AN INVESTIGATION OF FERRIMAGNETIC

COBALT DOPED GAMMA FERRIC OXIDE
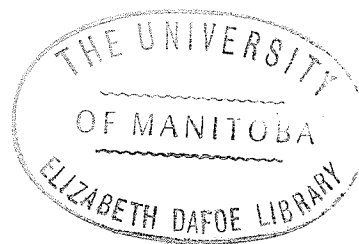
MICROPOWDERS

A Thesis

Submitted To

The Faculty of Graduate Studies, University of

Manitoba, in partial fulfillment of the requirements

of the degree of Master of Science

By

Dorothy Khalafalla

Winnipeg   Manitoba

March   1971

© Dorothy Khalafalla 1972

ABSTRACT

The magnetic properties of cobalt doped gamma ferric oxide micropowders were measured including the magnetic moments and coercive forces and Mössbauer spectra were taken at room temperature and 4.2° K. It was found that the coercive force greatly increased with increased cobalt content and exhibited a strong temperature dependence. This was accounted for by using the one ion model of Slonczewski for the anisotropy of Co^{2+} ions in ferrites. Other magnetization measurements were less significant and the magnetic moments were found to change little with cobalt doping.

An increase in lattice parameter was observed for the cobalt doped samples. The conversion to αFe_2O_3 was studied and the coercive forces of partially converted samples was found to be high and complete conversion was never obtained. The magnetic moments of the heated samples were found proportional to the cobalt content.

There was no change observed in the area ratios of the recoil free absorption peaks in the Mossbauer spectra and no change in hyperfine field or isomer shifts were observed. It was found that at low temperatures the samples

were not saturated even at 50 kOe.

Most results indicated that the cobalt ion was in the lattice and not present in clusters. The experiments also suggested that the cobalt ion was in the B sites, both iron and vacancy sites in approximately equal proportions, and that the micropowder consisted of single domain particles whose magnetization vectors reversed coherently.

ACKNOWLEDGEMENTS

TABLE OF CONTENTS

FIGURES

TABLES

CHAPTER I

THE PROBLEM, DEFINITIONS, REVIEW AND PROCEDURE

A. THE PROBLEM

This thesis gives the results of an investigation of the properties of cobalt doped γFe_2O_3 micropowders. Pure acicular γFe_2O_3 particles with high anisotropy are used for the coatings of magnetic recording tapes. Because a small amount of cobalt in γFe_2O_3 greatly increases the coercive force, it was thought that these cobalt doped particles could also be used for magnetic tapes. However more high frequency losses of recording signal occur than for pure samples from friction between the tape and the head. Conversion to αFe_2O_3 which occurs irreversibly in pure γFe_2O_3 above about 400° C, occurs with a greatly increased activation temperature in cobalt doped samples. Thus these particles may be useful for coating tapes that are stored at high temperatures, and used at lower temperatures where the coercive force is greater. Therefore it is of interest to know the exact temperature dependence of the coercive force, the relationship between the magnetic properties and the cobalt doping, the effect of the

cobalt ion on the crystallographic structure and the position of the ion in the lattice.

B. DEFINITIONS

Anisotropy

Anisotropy energy is defined as the work required to make the magnetization lie along a certain direction compared to the easy direction. Thus the easy direction is that along which the magnetization vector lies for the energy to be a minimum. The anisotropy can be due to shape, where the easy direction is along the polar axis of an elongated particle. Particles subjected to tension or compression have strain anisotropy, and the easy direction is along the strain axis or perpendicular to it. When the magnetization tends to lie along certain crystallographic axes, the material has crystalline anisotropy. The crystalline anisotropy constants K can be expressed in terms of the free energy, F_k, for cubic symmetry.

$$F_k = K_1 (a_1^2 a_2^2 + a_2^2 a_3^2 + a_3^2 a_1^2) + K_2(a_1^2 a_2^2 a_3^2)$$

where a_1, a_2, a_3 are the direction cosines of the angles between the magnetization direction and the easy directions.[1]

Single Domain Particles

Magnetic materials in general contain many domains. Each domain is spontaneously magnetized and the direction of magnetization may vary from one domain to another. The domain configuration is a function of the applied field. When the particle is very small it may consist of a single domain; that is the exchange forces may dominate the demagnetization energy so that the particle is uniformly magnetized when no field is applied. There is a theoretical critical size below which the particle will be single domain, but experimentally[1] no sudden discontinuity is observed and the coercive force continues to increase below the critical size.

Coherent and Incoherent Rotations

Coherent rotations are those in which the magnitude of the magnetization remains constant (uniform) during reversible and irreversible changes in a field. The field at which the magnetization becomes non-uniform is called the nucleation field. Reversible magnetization changes occur coherently, whereas irreversible changes may be incoherent. A lower coercive force is expected for incoherent

reversals. Several modes of incoherent reversals have been proposed.[2] For particles in the form of infinite cylinders buckling and curling take place; in an elongated particle consisting of several spheres attached together, the magnetization reverses by rotations of the uniform magnetization vectors of each sphere in opposite directions, this is known as fanning. Information on the method of rotation of single domain particles can be obtained from measurements on aligned particles.[2,3] A maximum in the coercive force at about 50° occurs for incoherent rotations, when the coercive force is measured as a function of the angle from the alignment direction. However, it has also been proposed that coherent reversals in partially aligned particles give rise to maxima at various angles depending on the degree of alignment.[4]

For coherent rotations of spherical particles with cubic crystalline anisotropy, oriented at random, the coercive force H_c is[5],

$$H_c = \frac{0.64 \ K_1}{M}$$

where M is the magnetic moment. However the coercive force is often much lower than this experimentally.

Spinel Structure

The spinel ferrite structure may be represented by $M^{2+}Fe_2^{3+}O_4$. The oxygen ions form a face centred cubic lattice. The cations occupy interstitial positions such that they are either surrounded by four oxygen ions at the corners of a tetrahedron, A sites, or they are surrounded by six oxygen ions at the vertices of an octahedron, B sites. The smallest cubic unit cell consists of 32 oxygen ions. A normal spinel may be represented $M^{2+}(Fe_2^{3+})O_4$ where the brackets enclose the ions on the B sites, and the ions to the left are on the A sites. An inverse spinel has the distribution $Fe^{3+}(M^{2+} Fe^{3+})O_4$. Partially inverse structures are also possible. For spinels the angles and the distances between the ions are favourable for superexchange between the sublattice; the weakest interaction is that between the A site ions. From this factor and the results of neutron diffraction experiments, it is assumed that the sublattice magnetizations are antiparallel, although there are exceptions when the magnetization vectors are canted with respect to each other.

Mole % Weight %

When there is m mole per cent of cobalt in substance Q,

$$m = \frac{\dfrac{\text{weight of cobalt}}{\text{atomic weight of cobalt}}}{\dfrac{\text{weight of Q}}{\text{molecular weight of Q}}} \times 100$$

When there is w weight per cent of cobalt in substance S,

$$w = \frac{\text{weight of cobalt}}{\text{weight of S}} \times 100$$

These definitions are stated to clarify such formulae as $Co_xFe_{2-x}O_3$ where m = 2x, and $Fe(Fe_{5/3-y}Co_y\square)$, where $\square$ denotes a vacancy, and then m = $\frac{8}{3}$ y.

C.   REVIEW OF GAMMA FERRIC OXIDE

Structure

Gamma ferric oxide has the spinel structure with ordered vacancies in the B sites. The lattice parameter is 8.33 A if a cubic unit cell is used for indexing, extra X-ray lines that are due to ordering of the vacancies, may be accounted for by using a larger, tetragonal unit cell. The structure is usually represented by $Fe^{3+}(Fe_{5/3}^{3+}\square_{1/3})O_4$ where $\square$ denotes vacancies, but there is evidence that there may be water in the lattice.[7,8,9] The X-ray diagram of γ Fe_2O_3 (including the superstructure

lines) is very similar to that of $LiFe_5O_8$. By comparing these two structures[7] it is found that the composition ideal for ordering is $Fe^{3+}(Fe_{3/2}^{3+}H_{1/2})O_4$. A mixture between the phase with hydrogen (that may be due to the presence of water during preparation), and that without has also been proposed.[9] Gamma ferric oxide particles are usually acicular with the polar axis along the (110) direction.

Magnetic Moment

The magnetic moment of γFe_2O_3 has been measured as 71 - 74 emu/gm[9,11,12,13] at room temperature, and $3.5\,\mu_B$/formula unit (82.5 emu/gm) at 4.2° K[9,14]. The latter corresponds closely to the theoretical spontaneous moment with spins on the A and B sites antiparallel $3.33\,\mu_B$/formula unit). The saturation moment at room temperature is 0.9 of that at 0° K.[15] As most authors quote the saturation moment and not the spontaneous moment, and the values are consistently low (the expected moment at room temperature is about 79 emu/gm), there is still a discrepancy between the theory and most experimental results. The presence of non-magnetic γFe_2O_3 has been proposed[16], and also the structure $Fe^{3+}(Fe_{3/2}^{3+}H_{1/2})O_4$ gives a lower moment. The moment measurements have been used to verify the existence of the phase with hydrogen in the lattice.[9]

Coercive Forces

Most experiments have been done on acicular particles where shape anisotropy predominates. The polar axis length is usually about 400 A to 1μ and axial ratios vary from 1/7 to 5/7. The coercive forces vary between 100 oe and 350 oe at room temperature, rising to 200 oe to 400 oe at 77° K.[11,12,17,18,19] The coercive force due to crystalline anisotropy only, has been calculated[11] as about 80 oe at room temperature and about 190 oe at 100° K. As the predominant anisotropy is usually due to shape, the coercive force is very dependent on shape and particle density.[17,18]

Critical Single Domain Size and Methods of Rotation

The critical single domain size for coherent reversals in γFe_2O_3 has been calculated to be about 0.1μ for the diameter of a spherical particle, and 3.4μ for the major axis length of an acicular particle with axial ratio $\frac{1}{10}$.

Incoherent reversal modes have been proposed for acicular γFe_2O_3 because the coercive force is very dependent on particle size.[11,21] The chain of spheres, fanning, model yields reasonable agreement with experiments. Also

measurements on aligned particles tend to indicate inco-
herent reversals.[3]

Conversion

Gamma ferric oxide converts irreversibly to αFe_2O_3
on heating above about $400^{\circ}C$. The degree of conversion
depends on the heating temperature and time. The conver-
sion process has been studied in detail[22] and a mechanism,
involving cooperative slipping of the oxygen planes and
subsequent movement of the cations, has been proposed.[23]
The temperature of conversion has been found dependent on
the purity[24] and the shape[25] of the specimens. Evidence
that both γ and α phases exist in the same particle of par-
tially transformed materials, has been found in the form of
exchange anisotropy between the two phases.[26,27]

Cobalt Doped Gamma Ferric Oxide

The coercive forces of cobalt doped γFe_2O_3 have been
found to be high, up to 7.1 kOe at 77° K, and strongly tem-
perature dependant.[22] In two investigations[16,22], the co-
ercive forces were found approximately proportional to dop-
ing, but no detailed work on this was done. In one inves-
tigation[11] it was found that for samples with between 3 and
6 mole % cobalt, the anisotropy was independent of doping

and a non uniform reversal mode was proposed. The aniso-
tropy of many ferrites[28,29,30,31] is greatly increased by
the addition of a small amount of cobalt and a one ion model
has been proposed to account for this.[32,33,34,35] It was
suggested[16] that this model might also apply to γFe_2O_3 but
the matter was not investigated further.

The effect of cobalt on conversion to αFe_2O_3 has
been examined[22] and a greatly increased activation temper-
ature was found.

D.   INVESTIGATION PROCEDURE

To investigate the dependence of the properties on
cobalt content a large range of dopings were used from 0
to 10 mole % cobalt, (10 samples). The amount of cobalt
in the samples was measured by X-ray fluorescence, and the
structure was examined and the lattice parameters were
measured by X ray diffraction. The magnetic properties,
coercive force, moment and others were measured on a vi-
brating sample magnetometer. The particles were heated
for various times and at different temperatures to inves-
tigate the conversion to αFe_2O_3. To determine the dis-
tribution of ions in the lattice, the Mössbauer effect

was used and spectra were taken at room temperature and at 4.2° K both with and without an applied field of 51kOe. The results of these experiments were correlated and various conclusions reached.

CHAPTER II

ELECTRON MICROSCOPE AND X-RAY ANALYSIS

Sample Description

Five of the samples were in powder form and were
ground to separate the particles before use in experiments.
The remainder were in paraffin wax which was removed with
successive washing with toluene and acetone for experi-
ments that required a powder. There may have been dif-
ferences between the particles due to ageing and oxidation
effects, that is differences in diffusion of vacancies, dif-
fusion of cobalt ions and absorption or release of water,
due to varying ages of the powders and whether or not they
were stored in paraffin. The samples were numbered and
their description given in Table I.

Sizes and Shapes of Particles

Some of the particles were ground and separated on-
to a glass slide; a carbon film was evaporated over them
and this film, containing the particles, was examined with
an electron microscope. The diameters of the particles
were measured in two perpendicular directions, the longest
and the shortest diameters were measured if any elongation

TABLE I

SAMPLE DESCRIPTION

Sample Number	Bottle Marking	Remarks
1	Pure γ Fe_2O_3	
2	$Co_{0.02}Fe_{1.98}O_3$	In paraffin, received circa 1960
3	1.2%	In paraffin, (12/29/61)
4	2%	In paraffin, (11/14/60)
5	3.08%	M.T.O.28265 L-35-K-1 Received Jan. 1971
6	3.5%	In paraffin, (11/14/60)
7	1.5% CoO	Received 1965
8	3% CoO	Received 1965
9	4.13%	M.T.O.28770,28268 Lot 2 Received Jan. 1971
10	7.37%	M.T.O.28770,28268 Lot 2 Received Jan. 1971

was present. Most particles (85%) were spherical although
some were square and protrusions appeared which may have
been small particles or larger particles with knobs. Some
particles appeared kidney shaped or hemispherical. The
axial ratio of the non spherical particles varied from
1/1.3 to 1/2. Many particles had blurred edges due to
carbon formation and interference of the magnetic field
of the particles with the magnetic focussing field of the
microscope. The results are shown in Figure 1 to Figure
6 and Table II.

In the following the particles are assumed spherical
and thus the anisotropy is assumed all crystalline. Shape
anisotropy would add about 200 oe to the coercive force for
all temperatures (from comparison with acicular pure samples),
and if 15% of the particles had shape anisotropy, the ad-
ditional term would be only 30 oe which is negligible in
comparison to coercive forces of the order of kilo-oersteds.
Thus the particles are assumed spherical with diameters of
about 800A.

Fluorescence Analysis

X-ray fluorescence analysis was carried out to deter-
mine the mole per cent of cobalt in each sample. Standards

FIGURE 1

Distribution of sizes of sample 7 ($4\frac{1}{2}$ mole % cobalt).
The arrow denotes the mean diameter.
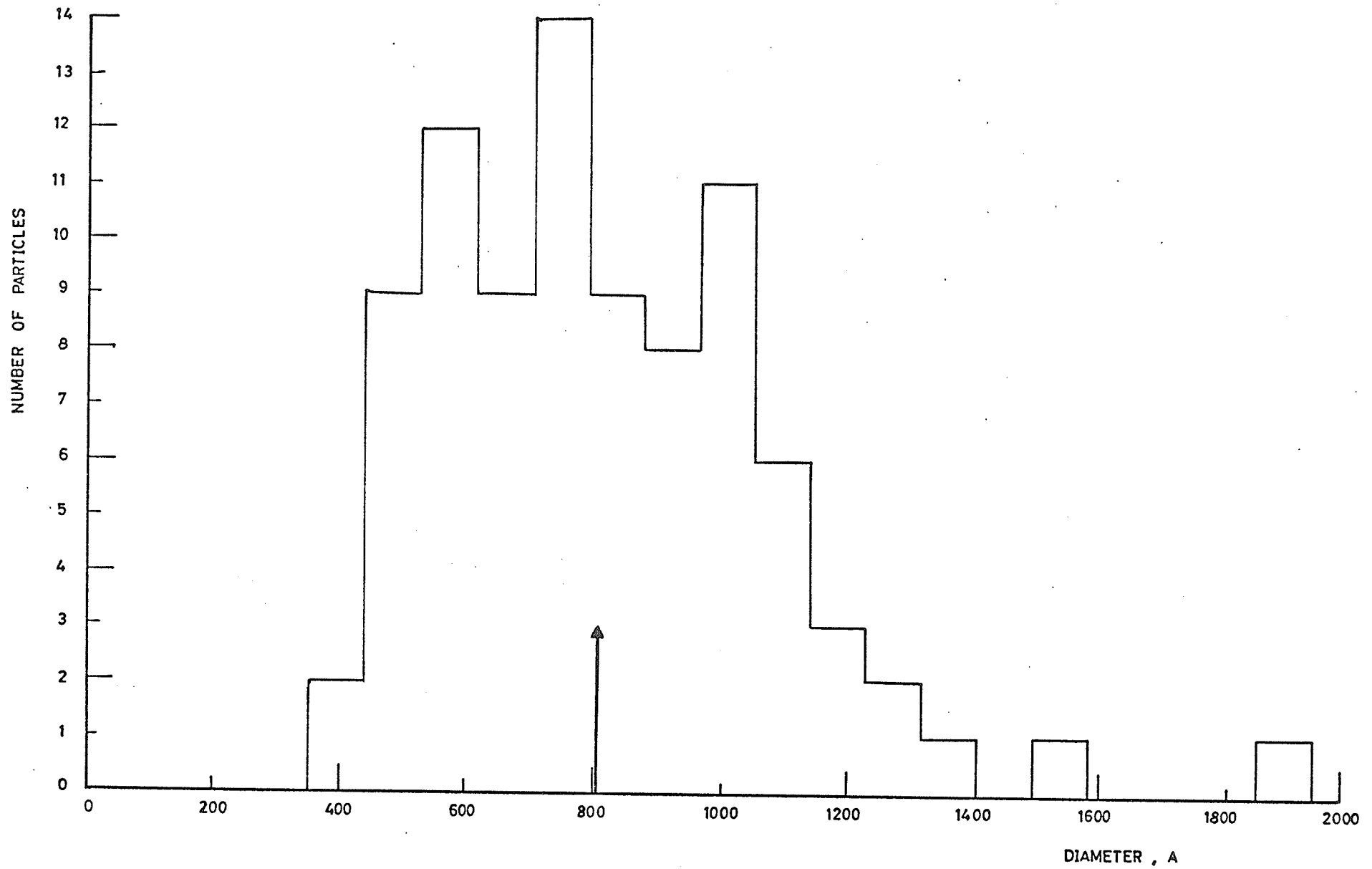
FIGURE 2

Distribution of sizes of pure γFe_2O_3 particles. The ar-
row denotes the mean diameter.
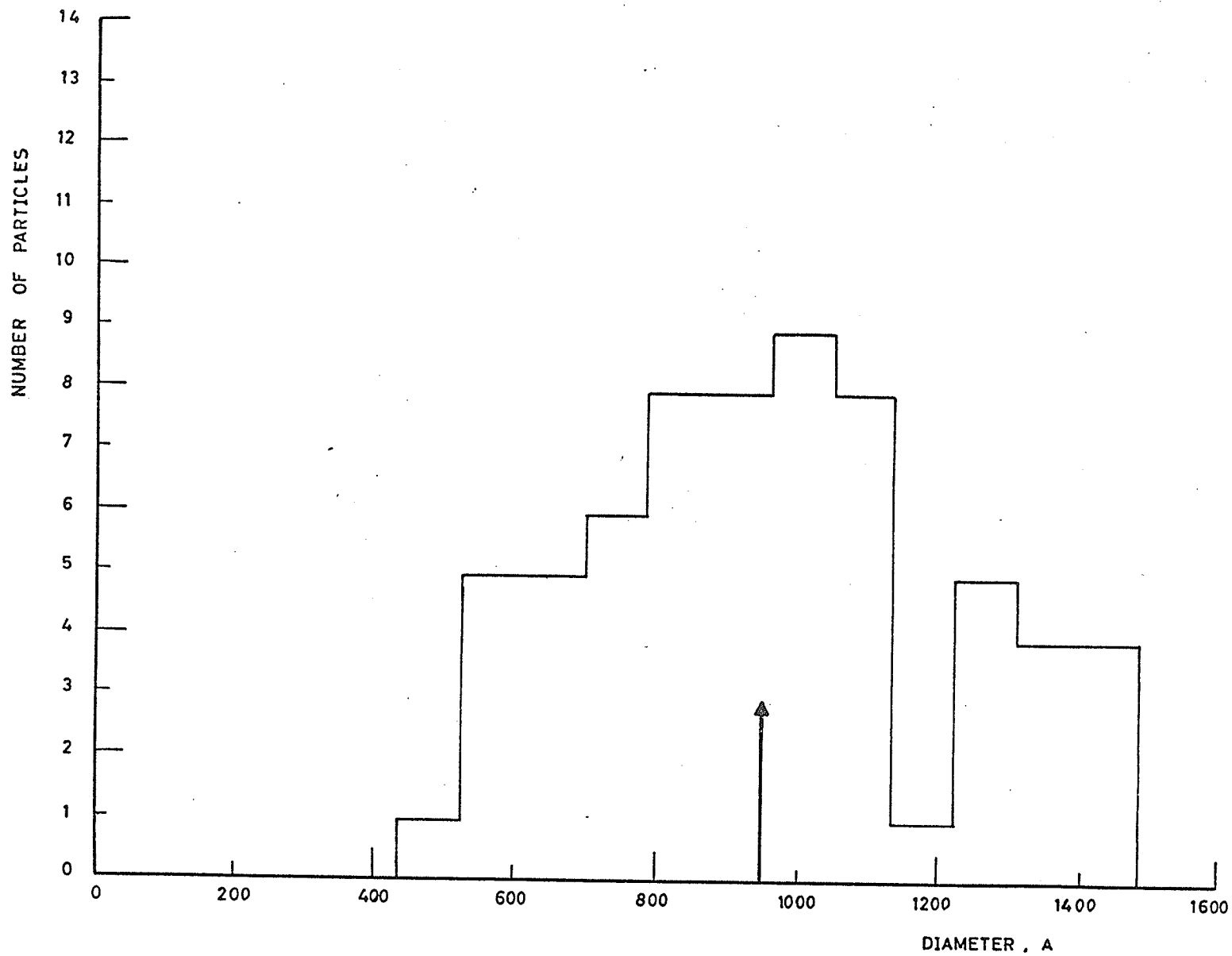
FIGURE 3

Distribution of sizes of sample 8 ($4\frac{1}{2}$ mole % cobalt).
The arrow denotes the mean diameter.
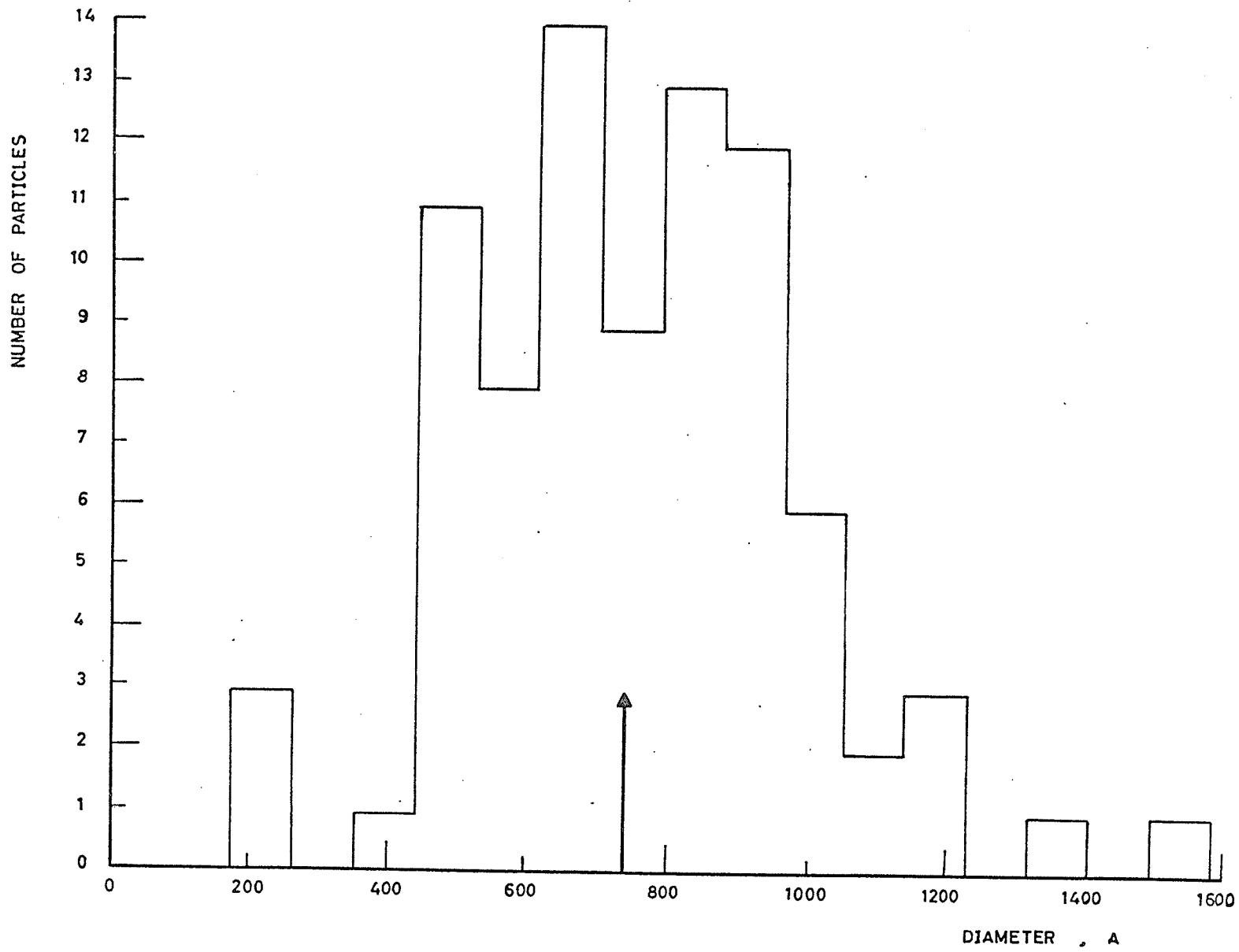
FIGURE 4

Electron microscope picture of pure γ Fe_2O_3 particles
(x 7990), showing predominantly spherical particles and
their tendency to stick together.
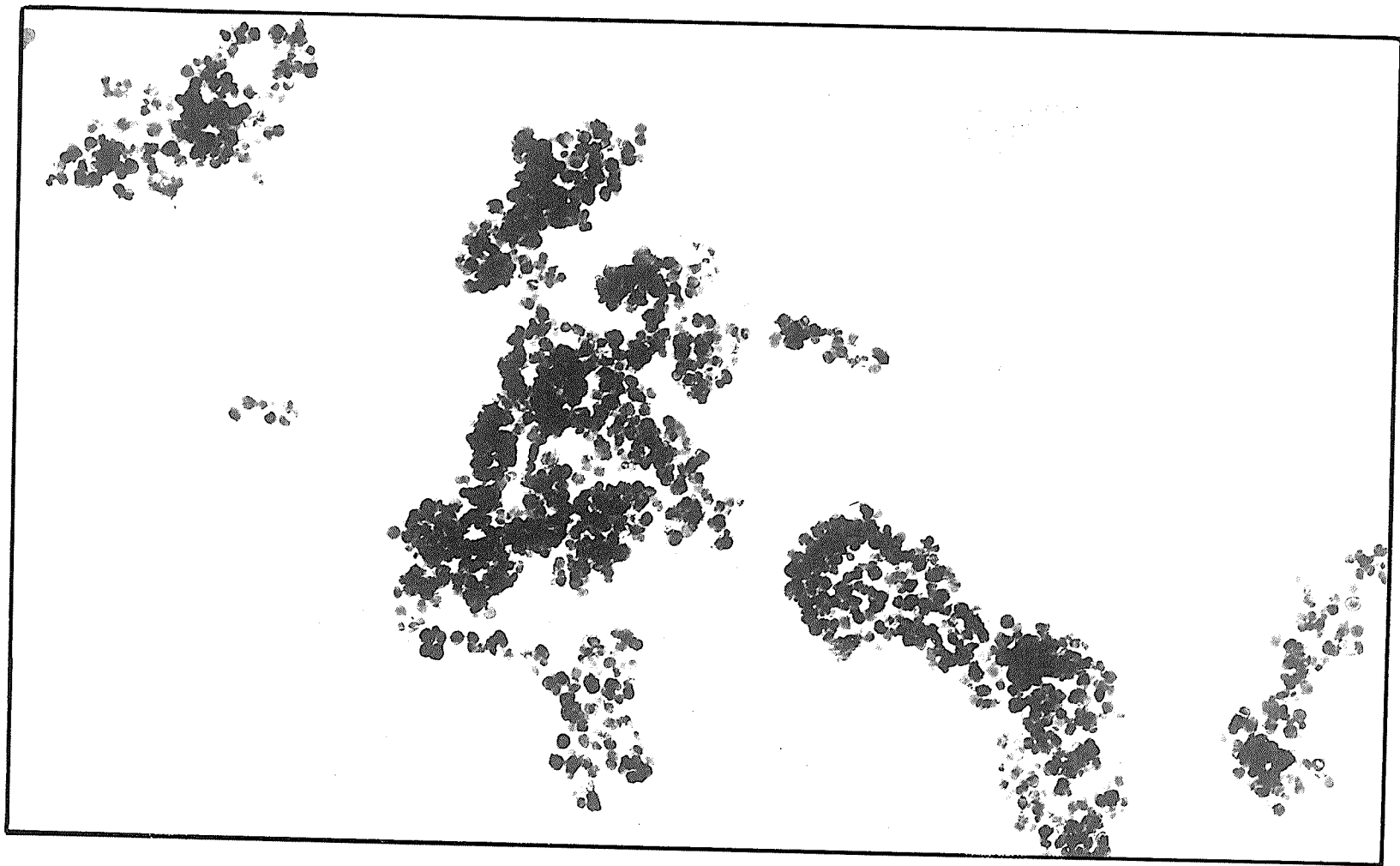
FIGURE 5

Electron microscope picture of pure 𝛾 Fe_2O_3 particles
(x 228000), showing predominantly spherical particles
with one elliptical particle.
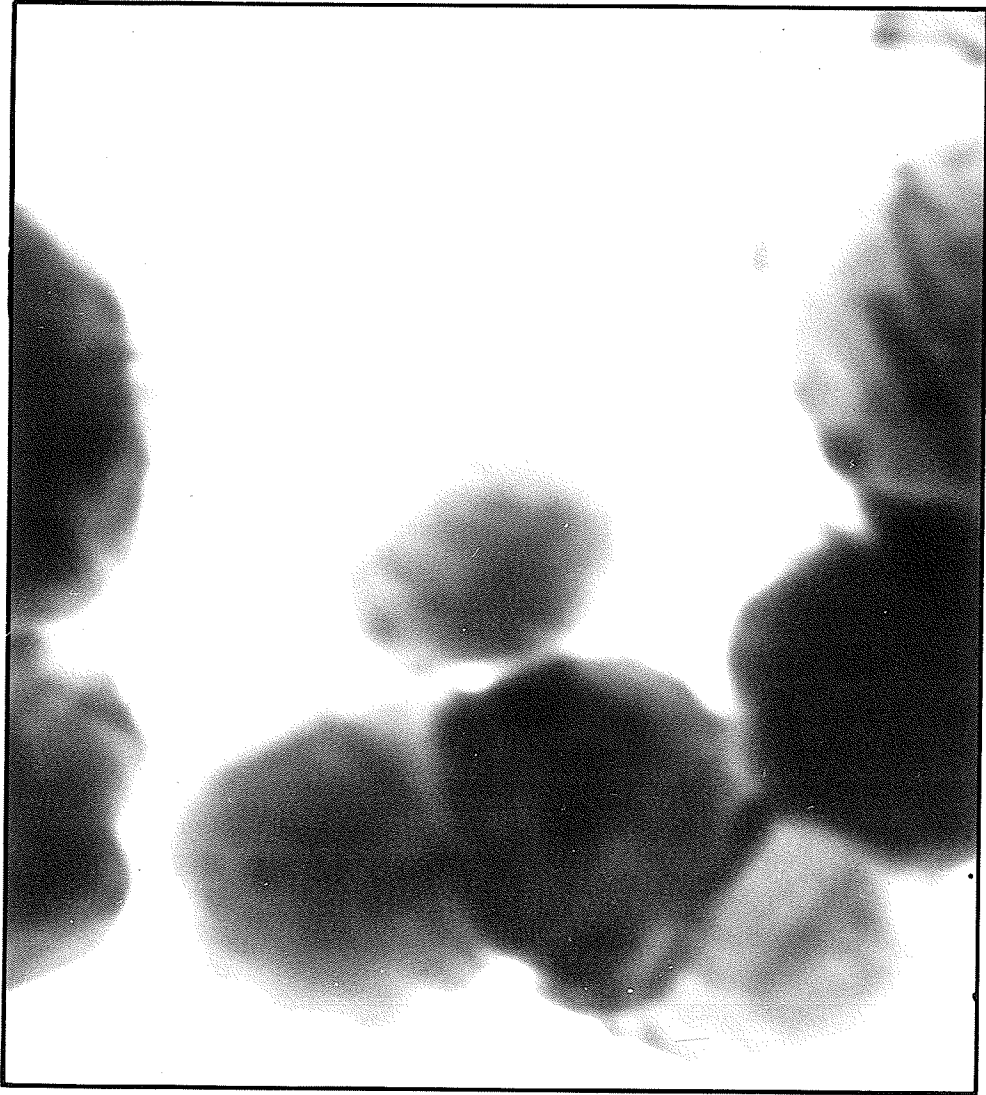
FIGURE 6

Electron microscope picture of sample 7 ($4\frac{1}{2}$ mole % cobalt)
(x 228000) showing a closely packed group of predominantly
spherical particles and one particle with a possible pro-
trusion.
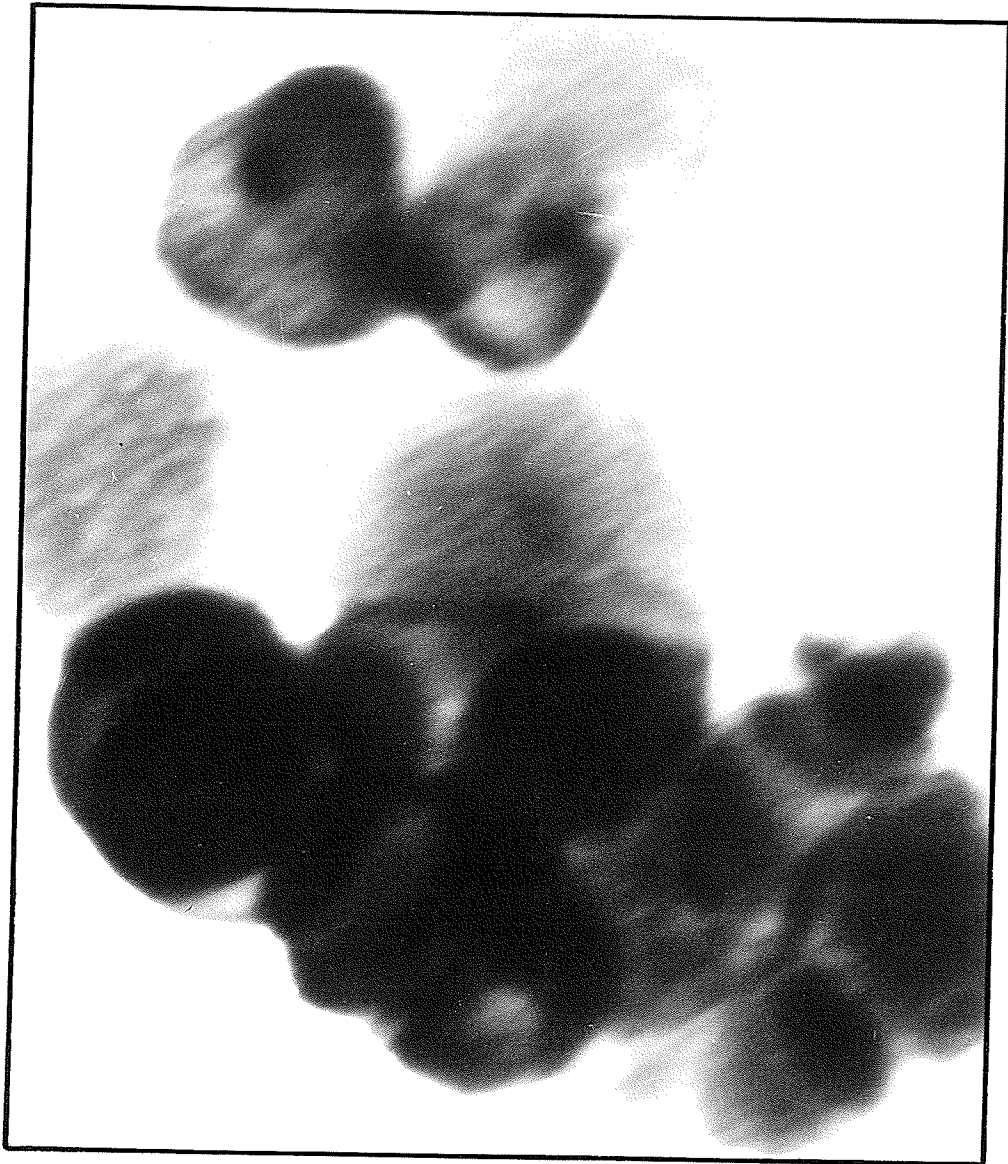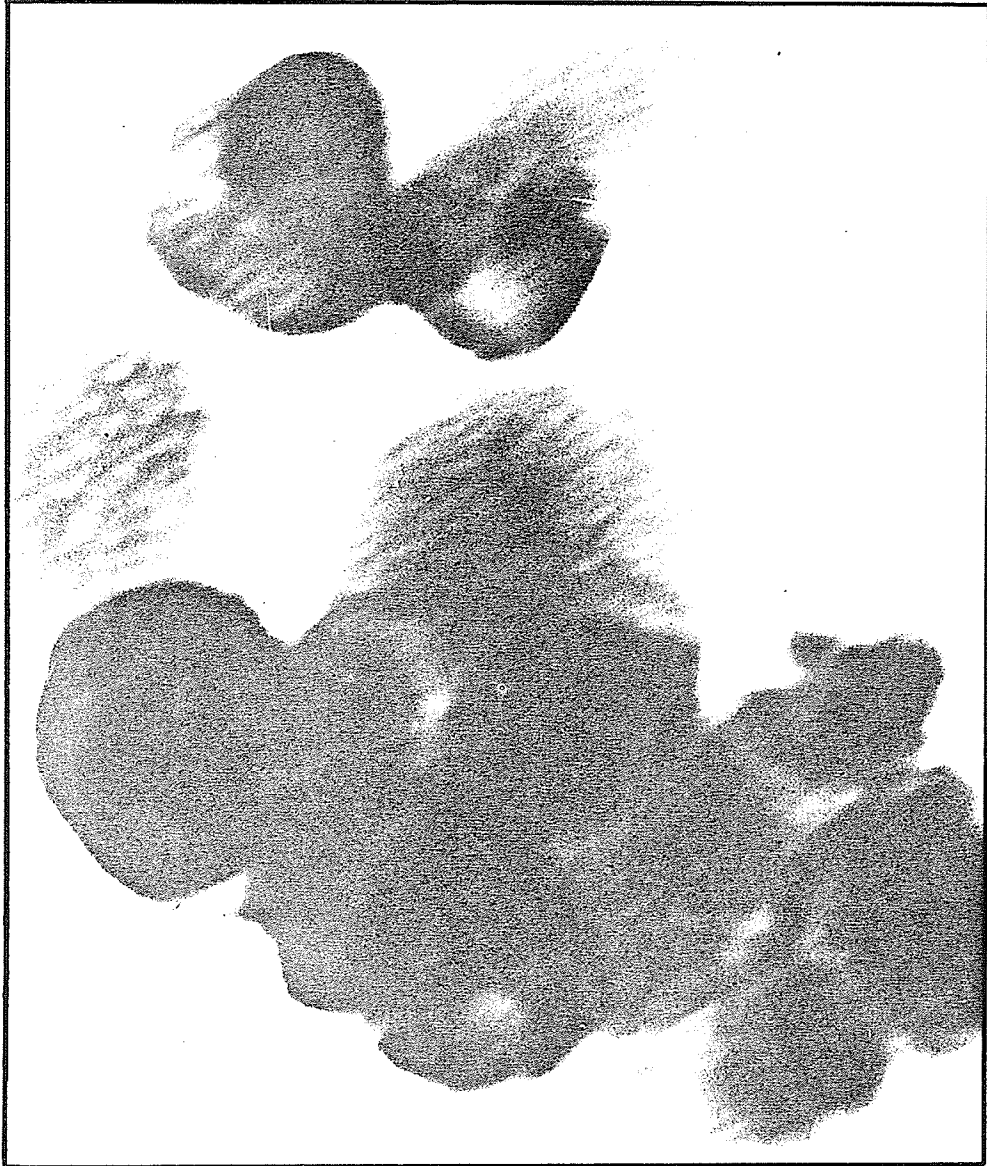
TABLE II

ELECTRON MICROSCOPE RESULTS

Sample Number	Mole % Co	Mean Diameter A	Maximum Diameter A	Minimum Diameter A	Fraction of particles with diameter greater than 1000 A
1	0	955	1500	400	0.34
7	4.5	806	1600	200	0.08
8	4.5	740	2000	400	0.16

were made by mixing known proportions of cobalt oxide and γFe_2O_3 and moulding them in a plastic disc. Silver radiation was used and a lithium flouride crystal. The bottle marking was found to correspond to the weight per cent of cobalt in most cases (Table III). Errors are of the order of or less than 10%. Five ratios of the iron K_α and K_β X rays to the cobalt K_α and K_β X rays were used and the error recorded is the spread of the readings.

Fluorescence analysis also yields information about possible impurities. All the samples were found to contain copper, nickel, manganese and some zinc. There was about twice as much nickel and copper in samples 5, 9 and 10 than the others. Small amounts of zinc were found in samples 9 and 10, twice this in sample 6 and four times this in sample 2. By comparing these intensities with other lines, it was found that most samples contained less than 1% impurities.

X-Ray Diffraction Results

X-ray powder diffraction pictures were taken with a cylindrical camera using iron radiation with a manganese filter. The lattice parameters were measured from about five high angle lines and for about two of these the α_1, α_2

TABLE III

MOLE PER CENT OF COBALT IN SAMPLES

Sample Number	Bottle Marking %	Mole % Measured	Mole % Co Corresponding to Bottle Markings of Weight %
2	1	0.95 ± .05	-
3	1.2	2.1 ± 0.2	1.6
4	2	3.25 ± 0.4	2.7
5	3.08	4.3 ± 0.3	4.16
6	3.5	4.4 ± 0.5	4.75
7	1.5	4.5 ± 0.5	-
8	3	4.5 ± 0.5	-
9	4.13	5.8 ± 0.6	5.6
10	7.37	9.9 ± 0.8	9.5

doublet was resolved. A cubic unit cell was used for indexing and the results extrapolated using the Nelson Riley extrapolation procedure. The results are shown in Table IV and Figure 7, a linear relationship between cobalt doping and lattice parameter can be made if sample 2 (1% Co) is excluded (which can be justified as it contains more impurities).

All samples except samples 5, 9 and 10 showed the characteristic γFe_2O_3 diffraction pattern. Samples 9 and 10 showed only the lines of the spinel structure and no lines corresponding to vacancy ordering. Sample 5 displayed the spinel lines and two of the most intense γFe_2O_3 superstructure lines, although these were of low intensity((106, 203), (213, 116)). The (103, 110) and (102) lines were not present in samples 5, 9 and 10. Also for these samples the high angle lines were not resolved resulting in an increased error in the lattice parameter. Interstitial ions, causing strain, or the presence of another phase and an imperfectly formed material, are possible causes for the lack of resolution.

The ionic radius of the Co^{2+} ion is 0.72 A and that of an Fe^{3+} ion is 0.64 A, also it is assumed that the size

TABLE IV

LATTICE PARAMETERS

Sample Number	Mole % Co	Lattice Parameter (A)
1	0	8.348 ± 0.002
2	1	8.351 ± 0.002
3	2.1	8.349 ± 0.002
4	3.25	8.353 ± 0.001
5	4.3	8.354 ± 0.005
6	4.4	8.353 ± 0.001
7	4.5	8.354 ± 0.001
9	5.8	8.357 ± 0.005
10	9.9	8.366 ± 0.005

FIGURE 7

The lattic parameter, a, as a function of cobalt doping.
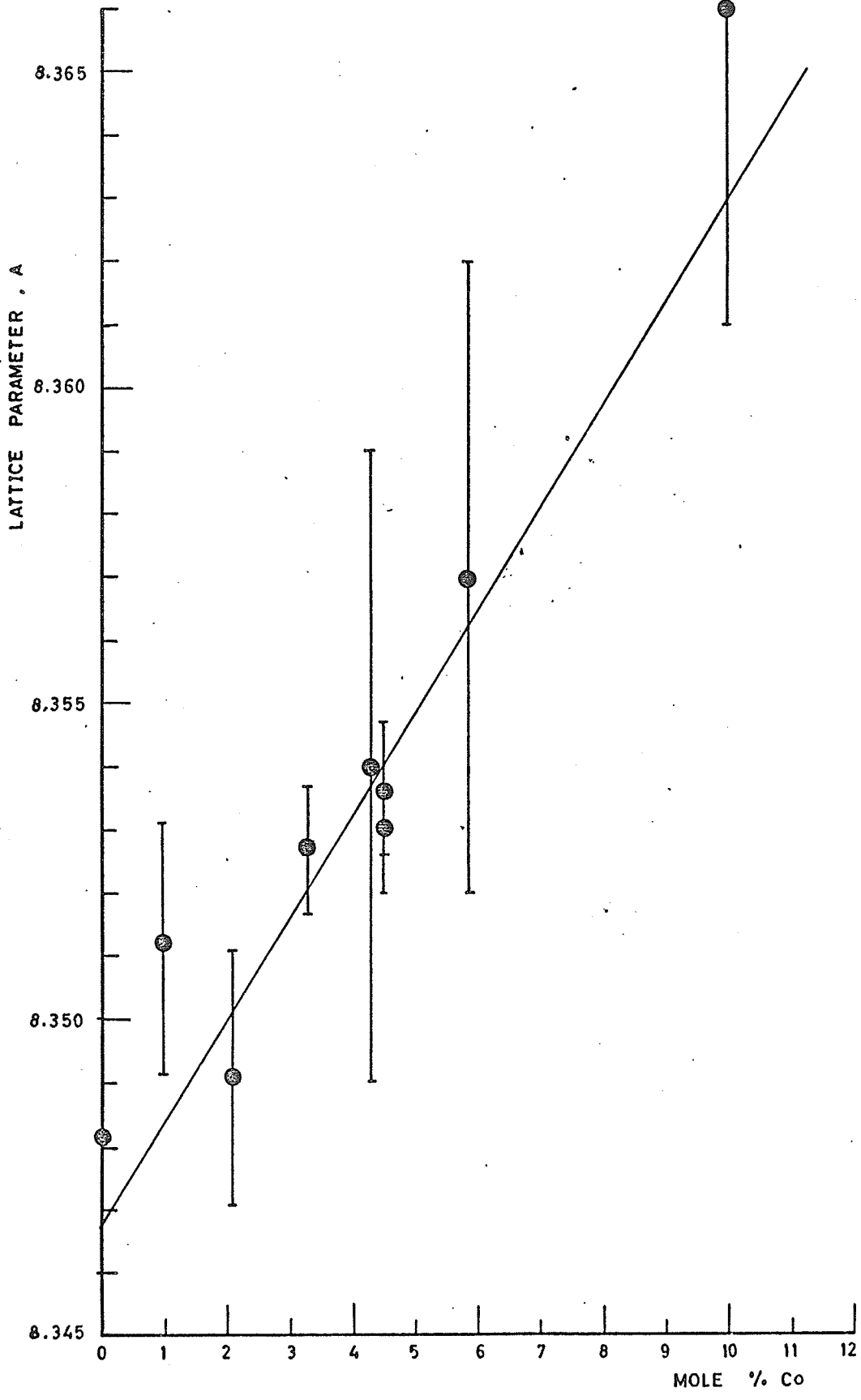
of a vacancy is about the same as that of an Fe^{3+} ion.
Thus if a cobalt ion replaced an iron ion on an A or B
site, or a vacancy, an increase in lattice parameter would
result. A cobalt ion on only iron A or B sites would need
an Fe^{3+} to change to an Fe^{4+} for charge balance; this
would result in a probable decrease in lattice parameter.
If a Co^{2+} ion filled only vacancies, some Fe^{3+} may become
Fe^{2+} to balance the charge, and as the ionic radius of an
Fe^{2+} ion is 0.74 an increased lattice parameter would be
expected.

Thus it seems that the cobalt ion does not go into
the iron A sites only or the iron B sites only.

CHAPTER III

MAGNETIZATION MEASUREMENTS

A.   EXPERIMENTAL METHOD

Each powder sample was mixed with paraffin wax, 50% by weight, resulting in a 15% packing density. The mixture was stirred over a water bath at 60°C to 80°C (to avoid conversion) and placed in an aluminum sample holder. The paraffin wax prevented movement of the particles. The samples used to measure the magnetic moment were made differently as an exact knowledge of the mass was necessary. The sample was weighed into the sample holder, wax was placed over it and the holder suspended in a water bath with copper wires. The melted paraffin soaked into the sample and avoided particle motion though may not have eliminated it, however this was not important as these samples were used only for moment measurements.

The measurements were made on a vibrating sample magnetometer using a dewar with liquid nitrogen and liquid helium for the low temperature measurements and a furnace for the high temperature measurements. A nickel sample was used for calibration.

B. MOMENTS

The results are shown in Figure 8 and Table V. Most cobalt doped samples had about the same moment as pure γFe_2O_3, but samples 2, 9 and 10 showed a decrease in moment of about 15%. The difference between the saturation moment (the applied field H extrapolated to infinity) and the spontaneous moment (H extrapolated to zero), increased for decreasing temperatures due to increased slope and possible lack of saturation. Table VI and VII show the expected changes in moment for the cobalt ions wholly in one type of site. The moment of a cobalt ion is assumed to be $3\mu_B$ but it may be as much as $3.5\mu_B$.[32]

Two observations can be made; firstly the cobalt may go into different positions for different samples, accounting for the scatter in the results, and secondly there may be a non-magnetic phase present or water in the lattice to account for the consistently low values of magnetic moment. Very low moments have previously been measured for cobalt doped γFe_2O_3 particles[16], (48 emu/gm) and the result attributed to a non-magnetic phase; these moments have also been measured as within 90% of the pure moment[11] but it was not stated whether this was an increase or de-

FIGURE 8

The magnetic moments of all samples at room temperature
and 77° K, for the applied field H extrapolated to zero
and infinity.
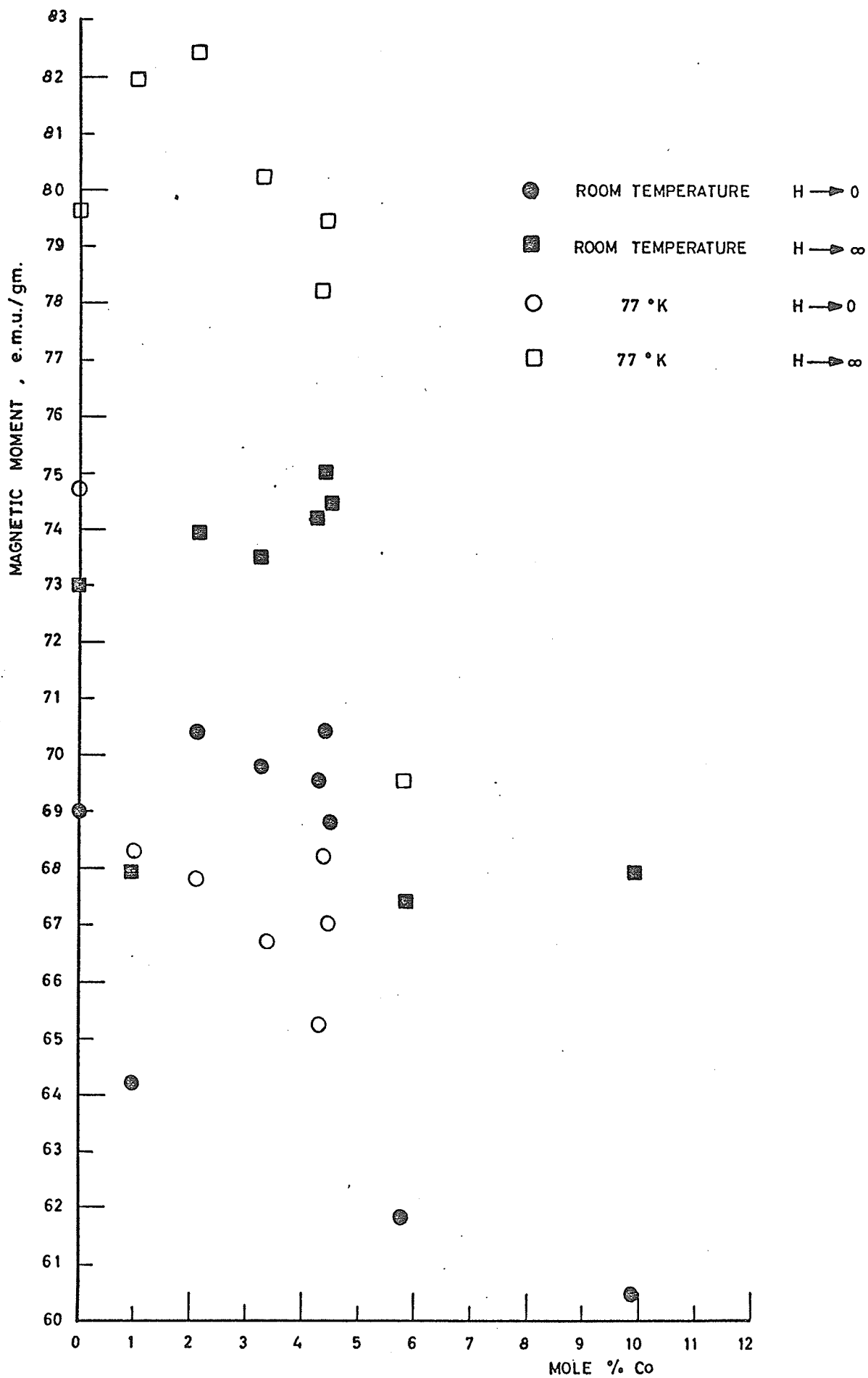
TABLE V

MAGNETIC MOMENTS

Sample Number	Mole % cobalt	Moment at Room Temperature			Moment at 77° K	
		$H \to 0$ emu/gm ±1	$\mu_B/Fe (Fe_{5/3}\square_{1/3})O_4$ ±.04	$H \to \infty$ emu/gm ±1	$H \to 0$ emu/gm ±1	$H \to \infty$ emu/gm ±1
1	0	69.0	2.64	73.0	74.7	79.6
2	.95	64.2	2.46	67.9	68.3	81.9
3	2.1	70.4	2.70	73.9	67.8	82.4
4	3.25	69.8	2.67	73.5	66.7	80.2
5	4.3	69.5	2.66	74.2	65.2	78.4
6	4.4	70.4	2.70	75.0	68.2	79.4
8	4.5	68.8	2.63	74.4	67.0	77.6
9	5.8	61.8	2.36	67.4	58.8	69.5
10	9.9	60.5	2.31	67.9	–	–

TABLE VI

CHANGES IN MAGNETIC MOMENT PRODUCED BY THE COBALT ION IN ONLY ONE TYPE OF SITE IN $Fe(Fe_{5/3}\square_{1/3})O_4$

(Theoretical pure moment 87.5 emu/gm at $0°$ K)

Cobalt Ion Replaces	Changes Needed For Charge Balance	Moment Change per Formula Unit, $0°$ K (m is mole % Co)	Moment Change emu/gm $0°$ K	Moment Change emu/gm, room temperature
Vacancies only	twice as many Fe^{3+} change to Fe^{2+}	2 2/3 m	70 m	63 m
Iron B Sites only	for each cobalt ion one Fe^{3+} changes to Fe^{4+}	-2 2/3 m	-70 m	-63 m
Iron A Sites only	for each cobalt ion one Fe^{3+} changes to Fe^{4+}	2 2/3 m	70 m	63 m
Vacancies only	Non stoichiometry of oxygen	8 m	210 m	190 m
Iron B Sites only	Non stoichiometry of oxygen	-5 1/3 m	-140 m	-126 m
Iron A Sites only	Non stoichiometry of oxygen	5 1/3 m	140 m	126 m

TABLE VII

CHANGES IN MAGNETIC MOMENT PRODUCED BY THE COBALT ION IN
ONLY ONE TYPE OF SITE IN $Fe(Fe_{3/2} H_{1/2})O_4$

(Theoretical pure moment 68.5 emu/gm at 0° K)

Cobalt Iron Replaces	Changes Needed for Charge Balance	Moment Change per Formula Unit, 0° K (m is mole % Co)	Moment Change emu/gm 0° K	Moment Change emu/gm, room temperature
Hydrogen in B Sites only	for each cobalt one Fe^{3+} changes to Fe^{2+}	5 m	137 m	123 m
Iron B Sites only	for each cobalt ion one Fe^{3+} changes to Fe^{4+}	-2.5 m	-68.5 m	-61.5 m
Iron A Sites only	for each cobalt ion one Fe^{3+} changes to Fe^{4+}	2.5 m	68.5 m	61.5 m
Hydrogen B Sites only	Non stoichiometry of oxygen	7.5 m	205 m	185 m
Iron B Sites only	Non stoichiometry of oxygen	-5 m	-137 m	-123 m
Iron A Sites only	Non stoichiometry of oxygen	5 m	137 m	123 m

crease or both.

C. COERCIVE FORCES

There was a large increase in coercive force with decreasing temperature from about 600 oe at room temperature to 9700 oe at 4.2° K. The rate of increase was greatest between room temperature and 77° K. The data is shown in Figure 9 to Figure 13, and all the data together in Figure 14. Above room temperature there was little change in coercive force (Figure 15) except a steady decrease to 100 .oe at 150°C and a subsequent slower decrease to about 50 oe at 300°C. Heating was done in air and helium gas as different results have previously been obtained from magnetic moments measured in air and helium[9], however no difference was observed here. The coercive force was measured at room temperature after heating and a slight increase in coercive force found; this may have been due to conversion.

Relationship Between Cobalt Content and Coercive Force

Figure 16 shows a reasonable linear relationship between the coercive force and mole per cent of cobalt up to about 5%. The anisotropy constant K_1 is proportional to the moment multiplied by the coercive force for single domain spherical particles. This was plotted in Figure 17;

FIGURE 9

The coercive force of pure γFe_2O_3 as a function of temperature. The full line joins the experimental points.
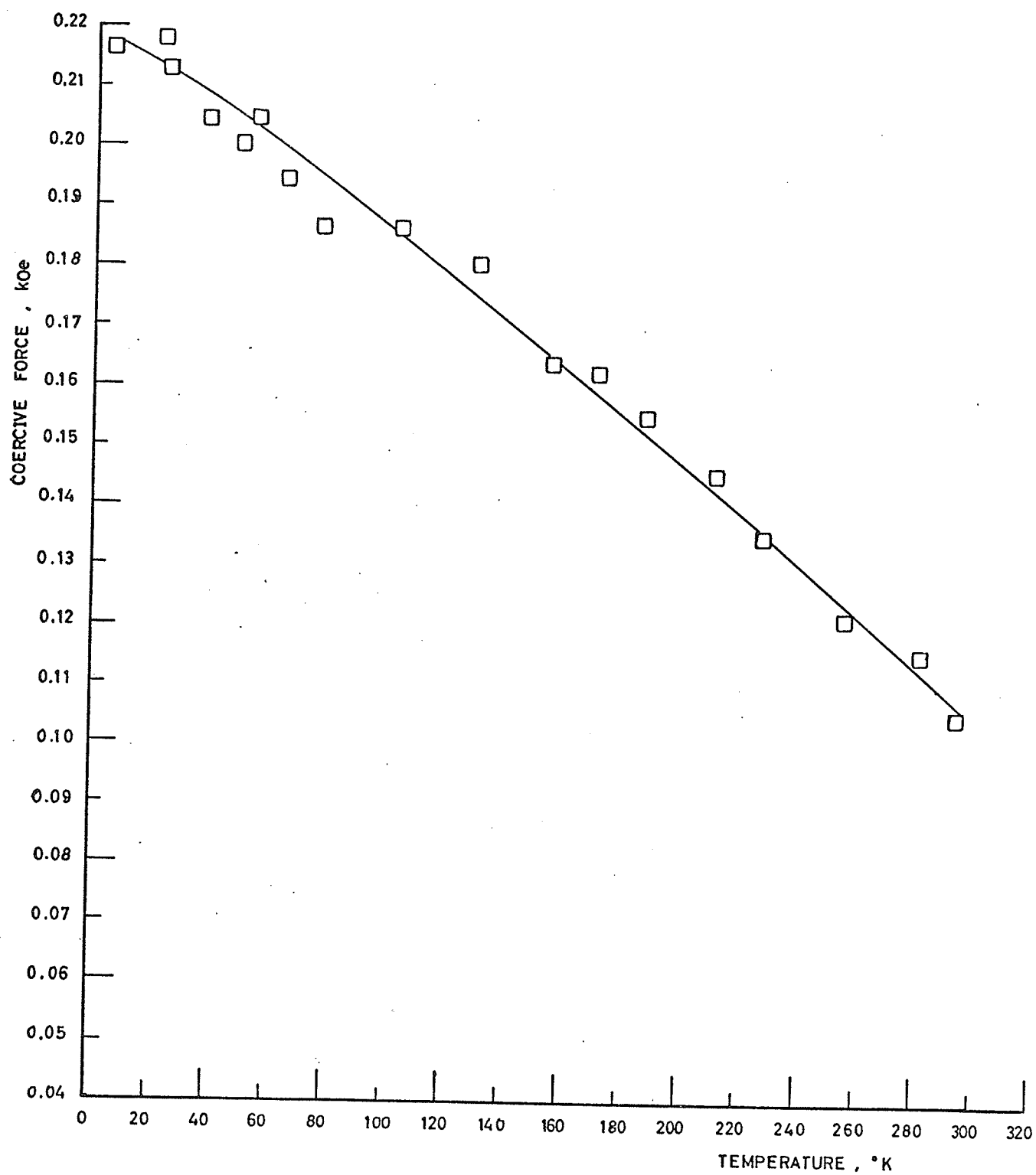
FIGURE 10

The coercive force of sample 2, (1 mole % cobalt) as a
function of temperature. The full line joins the experi-
mental points.
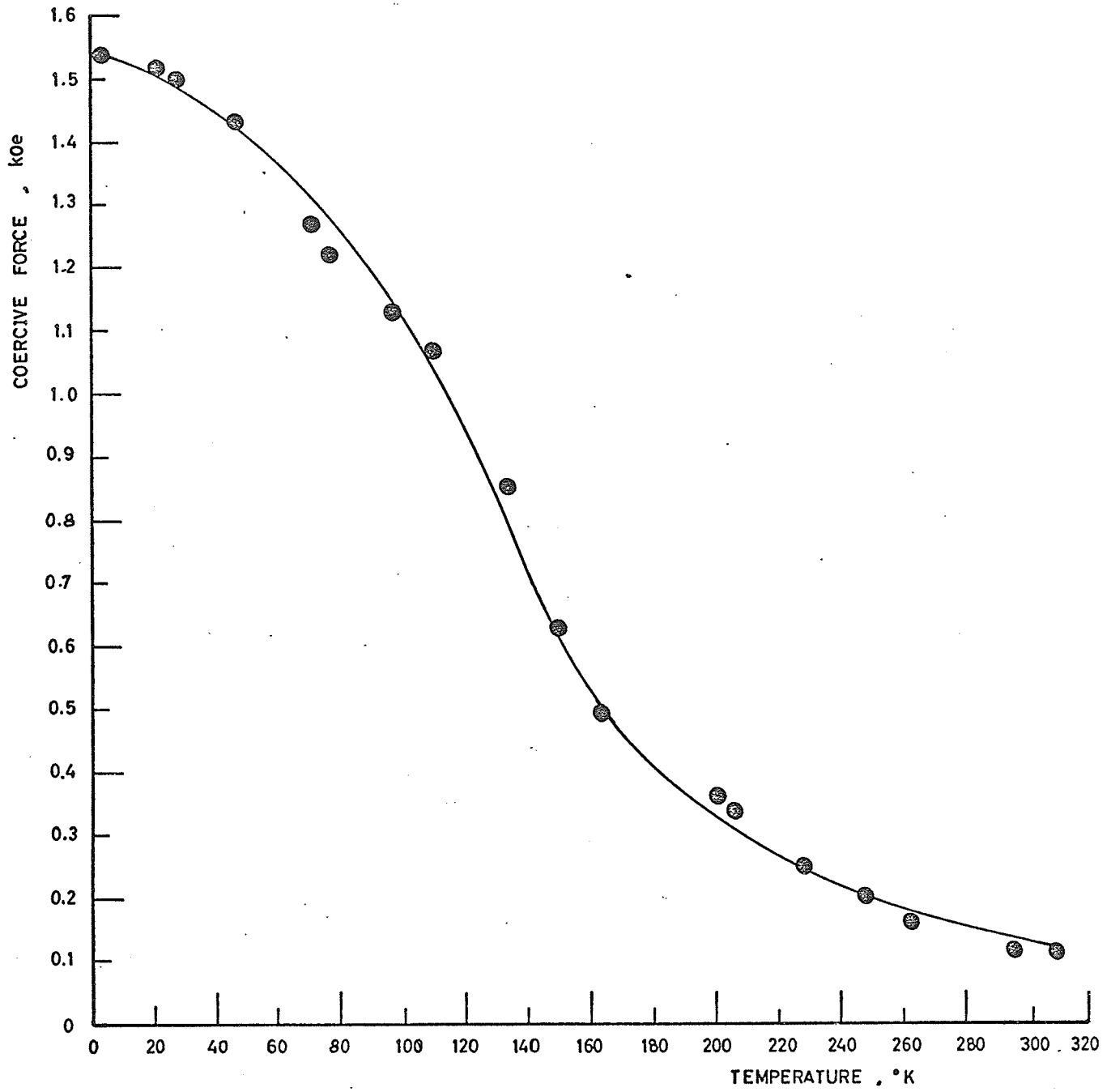
FIGURE 11

The coercive force of sample 3 (2.1 mole % cobalt) as a
function of temperature. The full curve joins experimen-
tal points.
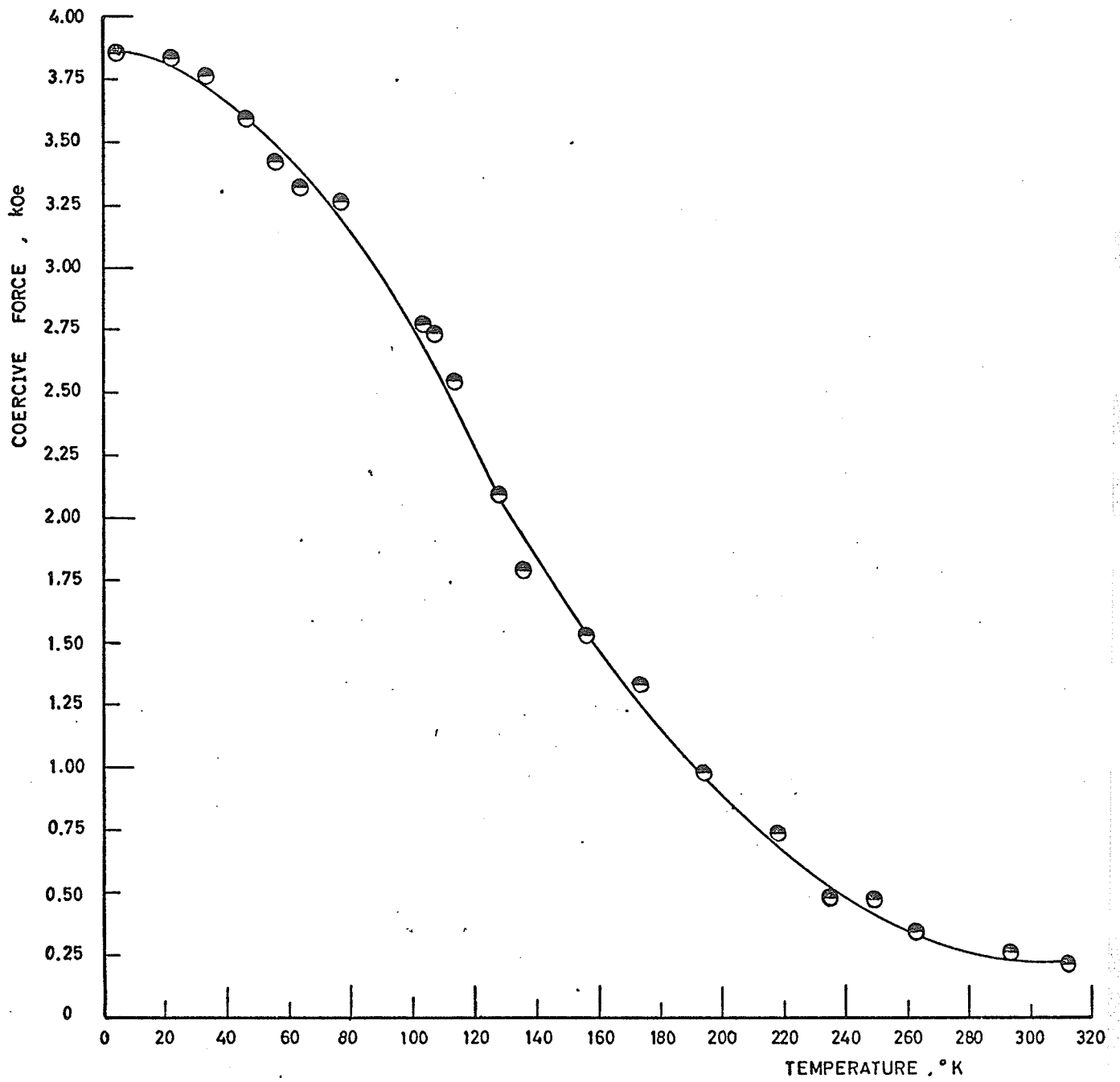
FIGURE 12

The coercive forces of samples 5, 9 and 10, (4.3 mole %, 5.8 mole % and 9.9 mole % cobalt) as functions of temperature. The full line joins the experimental points.
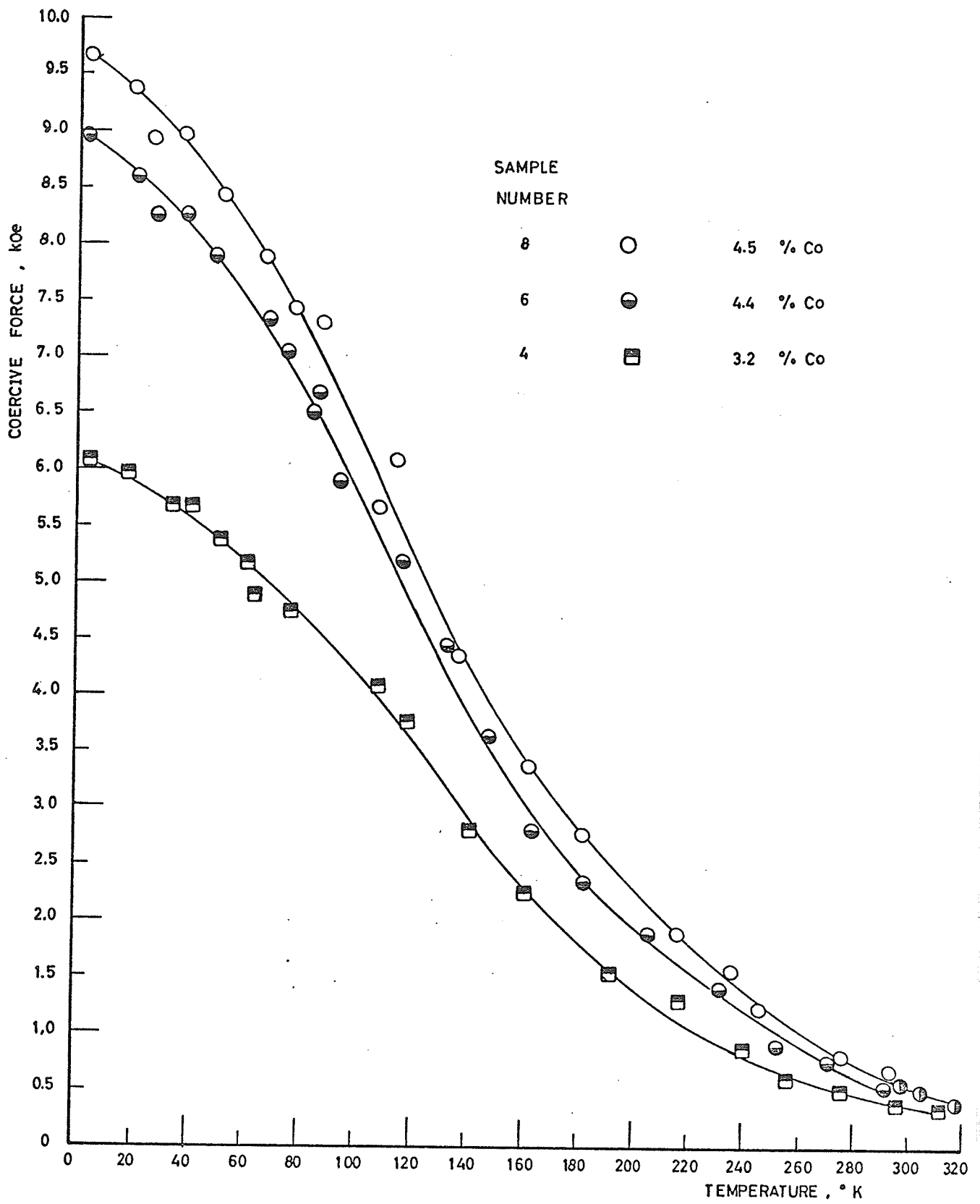
FIGURE 13

The coercive force as a function of temperature for samples
4, 6 and 8 (3.2 mole %, 4.4 mole % and 4.5 mole % cobalt).
The full curves join experimental points.
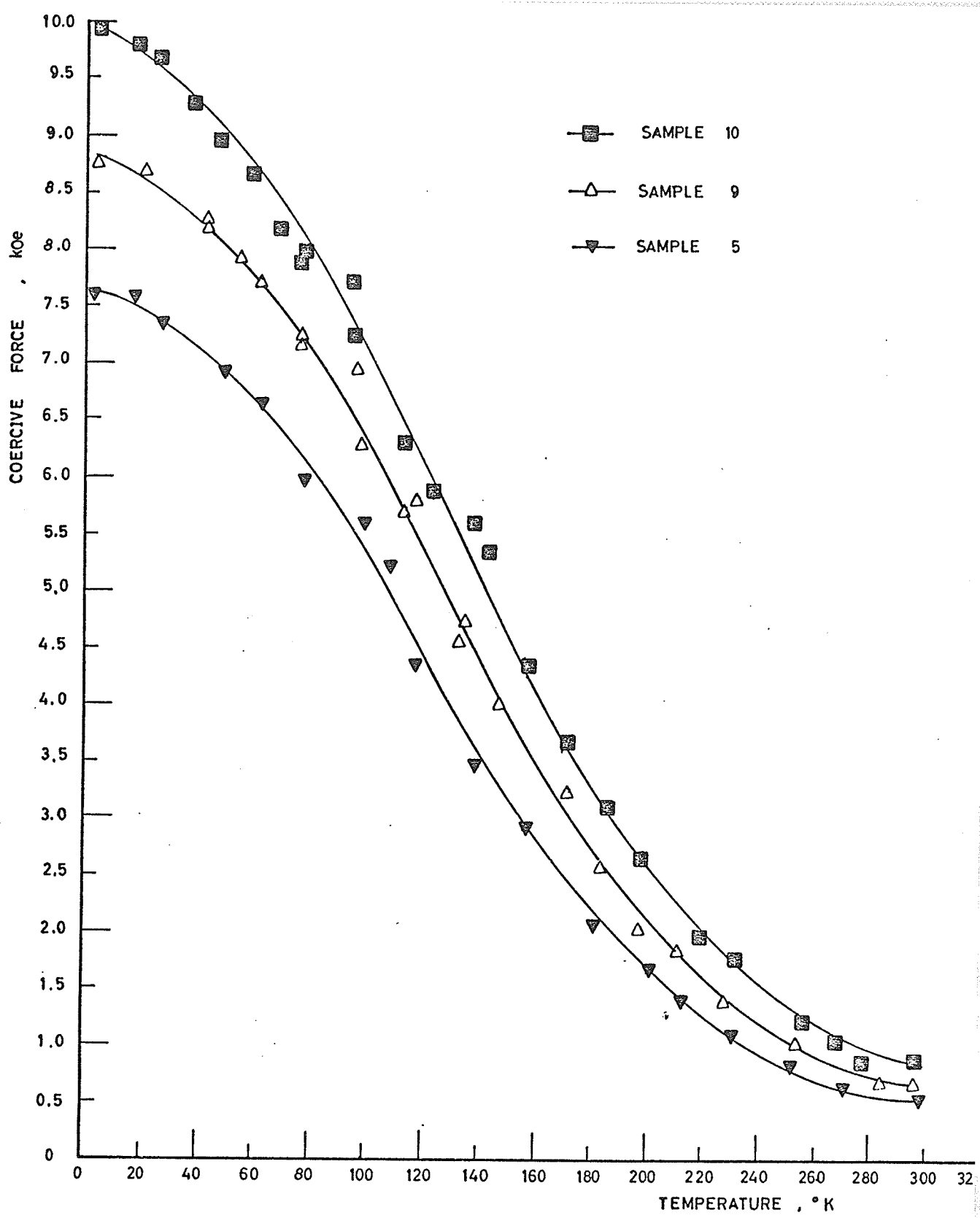
FIGURE 14

The coercive force of all samples as a function of temperature.
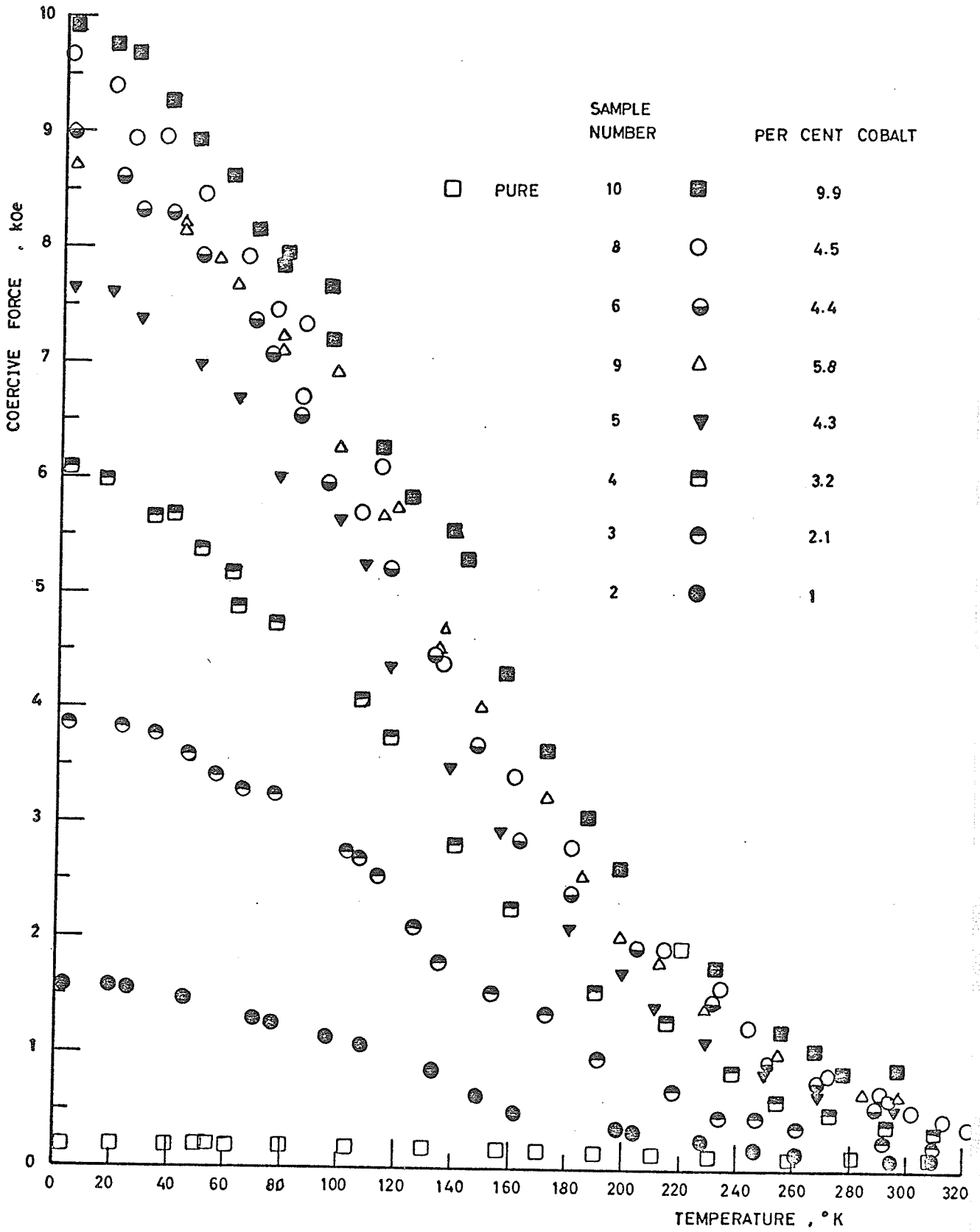
FIGURE 15

The coercive force as a function of temperature for samples 1 (pure) and 8 (4.5 mole % cobalt), above room temperature. After the coercive force at 563° K was measured, sample 8 was cooled and the coercive force was remeasured at room temperature.

COERCIVE FORCE , kOe

0.8

0.7

0.6

0.5

0.4

0.3

0.2

0.1

0

△   PURE

◯   SAMPLE 8   IN He   (⬤   AFTER   HEATING)

▨   SAMPLE 8   IN AIR (☐   AFTER   HEATING)

300   320   340   360   380   400   420   440   460   480   500   520   540   560   580
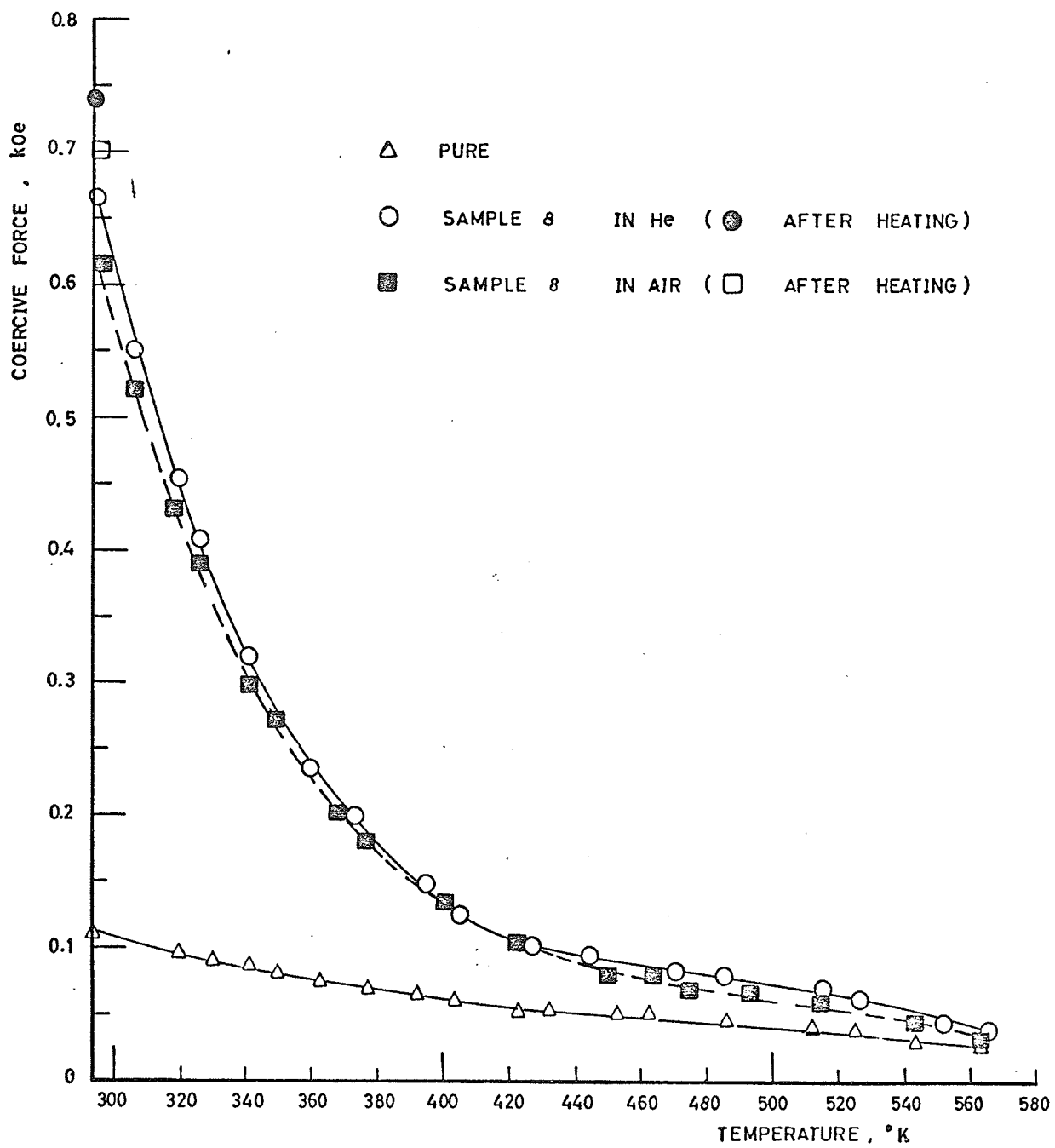
TEMPERATURE , °K

FIGURE 16

The variation of coercive force with mole % cobalt at
three temperatures. The straight lines are possible
linear fits to experimental data.
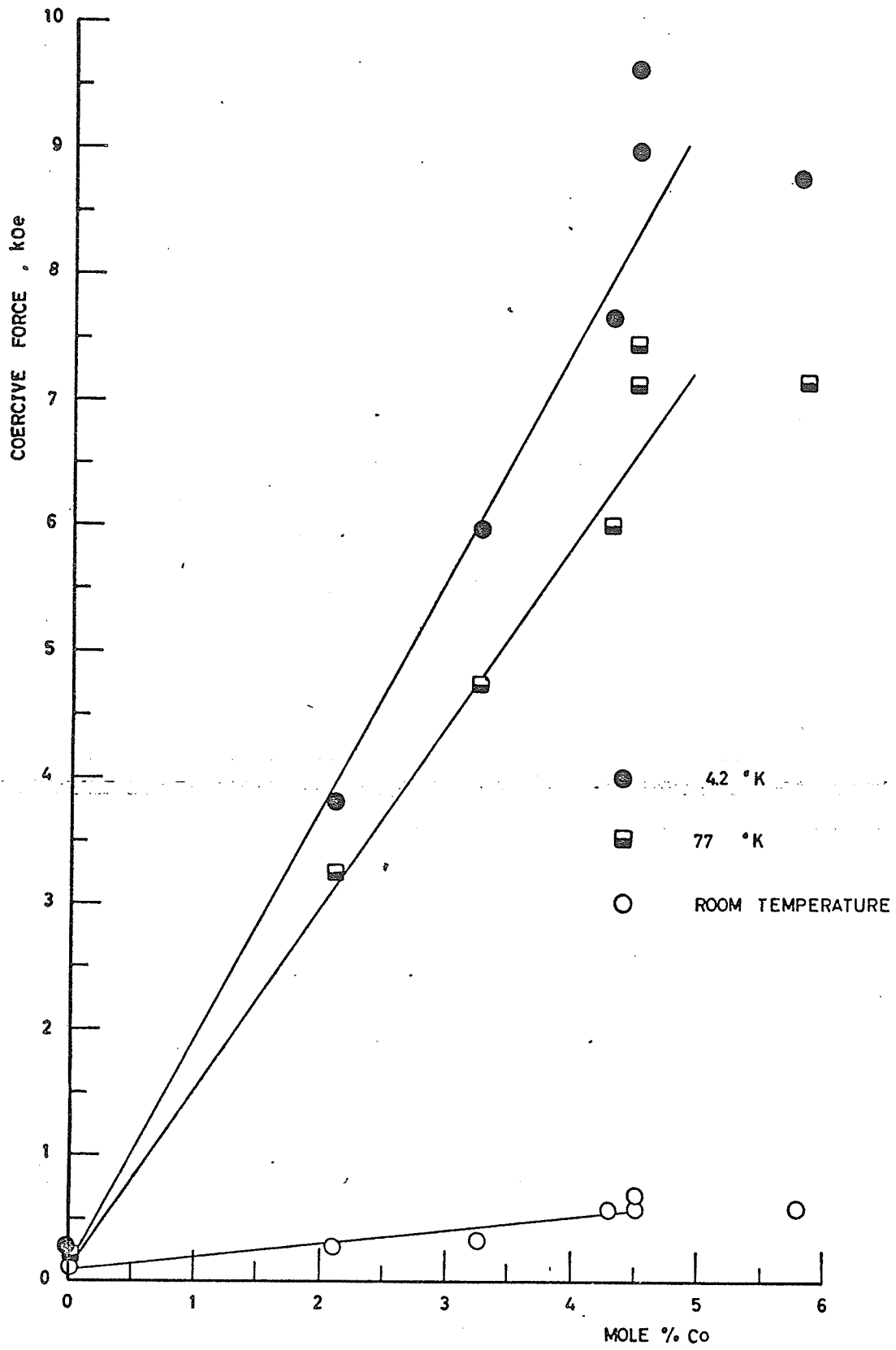
FIGURE 17

The relationship between coercive force multiplied by the
moment and the percentage of cobalt. The straight lines
are fits to experimental data.
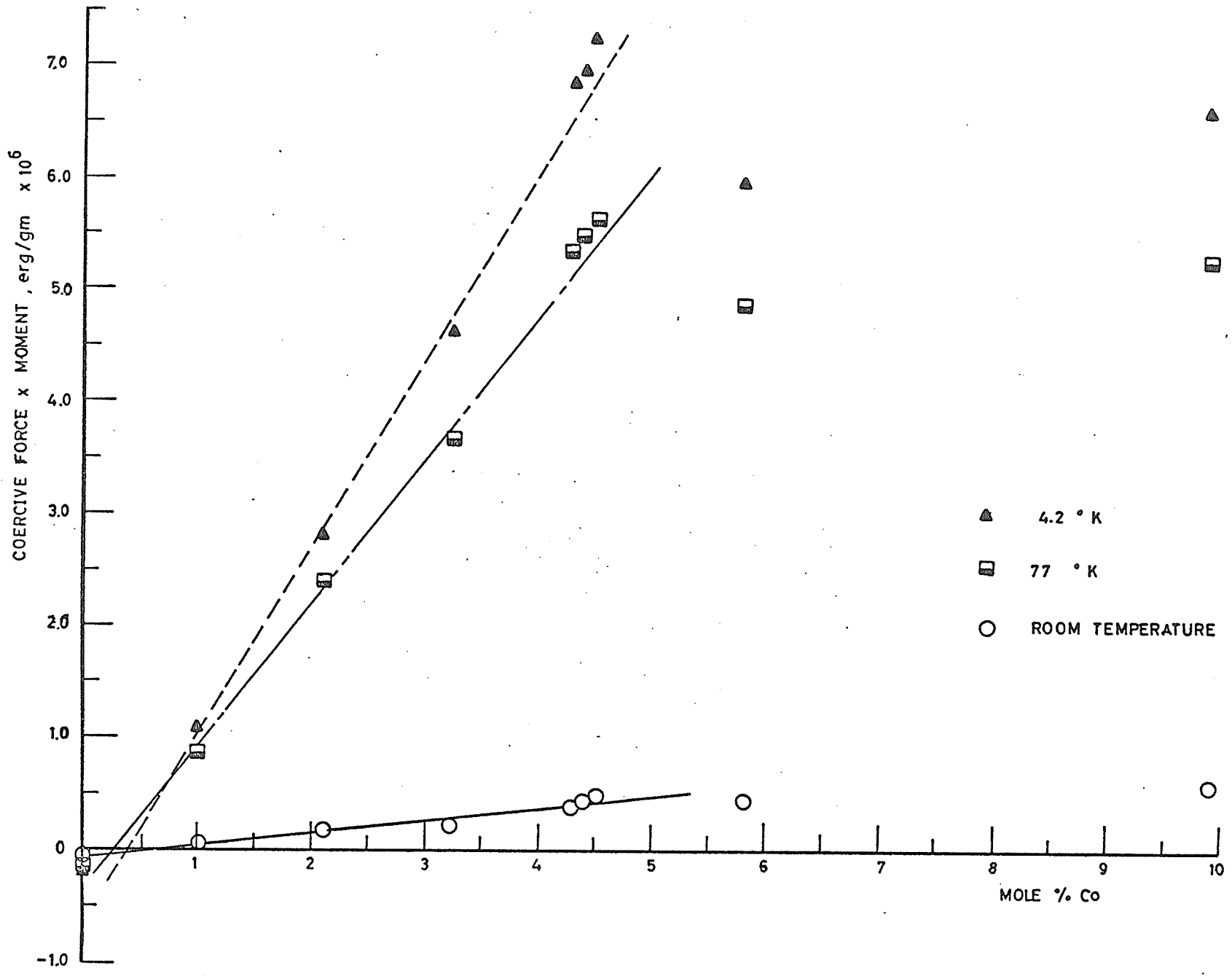
it is noticeable that a better straight line can be obtained if the anisotropy constant of pure γFe_2O_3 is assumed negative, and the effect of doping with cobalt is to add a positive contribution. Such an effect is observed in cobalt doped magnetite[29] which initially has a negative K_1, and positive contributions to K_1 are observed in cobalt doped nickel ferrite[30] and manganese ferrite.[31] However it seems that the anisotropy constant of the pure γFe_2O_3 was less than expected, this may be due to the particles not being single domain (Section E). Nevertheless it seems a linear relationship exists between anisotropy constant and cobalt content, for between 1% and 5% cobalt.

Single Domain Particles, Uniform and Non-Uniform Rotations

The size of these particles is about 800 A to 900 A, whereas the theoretical critical single domain size for coherent rotations is about 1000 A, thus it is probable that most particles are single domain if the rotations are uniform. Non-uniform rotations have been proposed for cobalt doped γFe_2O_3 particles[11], where the coercive force of 800 A 3 - 6% cobalt doped particles at room temperature was found to be 300 oe and a strong dependence on size was noted. For the samples used here there was no noticeable

size dependence and the coercive force of similar particles
to those in the reference was 660 oe. However the ratio
of the remanence to the saturation moment was greater than
80% at low temperatures, possibly indicating an incoherent
reversal mode. This matter was investigated further (Section E), and for the following, single domain particles
reversing coherently are assumed.

Particle Interactions

Particle interactions are less important for spherical particles whose anisotropy is predominantly crystalline, than for particles whose anisotropy is predominantly
due to shape. The packing fraction was 15% so even if particle interactions were important they would be very small,[17,18]
however there may have been some interactions present due to
a non-uniform distribution of powder in the paraffin. These
are neglected.

D. MODELS TO ACCOUNT FOR THE HIGH COERCIVE FORCE

Domain Boundary Model

A model has been proposed[36] to describe the behaviour
of $SmCo_5$ powders with coercive forces of about 10 kOe at

room temperature.[37] Domain boundaries may be present and move easily but a sufficiently large field will drive them out so that they must be renucleated.

However, this probably does not apply to cobalt doped γFe_2O_3 particles as the remanence and coercive force, when measured as a function of the previously applied field, do not increase at very high fields but become constant at comparatively low fields, of about twice the coercive force. (Figures 23, 24 and 25, Section F.)

Pinning Model

Wall pinning models have also been proposed for $SmCo_5$[38] and non-uniform magnetization pinning has been suggested in cobalt doped γFe_2O_3.[22] If the cobalt is not random but in clusters or a complex oxide, the non-uniform magnetization may be pinned resulting in a large coercive force. However such a good relationship between cobalt doping and coercive force would not be expected in this case, and the increase in lattice parameter with cobalt content shows that at least part of the cobalt goes into the lattice. Five percent of a second phase is necessary for it to be visible, so although no extra lines were observed in the X-ray diffraction patterns, the presence of another phase cannot be excluded.

One Ion Model

Slonczewski[33,34,35] obtained good agreement with experimental results of the anisotropy constant of cobalt doped Fe_3O_4[29] using a one ion model. The theory was extended to cobalt ferrite[32] and cobalt doped manganese ferrite[31,35], and later to cobalt doped nickel ferrite[30] with appropriate modifications. The model assumes the orbital angular momentum is not quenched but is constrained to lie parallel to the trigonal axis of symmetry, by the crystal field. The spin orbit energy L.S couples the spin to this axis also, accounting for the high anisotropy energy.

The anisotropy constant in cobalt doped magnetite[29] was linear in cobalt doping up to 5 mole % cobalt and exhibited a strong temperature dependance. Both of these features are observable in cobalt doped γFe_2O_3.

Slonczewski[33,34,35] derived the free energy F_c

$$F_c = -\tfrac{1}{4}kTN \sum_c \ln \cosh \left(\frac{3\alpha\lambda \cos\theta i}{2kT} \right)$$

and by using the phenomenological expression,

$$F_c = K_1 (\alpha_1^2 \alpha_2^2 + \alpha_2^2 \alpha_3^2 + \alpha_3^2 \alpha_1^2) + K_2 (\alpha_1^2 \alpha_2^2 \alpha_3^2)$$

the expression for the anisotropy due to the cobalt ions,

$$\Delta K_1 = kTN \quad 4 \ln \cosh \left(\frac{\sqrt{3}\alpha\lambda}{2kT} \right) - 2 \ln \cosh \left(\frac{3\alpha\lambda}{\sqrt{6}kT} \right)$$

was obtained, where k is Boltzmann's constant, T the absolute temperature, N the number of cobalt ions per c.c., θ_i is the angle between the magnetization vector and the trigonal axis, α is the ratio of the true angular momentum along (111) to that of the triply degenerate P state and λ is the spin orbit coupling constant. However the first equation for F_C cannot be written accurately in the form of the second equation for F_C except at high temperatures. There are two variable parameters $|\alpha\lambda|$ and $\mu_B H_e$, the exchange energy.

Trigonal symmetry is necessary for application of the theory, this was accounted for in magnetite by the rapid exchange between Fe^{2+} and Fe^{3+} ions. In nickel ferrite and cobalt ferrite half of the ions on the B sites are not Fe^{3+} so an extra term must be included for the non-symmetric crystal field due to these ions. Manganese ferrite is partially inverse, so about 10% of the B site ions are Mn^{2+}, but reasonable agreement is obtained (over a small temperature range however, 170 - 290° K) assuming a completely trigonal crystal field. In cobalt doped γFe_2O_3 17% of the B site ions are vacancies or 25% are hydrogen either of which would contribute to a non-symmetric

field at the cobalt ion. Thus it would be expected that a small extra term should be included to account for this.

Tachiki[32] introduced two different types of site for cobalt ions in cobalt ferrite each with an off diagonal matrix element a of the lower symmetry crystalline field. Again the conversion to the phenomenological K is not valid at low temperatures unless $\frac{a}{|\alpha\lambda|}$ is small. There are five variable parameters in this case.

Miyamoto et al[30] included only one type of site and only one a value and obtained good agreement with experiment for cobalt doped nickel ferrite using two unknown parameters and assuming $\mu_B H_e$ was infinite. The equation for the contribution to the anisotropy constant due to cobalt ions was then

$$\Delta K_1 = 2NkT \left(2 \ln \cosh \frac{3|\alpha\lambda|}{2kT}\sqrt{1/3 + r^2} \right) - \ln \cosh \left(\frac{3|\alpha\lambda|}{2kT}\sqrt{2/3 + r^2} \right)$$

$$- \ln \cosh \left(\frac{3|\alpha\lambda|}{2kT} r \right)$$

where r is $\frac{2a}{3|\alpha\lambda|}$. The details of the parameters is included in Table VIII.

To apply this theory to γFe_2O_3 two assumptions must be made. Firstly single domain particles reversing coherently are necessary so that

$$Hc = \frac{0.64K}{M}$$

however it was assumed here that Hc was only proportional to $\frac{K}{M}$

TABLE VIII

ONE ION MODEL

| Material | Temperature Range Used | Parameters for 2 Types of Site | | | Spin Orbit Parameter (cm^{-1}) $(\alpha \lambda)$ | Exchange Parameter $\mu_B H_e (cm^{-1})$ | Reference |
		(a_1) (cm^{-1})	(a_2) (cm^{-1})	$\frac{Na_1}{Na_2}$ *			
Fe_3O_4	$100^\circ K$-$350^\circ K$	0	0	-	132	(or 320[†])	33,34
$CoFe_2O_4$	$0^\circ K$-$350^\circ K$	140	$3(a_1)$	0.67	132	270	32
$CoFe_2O_4$	$0^\circ K$-$350^\circ K$	145		0.89	132	320	32
$MnFe_2O_4$	$170^\circ K$-$290^\circ K$	0	0	-	132	87	35
$MnFe_2O_4$	$0^\circ K$-$450^\circ K$	-	-	-	270	125	39[†]
$NiFe_2O_4$	$80^\circ K$-$300^\circ K$	102	0	-	97		30

* $\frac{Na_1}{Na_2}$ is the ratio of the number of ions in site 1 to those in site 2.

† These results were calculated from magnetostriction experiments.

where H_c is the coercive force and M the magnetic moment.
Secondly the majority of the cobalt ions must go into the
B sites and preferably though not necessarily into the va-
cancies or hydrogen sites to increase trigonal symmetry.
As the ions are similar to those in magnetite the parameters
for magnetite were used for preliminary guesses. The mag-
netic moment at room temperature was taken as 70 emu/gm
and the temperature variation of the moment was that in
Reference 15. A multiplying factor B was used so that the
coercive force was assumed only proportional to the aniso-
tropy constant. The data obtained from a least square fit
to the theory is shown in Table IX and Figure 18. If the
anisotropy of pure γFe_2O_3 was subtracted or added (due to
K being negative), there was very little difference in the
final results as it amounts to less than 1% of the aniso-
tropy. A multiplying factor of 3.24, that is

$$H_c = \frac{0.64 \ K}{3.24 \ M} = 0.2 \frac{K}{M}$$

was required to fit the data. In this case the same para-
meters as for magnetite can be used to 77° K (Figure 18)
however the theory does not hold below 77° K. By using an
extra term to include the non symmetric crystal field, good

TABLE IX

APPLICATION OF ONE ION MODEL TO GAMMA FERRIC OXIDE

Fixed Parameters	Parameters Calculated By Iteration	Initial Values	Final Values	Temperature Range ^{O}K
$\|\alpha\lambda\| = 132 \text{ cm}^{-1}$ $\mu_B H_e = \infty$	B^{*}	3.5	3.24	77 - 400
$\mu_B H_e = \infty$ $B = 3.5$	$\|\alpha\lambda\|$	132 cm^{-1}	97 cm^{-1}	4.2 - 400
$\mu_B H_e = \infty$ $\|\alpha\lambda\| = 132 \text{ cm}^{-1}$	B	3.5	1.9	4.2 - 400
$\|\alpha\lambda\| = 132 \text{ cm}^{-1}$ $B = 3.5$	$\mu_B H_e$	320 cm^{-1}	diverges	77 - 400
$\mu_B H_e = \infty$ $B = 3.5$	$\|\alpha\lambda\|$	132 cm^{-1}	129	77 - 400
$\mu_B H_e = \infty$ $B = 3.24$ $\|\alpha\lambda\| = 132$	$r = \dfrac{2a}{3\|\alpha\lambda\|}$	0.7	0.258	4.2 - 400
$\mu_B H_e = \infty$ $B = 3.24$ $r = 0.258$	$\|\alpha\lambda\|$	132 cm^{-1}	134.56	4.2 - 400

$*$ $H_c = \dfrac{0.64 \ K}{BM}$

very poor agreement

FIGURE 18

The one ion model for 1 mole % Co. The dotted line is the
one ion model for $|\alpha \lambda| = 132$ cm^{-1}, $\mu_B H_e = \infty$, B = 3.24 and
r = 0. The solid line is the one ion model for $|\alpha \lambda| = 134$ cm^{-1},
$\mu_B H_e = $, B = 3.24 and r = 0.26. The anisotropy of pure
γFe_2O_3 is assumed negative and that of the cobalt doped
sample positive.
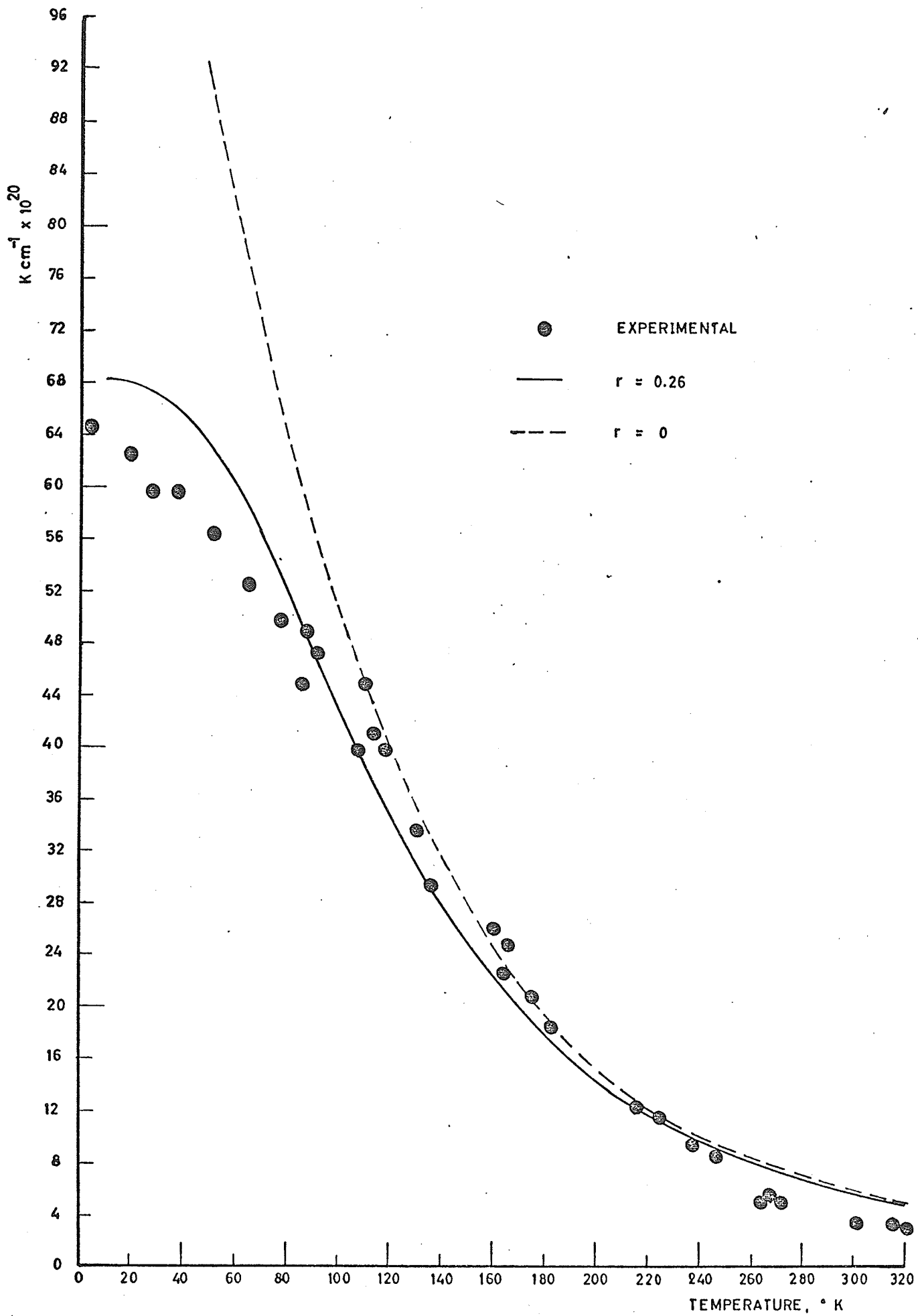
agreement could be obtained when a was set equal to 51.5 cm^{-1}.

Thus the coercive force temperature curve may be well approximated by

$$H_c = 1.62 \times 10^6 \frac{m}{M} T \left[2 \ln \cosh \left(\frac{182}{T}\right) - \ln \cosh \left(\frac{248}{T}\right) - \ln \cosh \left(\frac{744}{T}\right) \right]$$

where m is the mole % cobalt.

However no quantitative agreement can really be justified in that the coercive force was measured and not the aniso-tropy constant, and the factor of 3.24 was arbitrary, cal-culated from using the same $|M|$ and $\mu_B H_e$ as magnetite. Never-theless the qualitative temperature dependence holds, and the factor for the unsymmetric field is much smaller than that used for a completely inverse structure. The Curie temperature and the ions in the material are very similar to those in magnetite so the qualitative application at least can be justified.

Conclusions on Coercive Force Models

As the coercive force was found proportional to co-balt doping, at least qualitatively, (and quantitatively if the coercive force was considered proportional to the anistropy constant) the one ion theory of Slonczewski and

Tachiki holds, with logically consistent values of the
parameters, the particles are probably single domain, re-
versing coherently, and the anisotropy is probably all
crystalline and due to the single cobalt ion. Also as the
temperature dependence of samples 9 and 10 was like that
of the other samples it would appear that their anisotropy
is due to the same single ion. To account for the lack
of linearity, some cobalt ions may not be in the lattice
or if so not in the B sites. Clusters of interstitial ions
or inhomogeneities would also account for the blurred X-ray
pictures. Thus non-uniform magnetization and pinning by
clusters of cobalt cannot be eliminated, as the distribu-
tions of ions may not be that ideally required for the one
ion model and the ratio of the remanence to the saturation
moment is slightly more than 0.87 at very low temperatures.

E. MEASUREMENTS ON
PARTIALLY ALIGNED PARTICLES

Experimental

The samples were mixed with paraffin and placed in
sample holders in the furnace arrangement for the vibrating
sample magnetometer. They were heated to $150^{\circ}C$ for one hour

and cooled in a field of 14kOe for one hour, until room temperature was reached. The heating and cooling rates were constant for all samples. The magnetization curves in the alignment direction and perpendicular to it were measured, and the remanence and coercive force were measured as a function of the angle from the alignment direction. Narrow trenches were seen in the surface of the sample after alignment and it appeared that some paraffin had evaporated.

Results

The differences in remanence and coercive force before and after alignment, and parallel and perpendicular to the alignment direction are given in Table X and Figures 19, 20 and 21. The magnetization curves for sample 4 are shown in Figure 19 and the remanence as a function of angle for sample 8 is shown in Figure 21, the other samples gave very similar results.

There was no significant increase in coercive force after alignment and that which did occur may have been due to conversion, although there is a possibility of induced uniaxial anisotropy as occurs in many materials containing cobalt, this matter was not investigated further. The

TABLE X

COERCIVE FORCES AND RATIO OF REMANENCE TO SATURATION
MOMENT BEFORE AND AFTER ALIGNMENT (AT ROOM TEMPERATURE)

Sample Number	Mole % Cobalt	Coercive Force Initially (oe)	Coercive Force Finally (oe) 0°*	90°	$\frac{\text{Remanence}}{\text{Saturation}}$ Initially	$\frac{\text{Remanence}}{\text{Saturation}}$ finally 0°	90°
1	0	105	107	110	0.16	0.20	0.17
2	1	115	118	119	0.22	0.26	0.18
3	2.1	260	266	262	0.34	0.44	0.33
4	3.2	350	390	383	0.41	0.56	0.44
6	4.4	595	626	618	0.59	0.67	0.61
8	4.5	660	665	642	0.63	0.66	0.61

* Angle from alignment direction

FIGURE 19

The magnetization curves of aligned sample 4 parallel and
perpendicular to the alignment direction.

PARALLEL TO ALIGNMENT DIRECTION

PERPENDICULAR TO ALIGNMENT DIRECTION

APPLIED FIELD , kOe
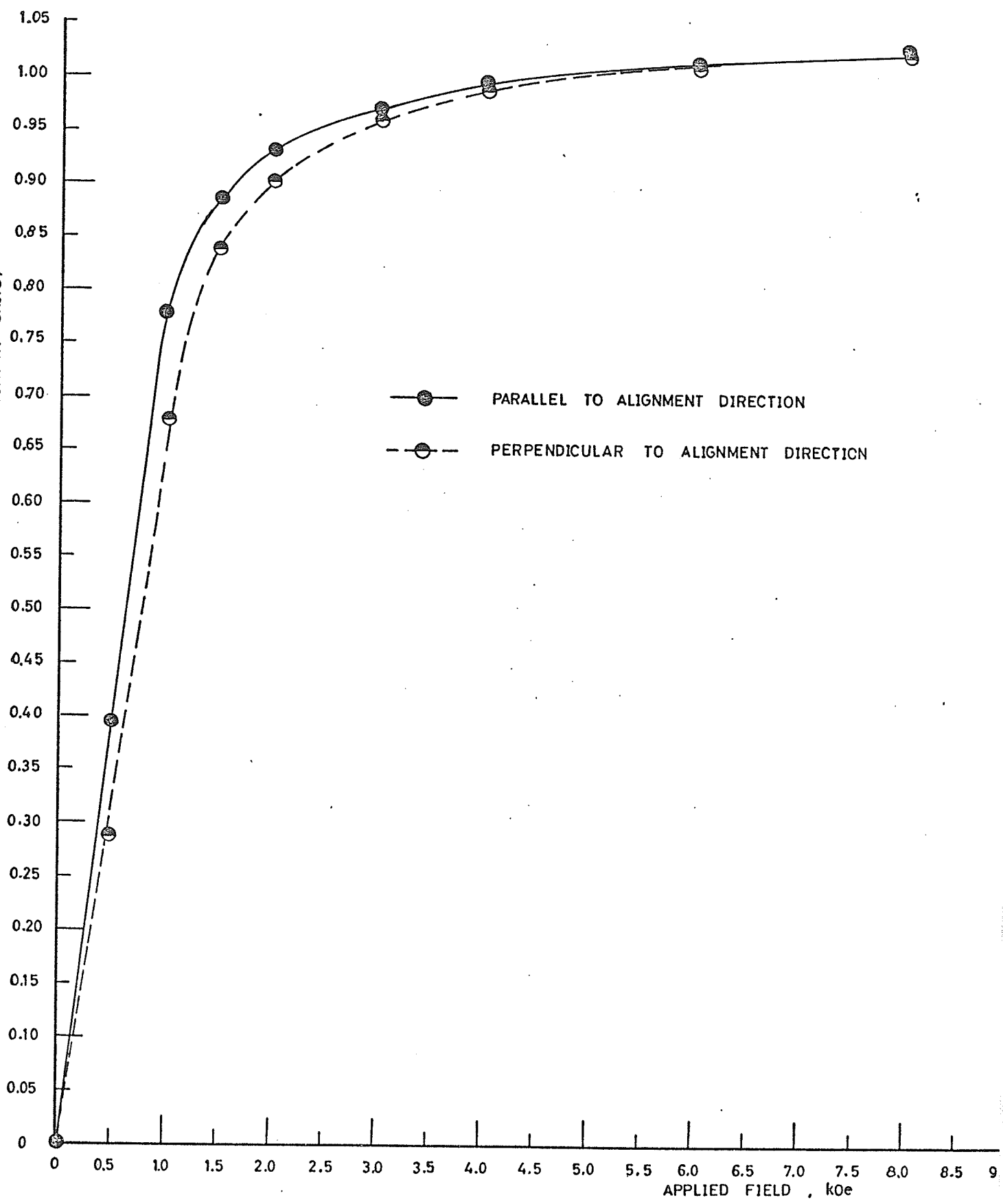
FIGURE 20

Relationship between coercive force and angle from the alignment direction, for samples 1, 2, 3, 4, 6, 8.
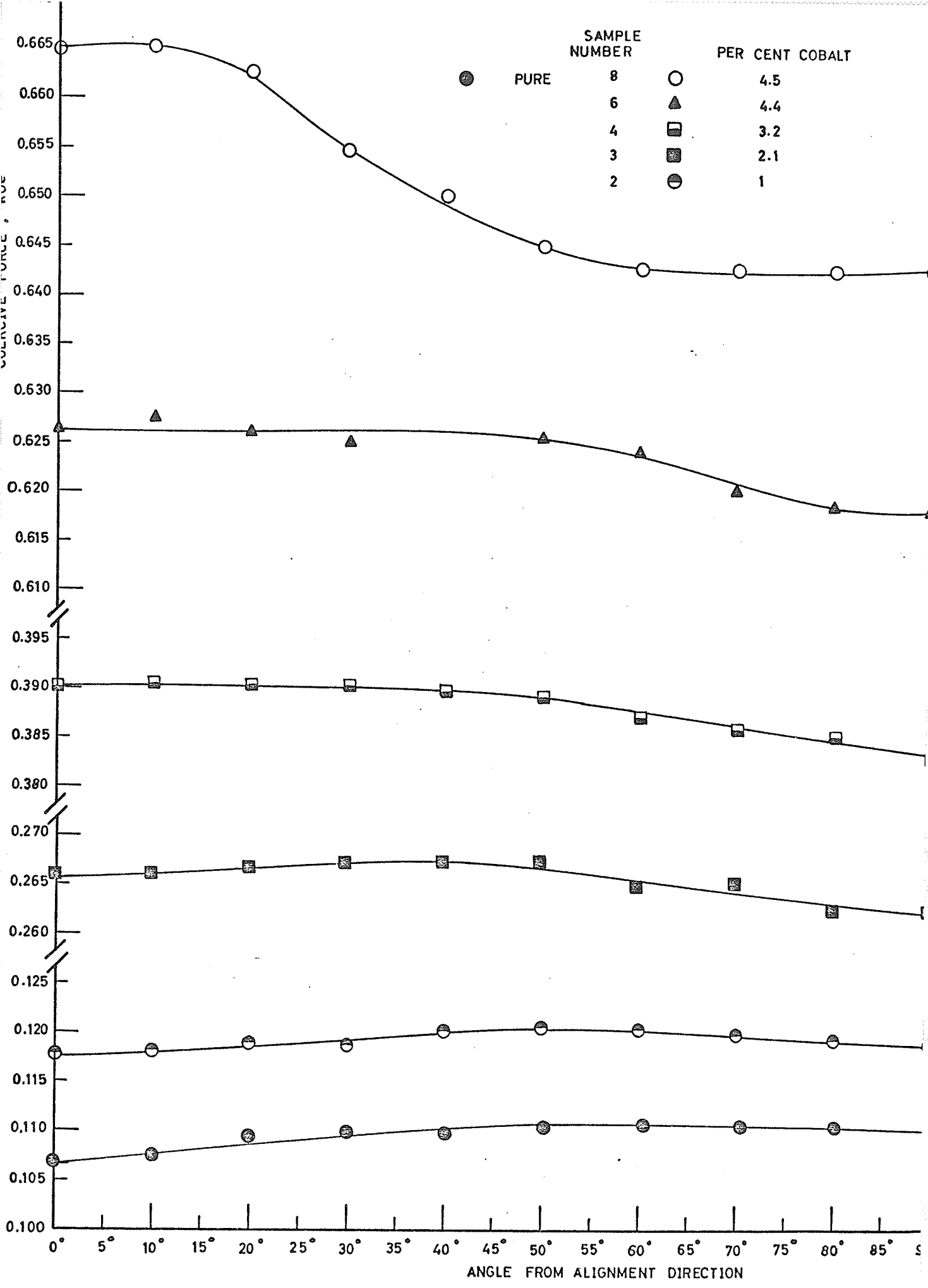
COERCIVE FORCE, OE (vertical axis)

ANGLE FROM ALIGNMENT DIRECTION (horizontal axis)

	SAMPLE NUMBER		PER CENT COBALT
PURE	8	○	4.5
	6	▲	4.4
	4	▱	3.2
	3	▨	2.1
	2	◓	1

FIGURE 21

The ratio of the remanence to saturation as a function
of the angle from the alignment direction, for sample 8.
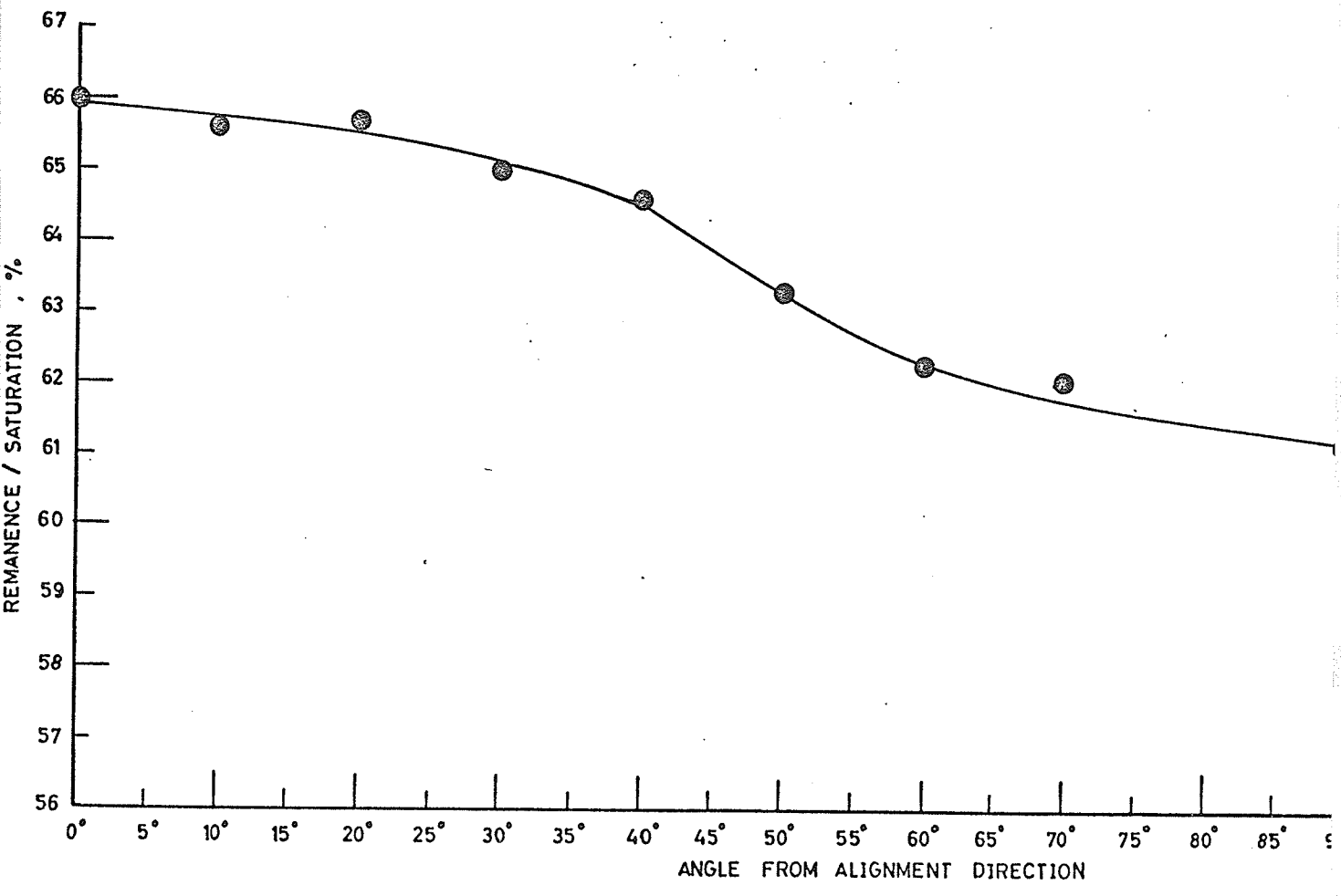
remanence to saturation ratio increased indicating that
alignment had taken place, however the values indicate
that the alignment was only partial as a ratio of unity
would be expected for complete alignment. There was very
little difference in the magnetization curves parallel
and perpendicular to the alignment direction, although
the cobalt doped samples displayed slightly greater dif-
ferences than did the pure sample.

Conclusions

Experiments similar to those described above were
carried out by Shur et al[42] and Ivanov et al[43] where the
transition from multidomain to single domain particles in
cobalt ferrite powders was examined. The increasing dif-
ficulty of the magnetization reversal process that occurs
when the size decreases is due to the increasing difficulty
of displacement of the domain boundaries and the growth
of magnetization reversal nuclei. As the angle from the
alignment direction increases the displacement of the 180°
boundaries becomes more and more difficult since the mag-
netic field component along the easy axis, causing displace-
ment, becomes weaker. If the coercive force perpendicular
to the alignment direction is less than that parallel to

it, the only explanation can be that the reversal is caused by rotation of the magnetization vector. For a uniaxial particle the coercive force would be zero perpendicular to the alignment axis[1], for cubic particles (such as γFe_2O_3) a decrease would be expected but not zero as the magnetization of the majority of the particles lies in the plane perpendicular to the alignment axis.

The boundary or domain wall energy density is the sum of that due to the crystalline anisotropy and exchange forces, and that due to the magnetostatic energy of the walls. Thus if the anisotropy constant increased and other factors remained the same the critical single domain size would increase. The data in Figure 20 shows a decrease in coercive force perpendicular to the alignment axis for all samples except sample 1 (pure) and 2 (1% Co). The decrease increased in magnitude for particles with a larger cobalt content. This is consistent with the pure γFe_2O_3 particles being mostly not single domain, and the 1% cobalt sample being mostly very nearly single domain and the others being completely single domain.

Another noticeable feature of Figure 20 is the maximum in coercive force that occurs between 0° and 90°. Much

work has been done[2,3] on incoherent reversals in elongated single domain particles for which a maximum occurs at 50°, and is accounted for by buckling, fanning or curling. Completely aligned single domain particles reversing coherently should show a decrease and no maximum in the coercive force when measured as a function of the angle. However it has been found[4] that partially aligned particles reversing coherently show maxima. It appears from Figure 20 that the maxima occur at different angles for different particles, most noticeable is the decrease in maximum angle from pure to 2 mole % cobalt. Wohlfarth[4] considered uniaxial partially aligned particles making angles θ in a cone along the alignment direction, where

$$\cos \theta = \frac{\text{remanence}}{\text{saturation moment}}$$

for uniaxial particles. The coercive force would then have a maximum value at angle θ from the alignment axis. For particles with cubic anisotropy a maximum at θ would also probably be expected. For these cobalt doped γFe_2O_3 particles the remanence to saturation ratio increases with cobalt content indicating a possible increase in degree of alignment. The corresponding decrease in the angle of

the maximum coercive force is observed. However a qualitative agreement does not hold.

Thus the results of experiments on partially aligned particles seem to indicate that most of the particles are single domain, and that reversals are coherent. The exceptions are the pure γFe_2O_3 and the 1 mole % cobalt doped samples which are almost single domain.

F. OTHER MAGNETIZATION MEASUREMENTS

Coercive Force as a Function of the Applied Field

Due to the large slope in the saturation magnetization curves, it was suspected that the samples may not have been saturated. To examine this point and for comparison with $SmCo_5$[36] the coercive force and remanence were measured as a function of the applied field at room temperature and 77° K. The results are shown in Figures 22, 23 and 24 and Table XI. Some hysteresis loops are shown in Figures 25 and 26, and the saturating field found from them is recorded in Table XII.

It was found that the coercive force came to a constant value at comparatively low fields; it became constant

FIGURE 22

The variation of remanence and coercive force with applied
field for sample 6 (4.5 mole % cobalt) at 77° K.
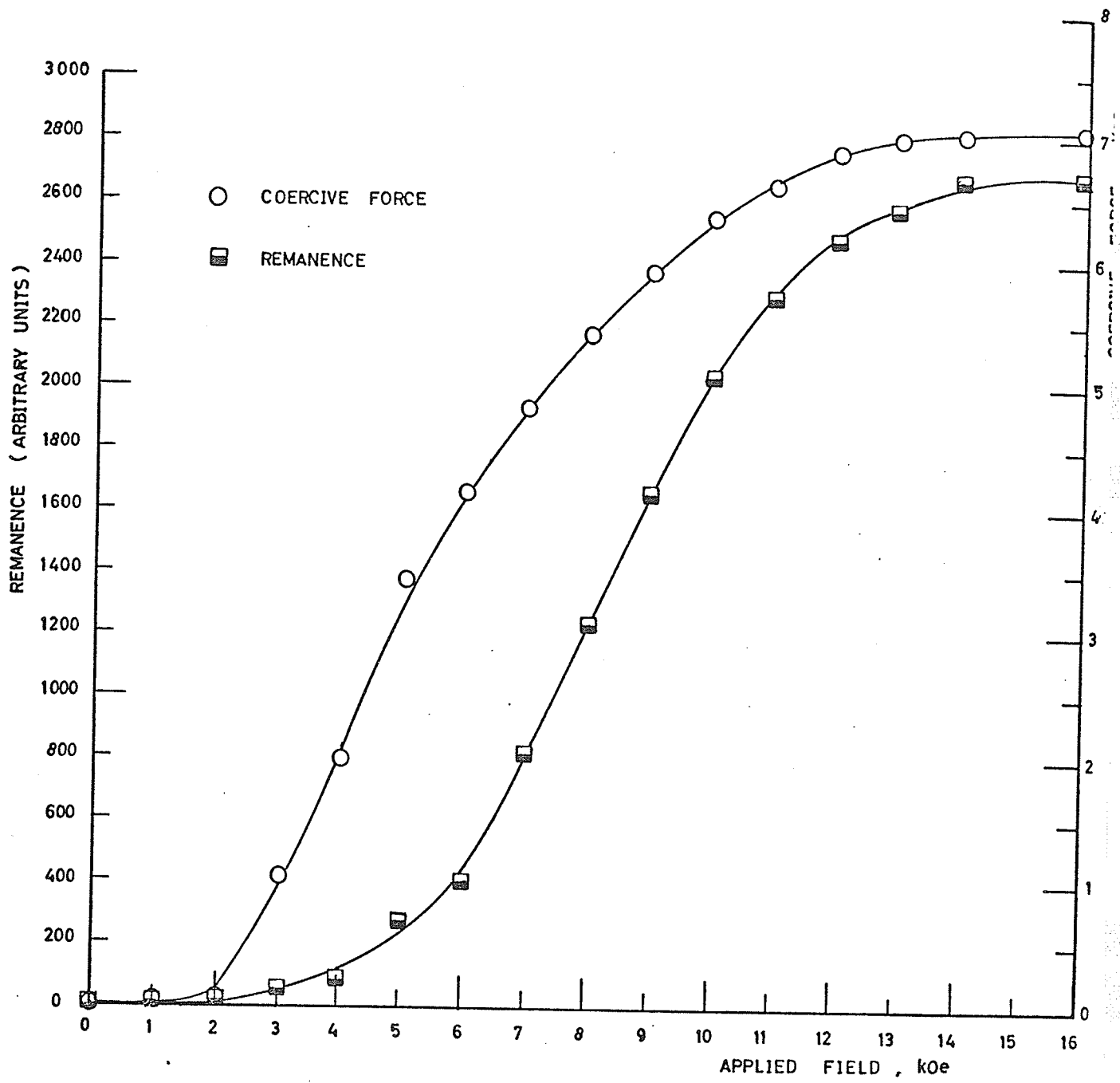
FIGURE 23

The variation of remanence and coercive force with applied
field for sample 6 (4.5 mole % cobalt) at room temperature.
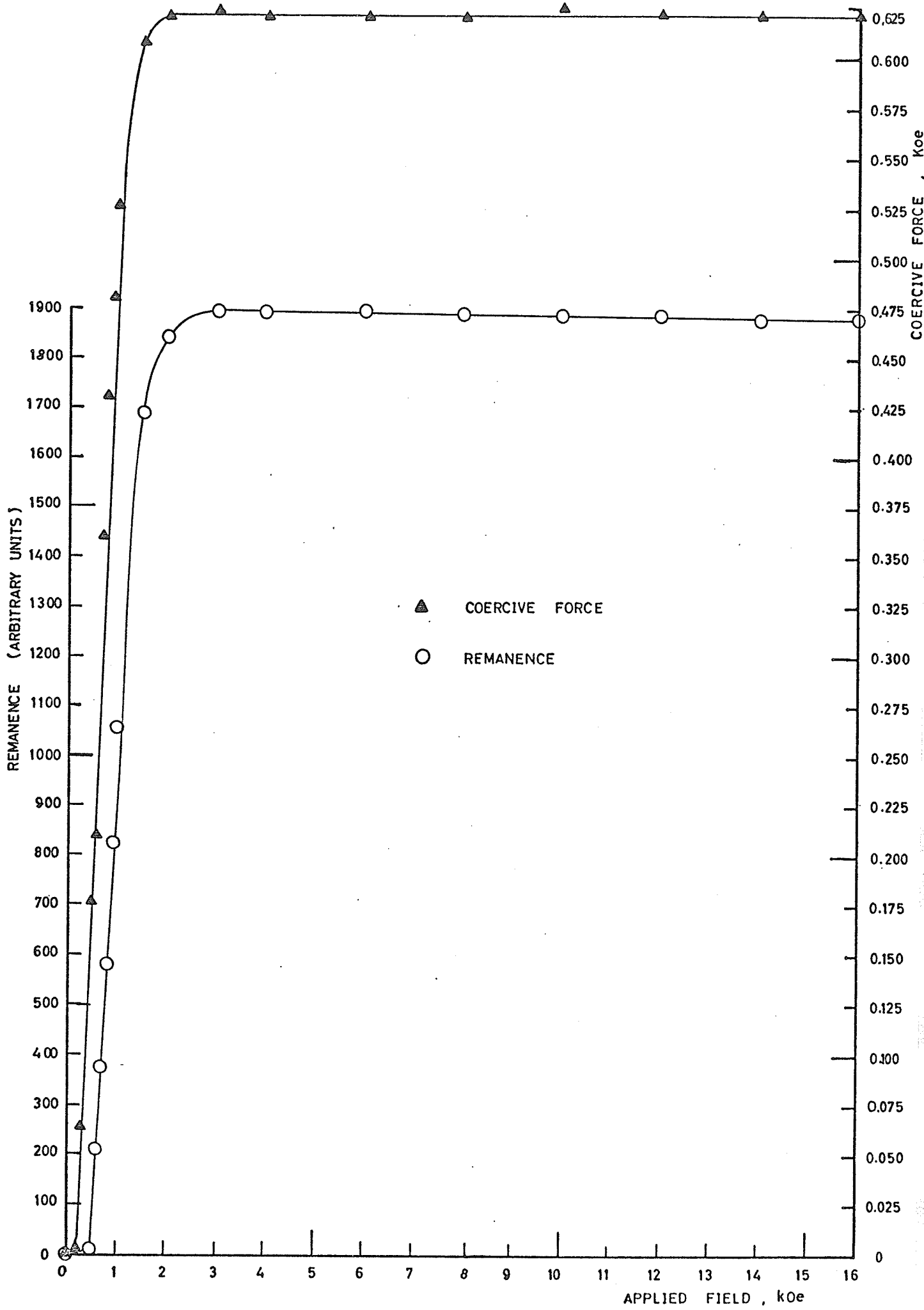
FIGURE 24

The variation of remanence and coercive force with applied field for sample 10 (9.9 mole % cobalt) at 77° K.
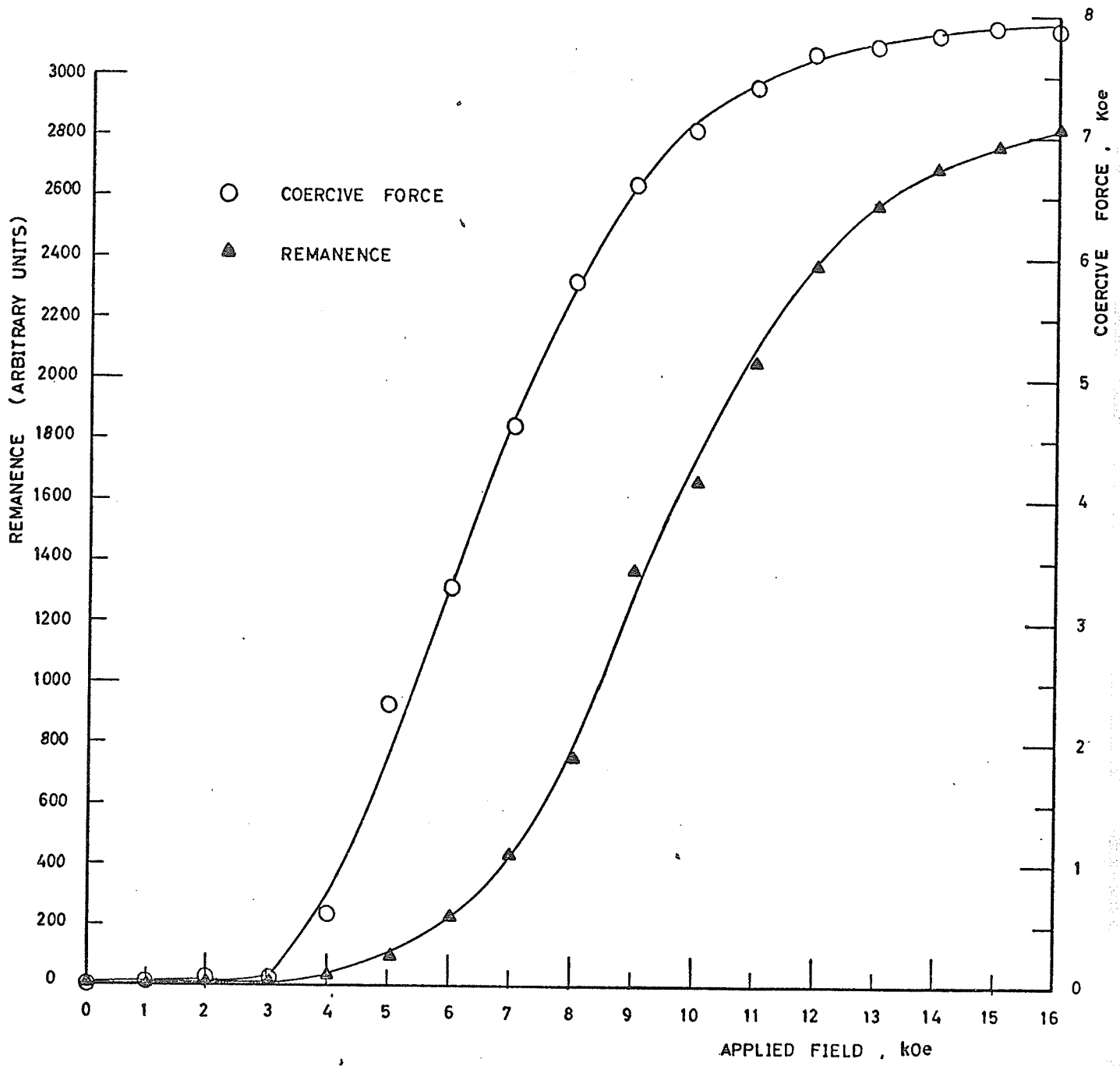
TABLE XI

COERCIVE FORCE AND REMANENCE AS A FUNCTION OF
APPLIED FIELD

Sample Number	Mole % Cobalt	Temperature	Field After Which the Coercive Force Became Constant (kOe)	Field After Which the Remanence Became Constant (kOe)
1	0	room temp.	0.9	0.8
1	0	77° K	2.0	2.0
6	4.4	room temp.	2.0	3.0
6	4.4	77° K	14.0	14.0
10	9.9	77° K	15.0	not constant at 16 kOe

FIGURE 25

Hysteresis loops at room temperature for samples 1 (pure) and 8 (4.5 mole % cobalt).
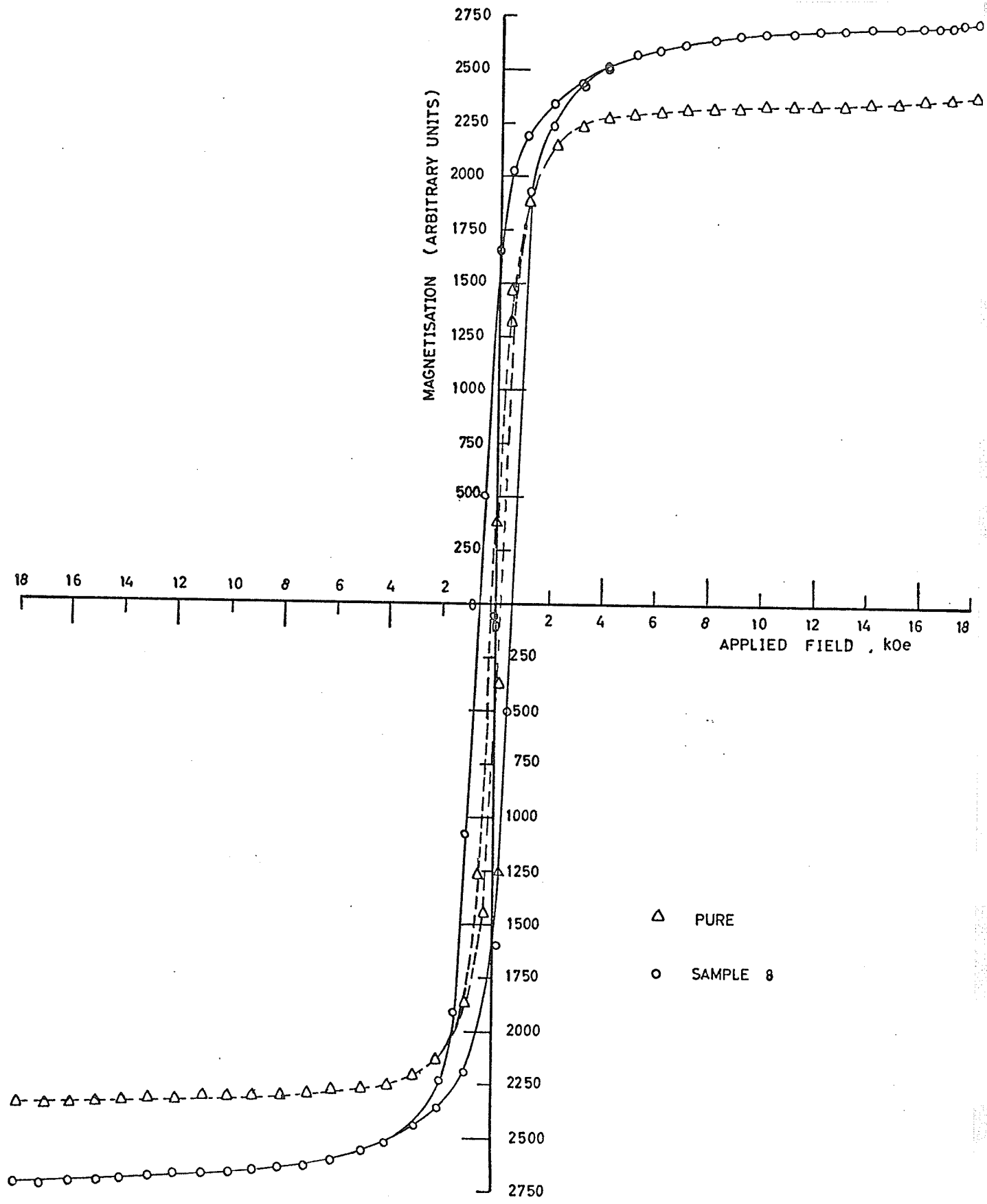
FIGURE 26

Hysteresis loops at 77° K for samples 8 (4.5 mole % cobalt) and 9 (5.8 mole % cobalt).
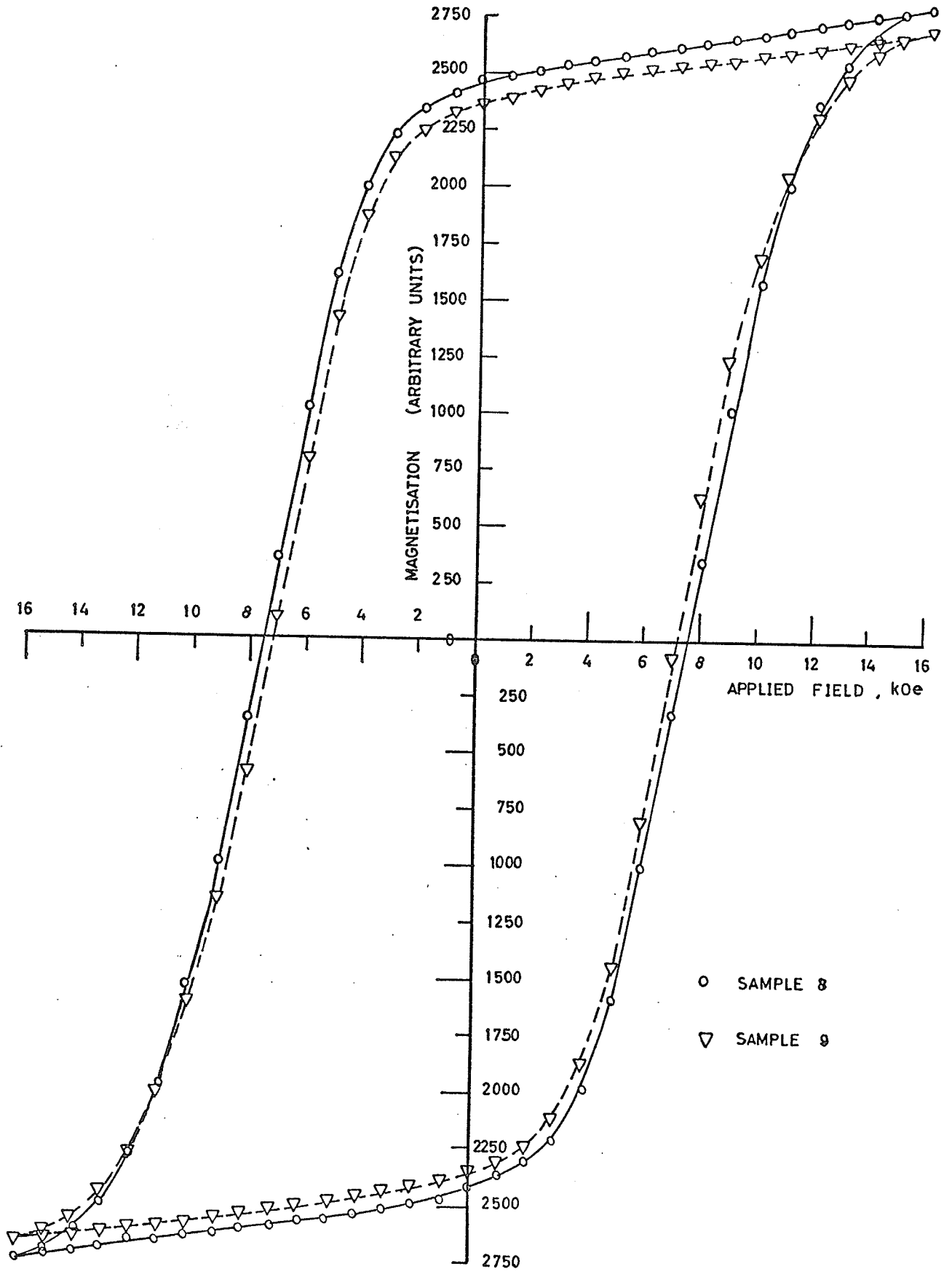
TABLE XII

SATURATION FIELDS

Sample Number	Mole % Cobalt	Field at Which Magnetization and Demagnetization Curves Coincide (kOe)	Temperature
1	0	2	room temp.
8	4.5	5	room temp.
8	4.5	16	77° K
10	9.9	16	77° K

at about 2 Hc for samples 10 (10 mole % cobalt) and 6
(4.5 mole % cobalt) at 77° K and about 3Hc for sample
6 at room temperature. However pure γFe_2O_3 required a
field of about 10 Hc to bring the coercive force to a
constant value. The differences in the coercive forces
measured after cooling a sample in a field or saturating
it at the low temperature were examined. There was no
difference except for sample 10 at 77° K, so this sample
was cooled in a field for all measurements down to 4.2° K.

Ratio of Remanence to Saturation Moments

Theoretically the ratio of remanence to saturation
moment is 0.8 for single domain particles reversing co-
herently. This ratio was measured for all samples between
4.2° K and 300° K, and for one sample (4.5 mole % cobalt)
to about 600° K. The results are shown in Figures 27, 28
and 29. The ratio for the pure sample displayed an almost
linear relationship with temperature, with values from 0.12
to 0.26. The remanence to saturation ratio for the 1%
cobalt doped sample increased from 0.1 at room temperature
to 0.8 at 4.2° K. The ratio for the other samples increased
from about 0.4 at room temperature to above 0.95 at and be-
low 77° K. The ratio found by using the saturation moment

FIGURE 27

Ratio of remanence to saturation of all samples as a function of temperature, below room temperature.
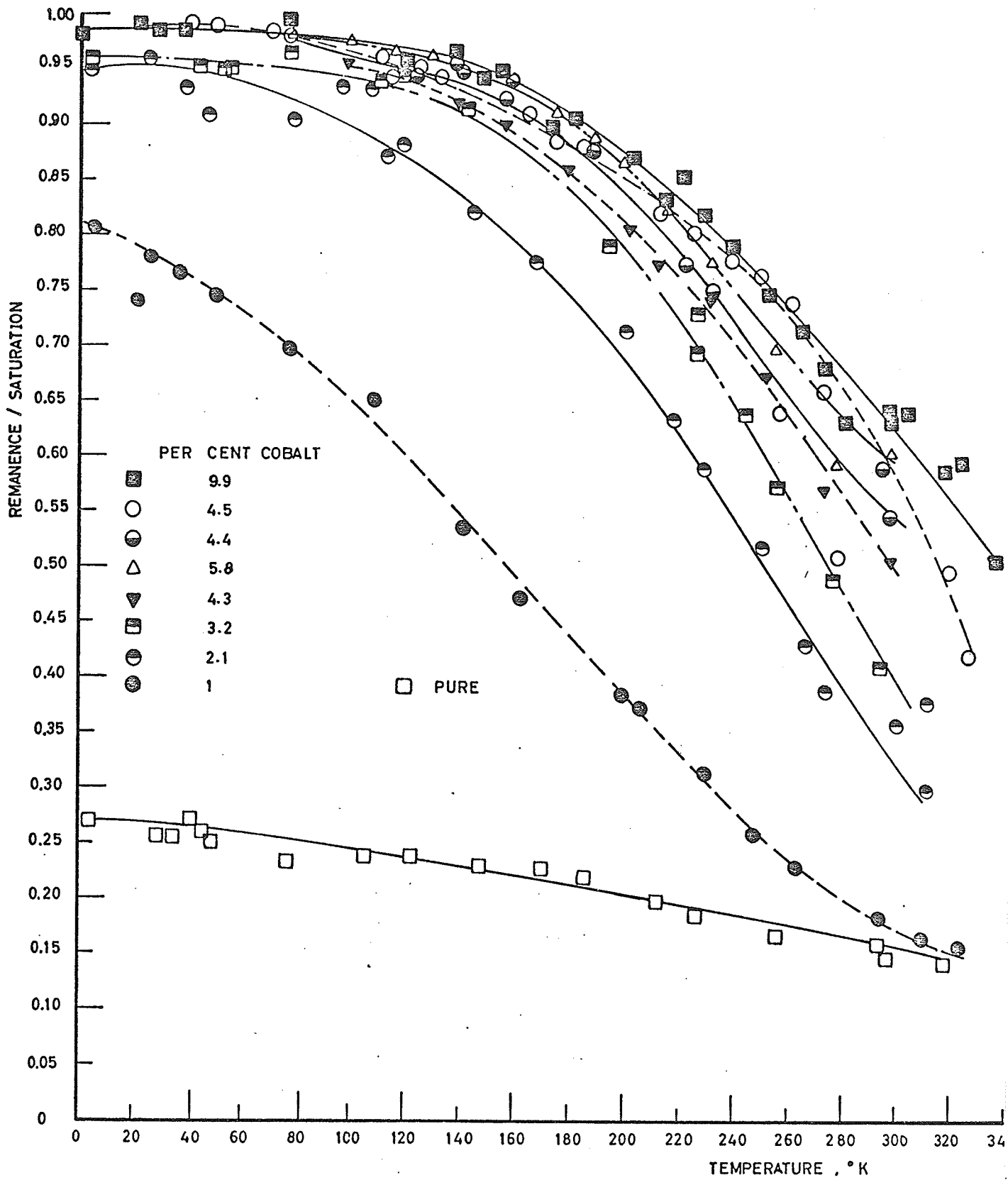
FIGURE 28

Ratio of remanence to saturation of sample 8 ($4\frac{1}{2}$ mole % cobalt) above room temperature as a function of temperature.
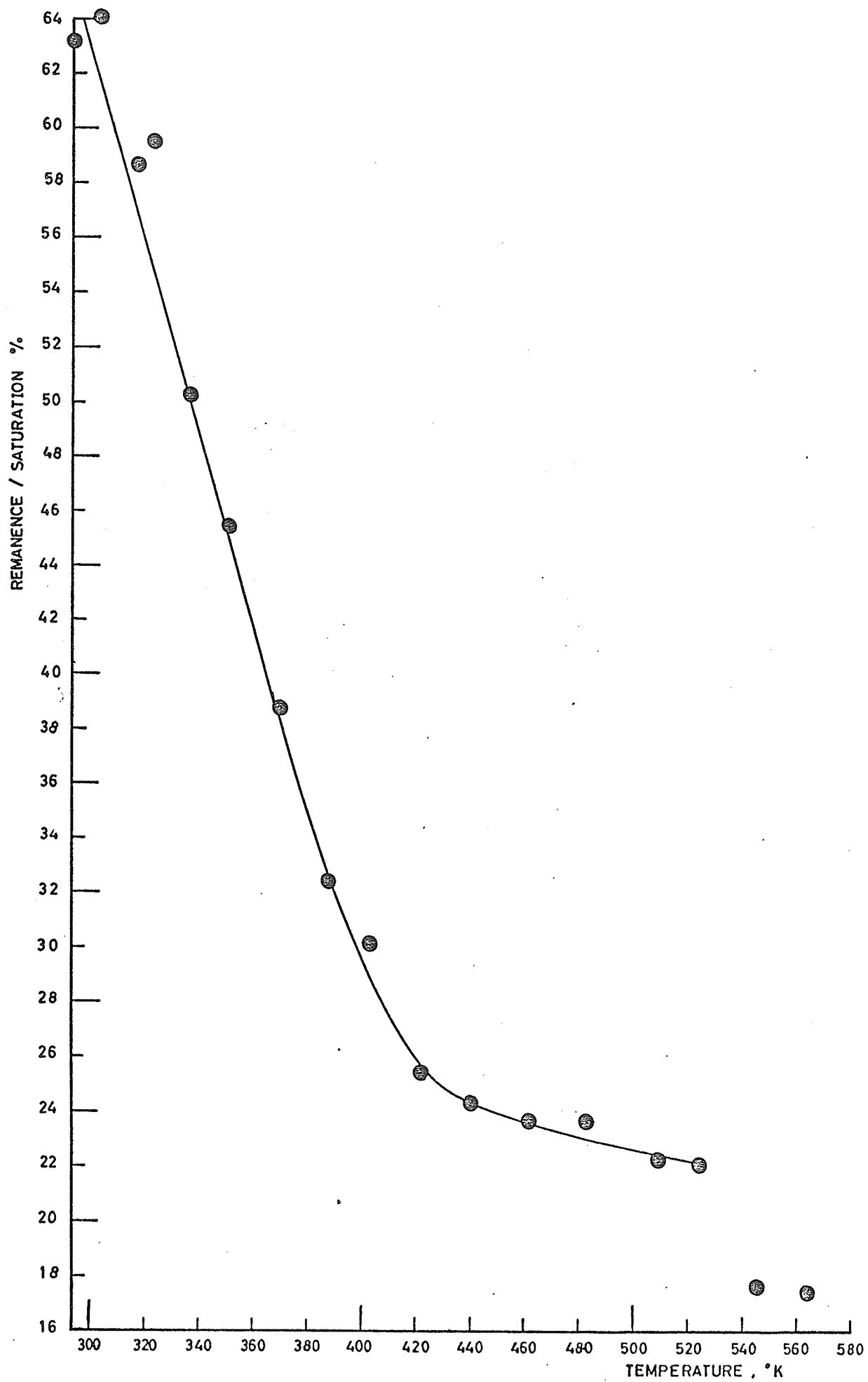
FIGURE 29

Comparison of the ratio of remanence to saturation moment
for sample 8 as a function of temperature as the applied
field H is extrapolated to zero and to infinity.
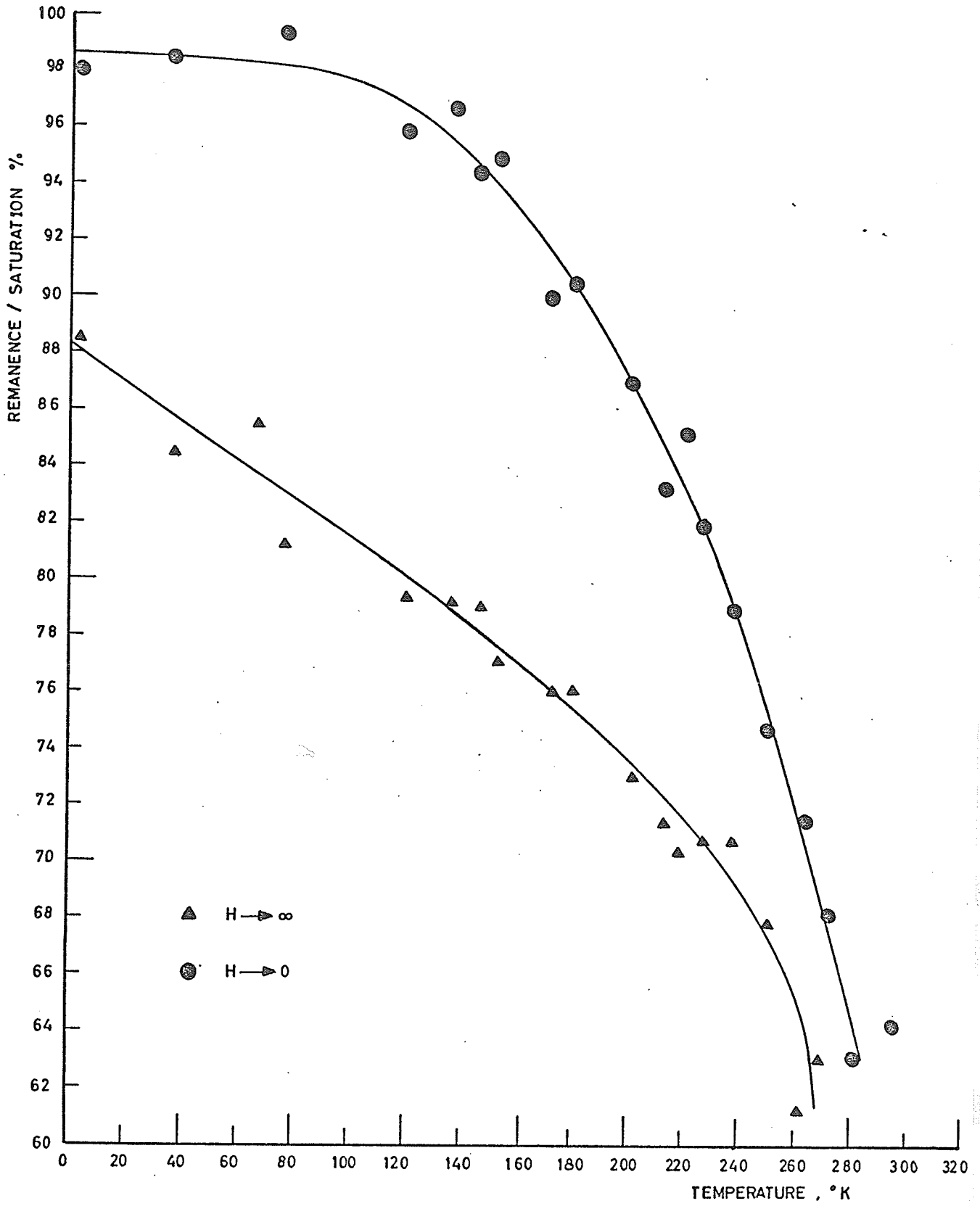
when the applied field is extrapolated to infinity is shown in Figure 29 and the increase is from 0.6 to a maximum of 0.88 for $4\frac{1}{2}$ mole % cobalt. The ratios in Figure 27 and Figure 28 were found by extrapolating the applied field to zero.

Wohlfarth[47] gives the ratio as 0.831 for random particles with cubic symmetry if the anisotropy constant is positive and 0.866 if the anisotropy constant is negative. If the material was not saturated the saturation moment found by extrapolation to zero applied field would be less than the actual saturation moment resulting in an increased remanence to saturation ratio. Also if there were clusters of cobalt and a non-uniform magnetization reversal mode the remanence to saturation ratio would be large.

However the results suggested that most particles are single domain reversing coherently and that the material is unsaturated at low temperatures.

G. CONCLUSIONS ON
    MAGNETIZATION MEASUREMENTS

The moment measurements indicated that the moment
was approximately constant with cobalt doping. The data
could not be fitted by considering the change in moment
caused by cobalt ions in only one type of site. The pos-
sibility that varying amounts of hydrogen were in the
lattice would account for the apparent randomness of the
moments. The coercive force data may be fitted with
Slonczewski's one ion model if a multiplying factor is
included, with logical values of the parameters. A good
linear relationship existed between the cobalt doping
and the anisotropy, which seems to indicate that the co-
balt goes in the same way for all samples, or if the one
ion model holds, the amount of cobalt that goes into the
B sites is proportional to the total amount of cobalt with
the same proportionality constant for each sample. Meas-
urements on aligned particles showed that most samples
were single domain and the reversals were coherent. The
ratio of the remanence to saturation moments possibly in-
dicate single domain particles reversing coherently with
a lack of saturation at low temperatures.

CHAPTER IV

CONVERSION

A. EXPERIMENTAL METHODS

A detailed study of conversion was not carried out but some experiments were done to examine the effect of heating on the properties of cobalt doped gamma ferric oxide. The samples were heated for various times, from 30 minutes to 10 days and at different temperatures, from $300^{\circ}C$ to $1200^{\circ}C$. Some were cooled slowly in the furnace and others were cooled quickly outside the furnace.

X-Ray Analysis

X-ray diffraction patterns of the heated products were of two types; for lower temperatures and shorter heating times they showed the γ structure (including the superstructure lines if they were present before heating) and for higher temperatures they showed the α structure with extra lines. The extra lines were always present indicating that total conversion to αFe_2O_3 cannot take place when there is cobalt in the lattice. The intensities of the extra lines increased with cobalt doping. The lattice parameter of the αFe_2O_3 lines were found to be the

same as pure αFe_2O_3 within experimental error. The extra

lines were found to correspond to the most intense lines

of either Fe_3O_4, γFe_2O_3 or $CoFe_2O_4$. Using these materials

to index, lines were found with (523), (642), (553, 731),

(800) and (555, 751) as the (hkl) values. The lattice para-

meter of the extra lines was found to be 8.40 ± 0.02 (Table

XII) which most nearly corresponds to Fe_3O_4 whose lattice

parameter is 8.39. The lattice parameters of γFe_2O_3 and

$CoFe_2O_4$ are 8.33. Also from the data it appears that the

lattice parameter is independent of the original doping and

the heat treatment, however the difference in lattice para-

meter between the pure and 10 mole % cobalt doped samples

was only 0.02 which is the experimental error in this case.

The experimental error is greater as no very high angles

were observed. To investigate the possibility of magne-

tite being present a Mössbauer spectrum at room tempera-

ture was taken. The spectrum consisted of broadened αFe_2O_3

lines and no evidence of Fe^{2+} or the characteristic $Fe^{2+}/3+$

line was present. From this result, and from the tempera-

ture dependence of the coercive force which showed no

anomaly at low temperatures, it would appear that no mag-

netite was present. As it has been shown that cobalt in

γFe_2O_3 increases the lattice parameter, it is probable that

additional phase is highly doped γFe_2O_3.

TABLE XIII

LATTICE PARAMETERS OF EXTRA LINES OF HEATED
COBALT DOPED GAMMA FERRIC OXIDE

Sample Number	Mole % Cobalt	Heating Procedure		Lattice Parameter a ±0.02
7	4.5	575°C	10 days	8.41
7	4.5	1200°C	30 mins. very slow cooling	8.40
7	4.5	680°C	30 mins. cooled in air	8.40
9	5.8	900°C	2 hours cooled in air	8.40
10	9.9	900°C	20 hours cooled in air	8.40

Coercive Forces

The coercive force of sample 7 ($4\frac{1}{2}$ mole % cobalt)
heated for 30 minutes at different temperatures was meas-
ured. Because the heating time was short, the temperature
may not have been constant and despite grinding, the par-
ticles tended to stick together; both factors lead to
scatter in results. All samples changed colour on heating,
the lower the doping the more red they became (from an
initially brown powder). The sample heated to 1200°C was
black and solid, the other samples remained as powders.
The results are shown in Figure 30.

The coercive forces increased significantly with
heat treatment from 660 oe to 2250 oe after heating for
10 days at 575°C and 2150 oe after heating for 30 minutes
at 950°C. This also indicates that the coercive force
becomes constant after a certain amount of heating.

The temperature dependence of the coercive force
of the sample heated for 10 days at 575°C was measured to
compare it to that of cobalt doped γFe_2O_3 (Figure 31).
This figure serves only to indicate the approximate tem-
perature dependence because of possible lack of satura-
tion, especially at low temperatures. The samples were

FIGURE 30

Coercive forces of sample 7 at room temperature after heating at the indicated temperature for 30 minutes. γ denotes X ray diffraction patterns like γFe_2O_3, $\alpha + \gamma$ denotes X ray diffraction patterns like αFe_2O_3 with extra lines.
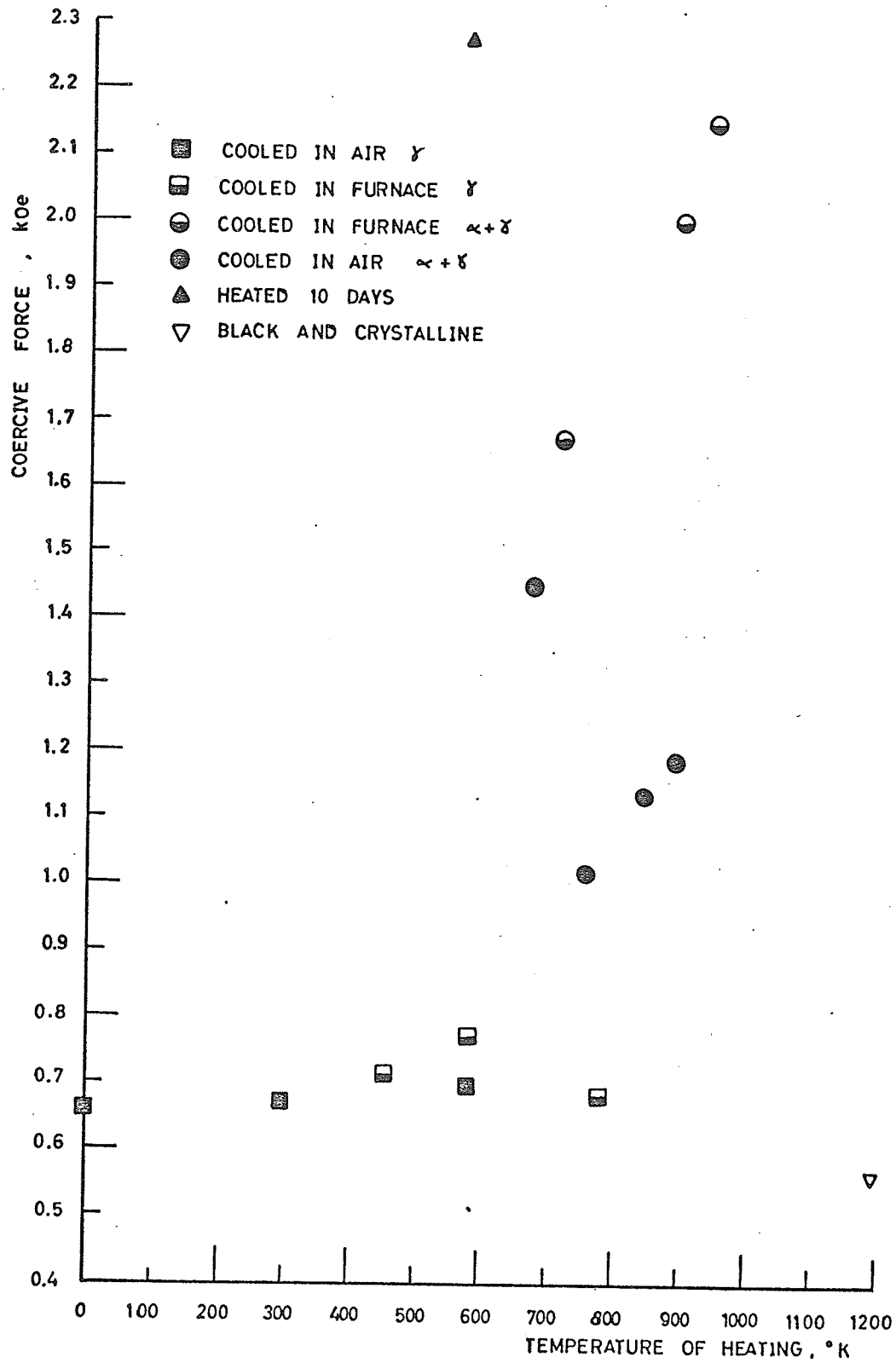
FIGURE 31

Variation of coercive force with temperature for sample 7 heated at 575ºC for 240 hours.
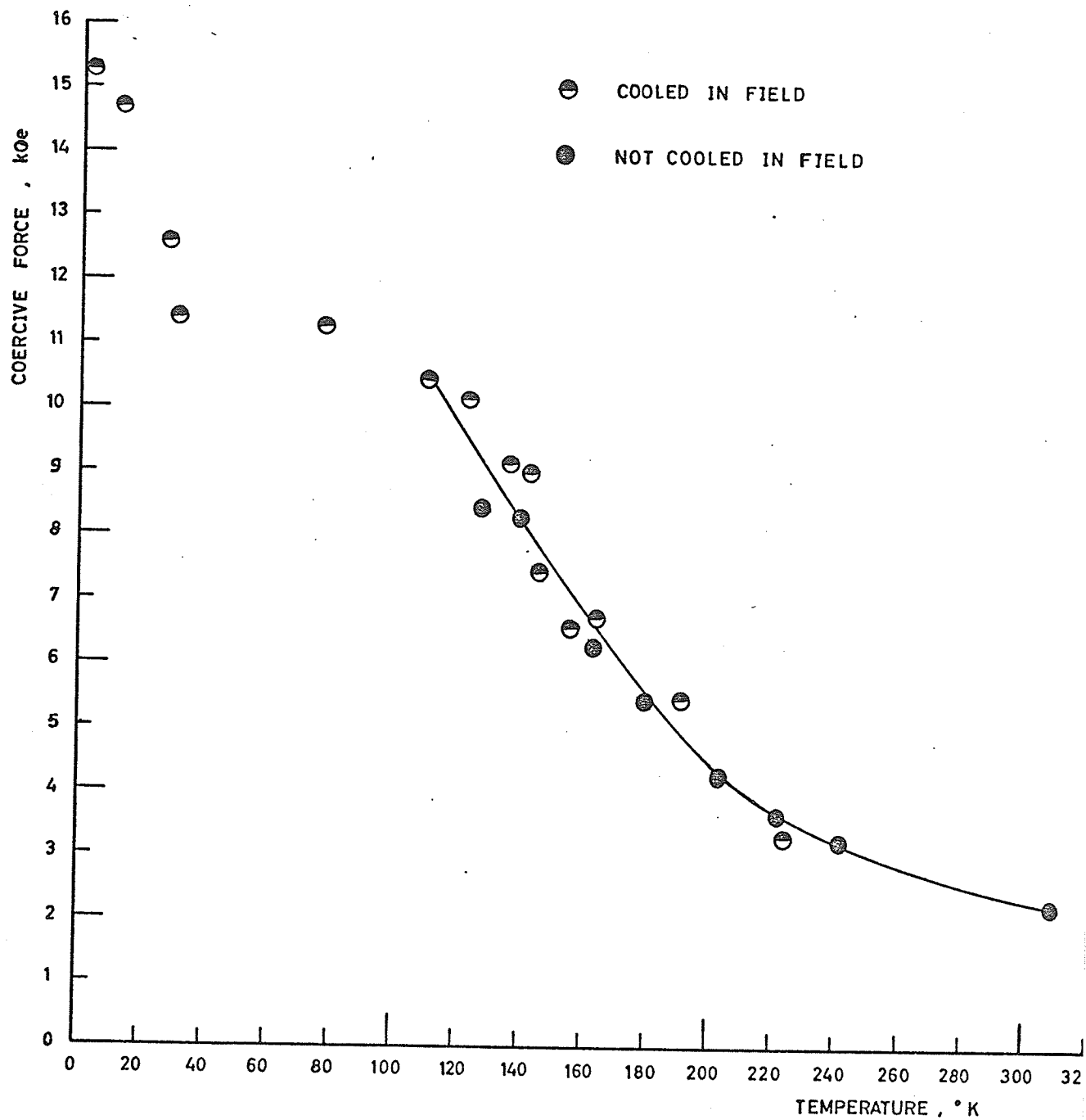
cooled in a field for most measurements as indicated on the graph. The coercive force reached 15.25 kOe at 4.2° K and 11.25 kOe at 77° K. The temperature dependence of the coercive force is less than that of cobalt doped γFe_2O_3 but more than that of cobalt ferrite.

The samples without superstructure lines gave a much smaller increase in coercive force on heating; the results are given in Table XIV.

Magnetic Moments

The magnetic moments of several heat treated samples were measured. Only small quantities of each were heated and the moments were small so the error was about 3%, the results are shown in Table XV. Despite the varying heat treatments the moment appears linear in cobalt doping (Figure 32). This indicates that if the same material is present for each sample (as would be expected from constant lattice parameters), the amount that is present, being proportional to the moment, is proportional to the amount of cobalt.

TABLE XIV

COERCIVE FORCES OF HEATED SAMPLES WITH INITIALLY
NO SUPERSTRUCTURE

Sample Number	Mole % Cobalt	Coercive Force Initially Room Temp. kOe	4.2°K kOe	Coercive Force Finally Room Temp. kOe	4.2°K kOe	Heat Treatment	
5	4.3	0.56	-	1.04	-	75 hrs	900°C
5	4.3	0.56	-	1.15	-	12½ hrs	950°C
9	5.8	0.69	8.75	0.80	9.96	20 hrs	950°C
10	9.9	0.92	9.94	0.80	10.03	15½ hrs	900°C

TABLE XV

MOMENTS OF HEAT TREATED SAMPLES

Sample Number	Mole % Cobalt	Heat Treatment		Moment emu/gm
5	4.3	575°C	240 hours	10.3
7	4.5	950°C	12½ hours	26.5
9	5.8	950°C	20 hours	15.6
10	9.9	900°C	15½ hours	26.5

FIGURE 32

Relationship between magnetic moment of heated samples and cobalt doping.
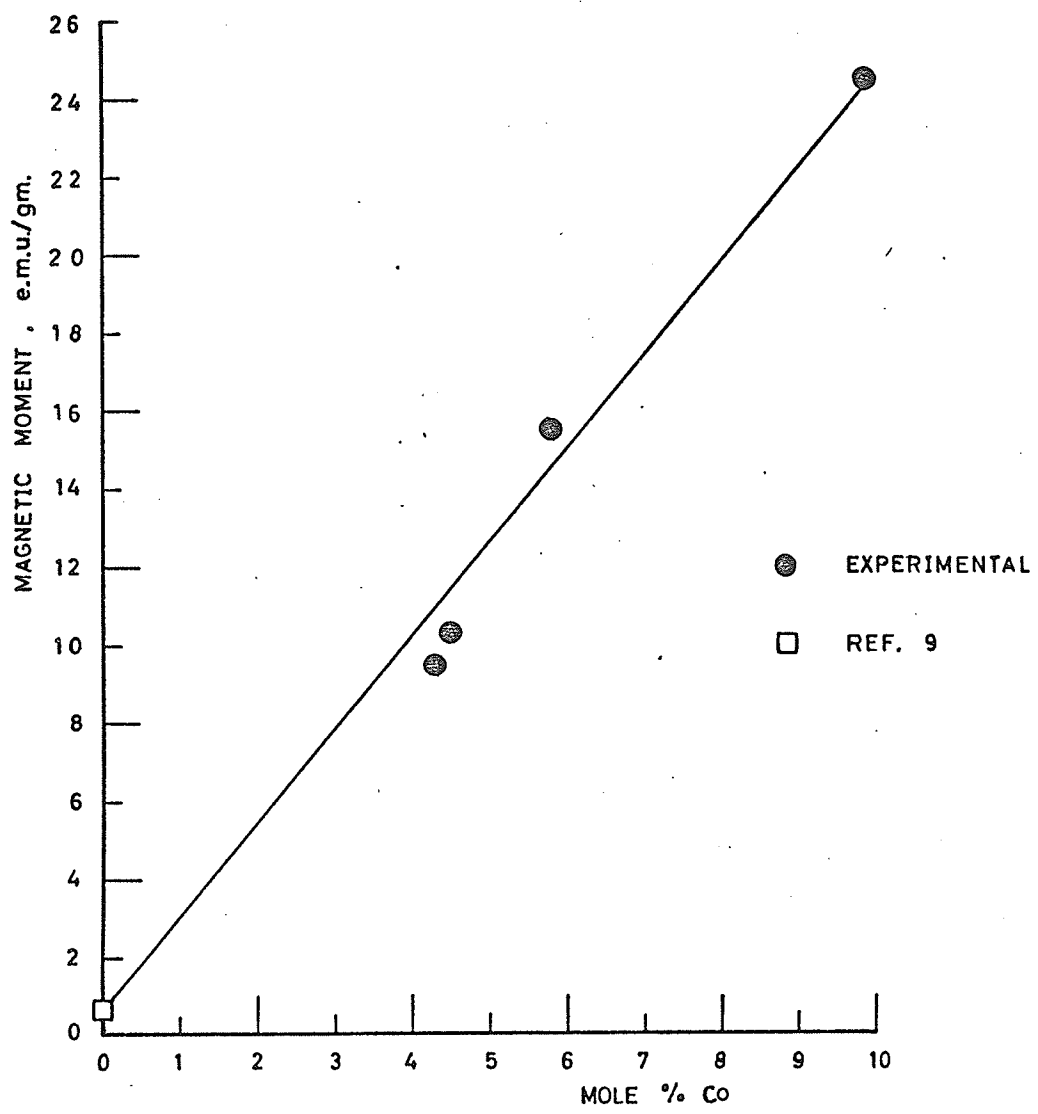
B. CONCLUSIONS ON CONVERSION EXPERIMENTS

The material with the αFe_2O_3 appears to be the same
for each sample, probably highly doped γFe_2O_3 or, γFe_2O_3
or cobalt ferrite with an increased lattice parameter due
to distortion. The quantity of this material appears to
be proportional to the cobalt doping of the original sample.
The linearity of the moments demonstrate that the non-
linearity before heating was due to a factor that dis-
appeared on heating, for example interstitial ions may
have moved into the lattice or hydrogen may have been driven
out. The anisotropy of the heated samples point to the
presence of extra forces that add an approximately tem-
perature independent term to the original anisotropy.
If one particle contained both α and γ phases, exchange
anisotropy between them could provide such an additional
term, also if small non-spherical regions were unconverted
there would be contributions from shape anisotropy. If
the original samples had a random distribution of dopings,
and those with sufficient cobalt did not convert the final
coercive force would be that of the most heavily doped par-
ticles. However the coercive force of a sample with $4\frac{1}{2}$
mole % cobalt exceeded that of a sample with 9.9 mole %
under approximately the same heat treatments, which is

not consistent with the latter model.

The lack of change in the sample 10 (9.9 mole % cobalt) coercive force, and the fact that the coercive force of sample 9 (5.8 mole % cobalt) approached that of sample 10 on heating, infers that sample 10 approaches the maximum doping for this type of doping. It is of interest to note that the percentage of vacancies to iron in Fe $(Fe_{5/3} \square_{1/3})O_4$ is 12% and that if all the vacancies were filled, conversion would be very difficult by Kachi's model. However if there were clusters of cobalt, there would be no conversion in some regions and also no change in coercive force, but the linearity of the moments does not confirm this.

Senno et al[26,27] found that partially converted γFe_2O_3 particles exhibited properties characteristic of exchange interaction between the ferrimagnetic and anti-ferromagnetic phases. They also found that below a critical value of the mole fraction of αFe_2O_3, γFe_2O_3 particles transformed directly into αFe_2O_3, but for mole fractions greater than this, individual particles existed in two phases. The critical mole fraction varied with size such that smaller particles tended to exist in two phases. The

size of the present particles is 800 - 900 A and for 1000A cubic particles the critical mole fraction was 0.65. The mole fractions of γFe_2O_3 in this case are 0.86 to 0.62 (calculated from the moments of converted samples). A direct comparison is perhaps not justifiable because of the greatly increased frequency factor[22] caused by cobalt doping, but if such a comparison was made it would indicate that most particles consisted of two phases.

Kachi et al[23] proposed a detailed model for the conversion from γFe_2O_3 to αFe_2O_3 by considering Iida's model[41] of the spinel, constructed by piling up two types of two dimensional trigonal lattices of cations between closely packed oxygen layers. The oxygen layers are re-stacked on heating by shifting every two layers with respect to the two below, and the metallic ions move co-operatively to form kagome lattices. These metallic two dimensional lattices then become the honeycomb lattice of αFe_2O_3 by cooperative migration of the ferric ions, due to the unsymmetric charge distribution around the regularly distributed vacancies. If the vacancies are not regular, twinning occurs which is eliminated on annealing. The final structure is represented by αFe_2O_3 separated

from γFe_2O_3 by a dislocation boundary region.

Thus if any cobalt went into a vacancy either no
conversion would take place or interstitial ions would be
present in the αFe_2O_3; cobalt in the B site iron positions
would not be expected to change the mechanism appreciably.
A possible model is proposed in which the cobalt ions are
trapped in the vacancies of the dislocation region and move
along with it by means of the remaining vacancies. Thus
all the cobalt ions may go to one part of the particle such
as the edges or the centre, in such a region all the vacan-
cies would be filled and no more conversion could take
place. Initial clusters of cobalt in the particle may pin
the dislocation regions. The coercive force would then de-
pend on where the dislocations were found and the shape
of the final unconverted region (for shape anisotropy),
resulting in randomness in the coercive force, heating
relation. The original highly doped samples may not have
many vacancies so the cobalt ions would be unable to move
far, resulting in either small regions of varying doping
with interstitial ions or large regions of unconverted
γFe_2O_3 (sample 10 is 40% unconverted). With this model
it is possible for a sample with initially a lower cobalt

content to have a higher coercive force on heating, as
the latter is dependent on the shape and size of the final
particle (for shape anisotropy), and possibly the nature
of the boundary between the two phases (for exchange inter-
action).

Although this model is completely qualitative, it
accounts for the magnetic moments, the lattice parameters
and the coercive forces of all the heated samples.

CHAPTER V

APPLICATION OF THE MÖSSBAUER EFFECT

The Mossbauer effect is a very useful technique for measuring the cation distribution in crystallographically inequivalent sites. The distribution can be determined from the ratio of the areas under the recoilless resonant absorption peaks for Fe^{57} nuclei in A and B sites, provided the recoil free fractions are known. If the hyperfine fields are the same for the A and B sites, the peaks can be separated by applying a large external field that adds to the A site and subtracts from the B site hyperfine fields.

Experimental Procedure and Data Analysis

Each sample was ground and 125 mg was mixed with lucite and moulded into a disc for an absorber. The source was 25-m Ci of Co^{57} in a Cr matrix. Spectra of samples 1, 8 and 10 containing 0 mole %, 4.5 mole % and 9.9 mole % of cobalt were taken at room temperature with no applied field. A spectrum of a thicker sample (200 mg) was taken also to determine whether any Fe^{2+} was present. An applied field of 51 kOe was used to separate the A and B site lines and spectra of samples 1, 8 and 10 were taken with this

field applied parallel to the γ ray propogation direction.
To determine the recoil free fraction ratio of the A and
B sites, spectra of sample 7 (4.5 mole % cobalt) were
taken at 4.2° K with and without an applied field. The
details of the apparatus and the superconducting solenoid
are given elsewhere.[46]

The spectra taken in an applied field were fitted
to 8 Lorentzians with an IBM 360 computer. Firstly the
intensities and the full widths at half height of opposite
lines were constrained to be equal, and secondly no con-
straints were applied on the outer two pairs of lines and
the two sets of results compared. The spectra taken with-
out an applied field were fitted to 10 lines, two for each
of the two pairs of outside lines, and one for each of the
middle pair of lines as no useful information could be gained
from fitting them to Lorentzians. Constraints were neces-
sary for a reasonable fit in this case, and the intensities
and full widths at half height of opposite lines were con-
strained to be equal. Also the intensity ratio of the B
to A site lines were constrained to be equal to that found
from the spectra taken with an applied field.

Isomer Shifts and Hyperfine Fields

The spectra taken with no applied field consisted of six lines (Figure 33) with the A and B sites giving rise to broadened but unresolved lines. No Fe^{2+} line or $Fe^{2+/3+}$ line was observed, and no quadrupole interaction was noticed at room temperature. In an applied field the second and fifth lines disappeared; this demonstrated that the material was saturated and all the atomic moments were either parallel or antiparallel to the applied field. The first and sixth lines showed clearly resolved A and B site lines (Figure 34). The isomer shifts and hyperfine fields are shown in Table XVI.

The isomer shift depends on the difference in the nuclear radii of the ground and the excited states. A change in the S electron density such as might arise from a change in valence, would result in an altered Coulombic interaction which manifests itself as a shift of the nuclear levels. The isomer shifts of the cobalt doped samples are unchanged from pure γFe_2O_3. Thus there is no isomer shift change that would correspond to Fe^{2+} being present and the iron on the A and B sites is Fe^{3+} within experimental error.

FIGURE 33

Mossbauer spectrum of sample 8 (4.5 mole % cobalt) at room temperature with no applied field. The crosses are experimental points and the Lorentzians for the A and B site lines are shown inside each peak. The sum of these is the curve that fits the experimental points.
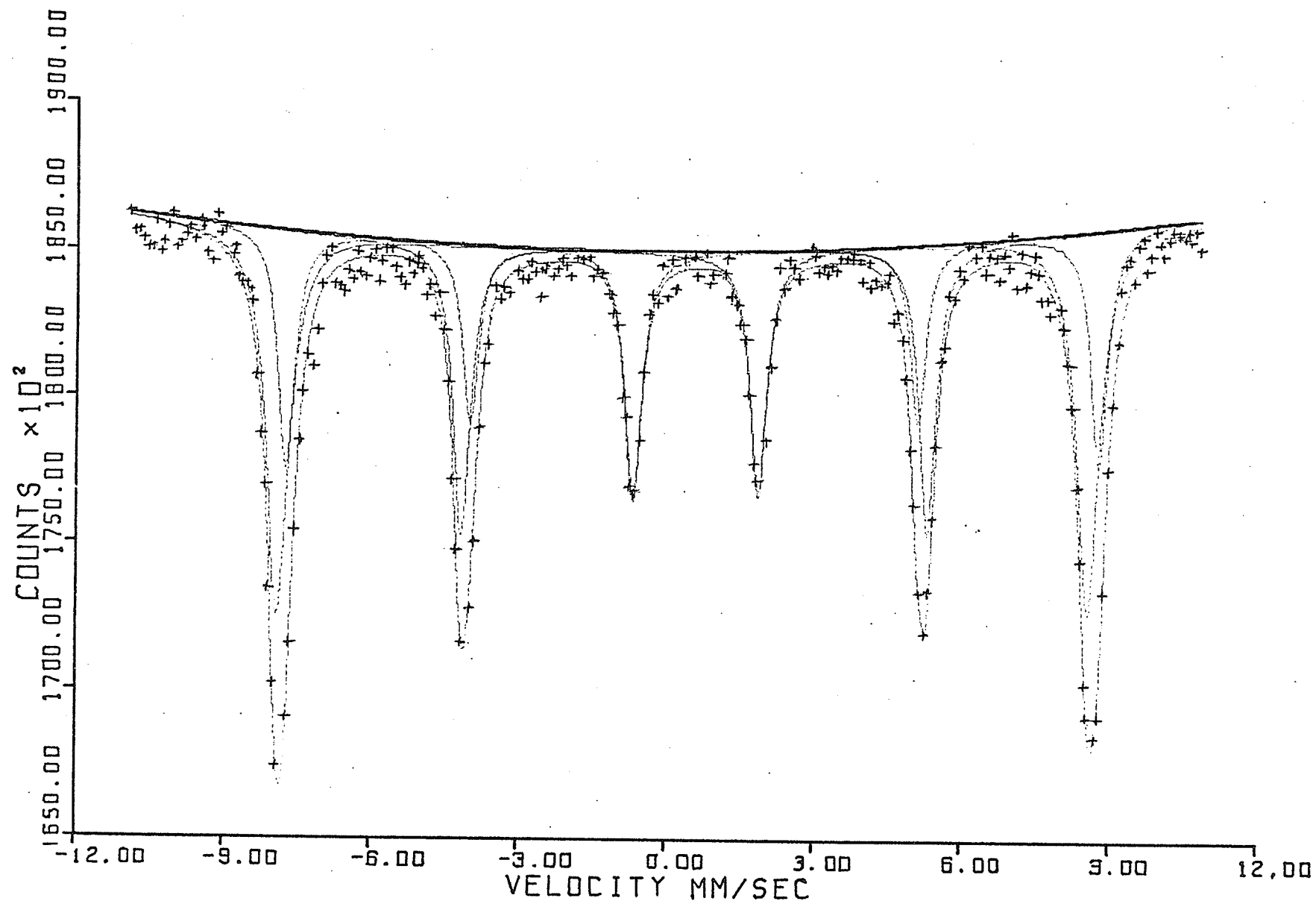
FIGURE 34

Mossbauer spectrum of sample 8 (4.5 mole % cobalt) at
room temperature with the applied field of 51 kOe. The
individual Lorentzians for the A and B sites are shown
and also the sum of these. The outer two pairs of lines
were fitted without constraints.
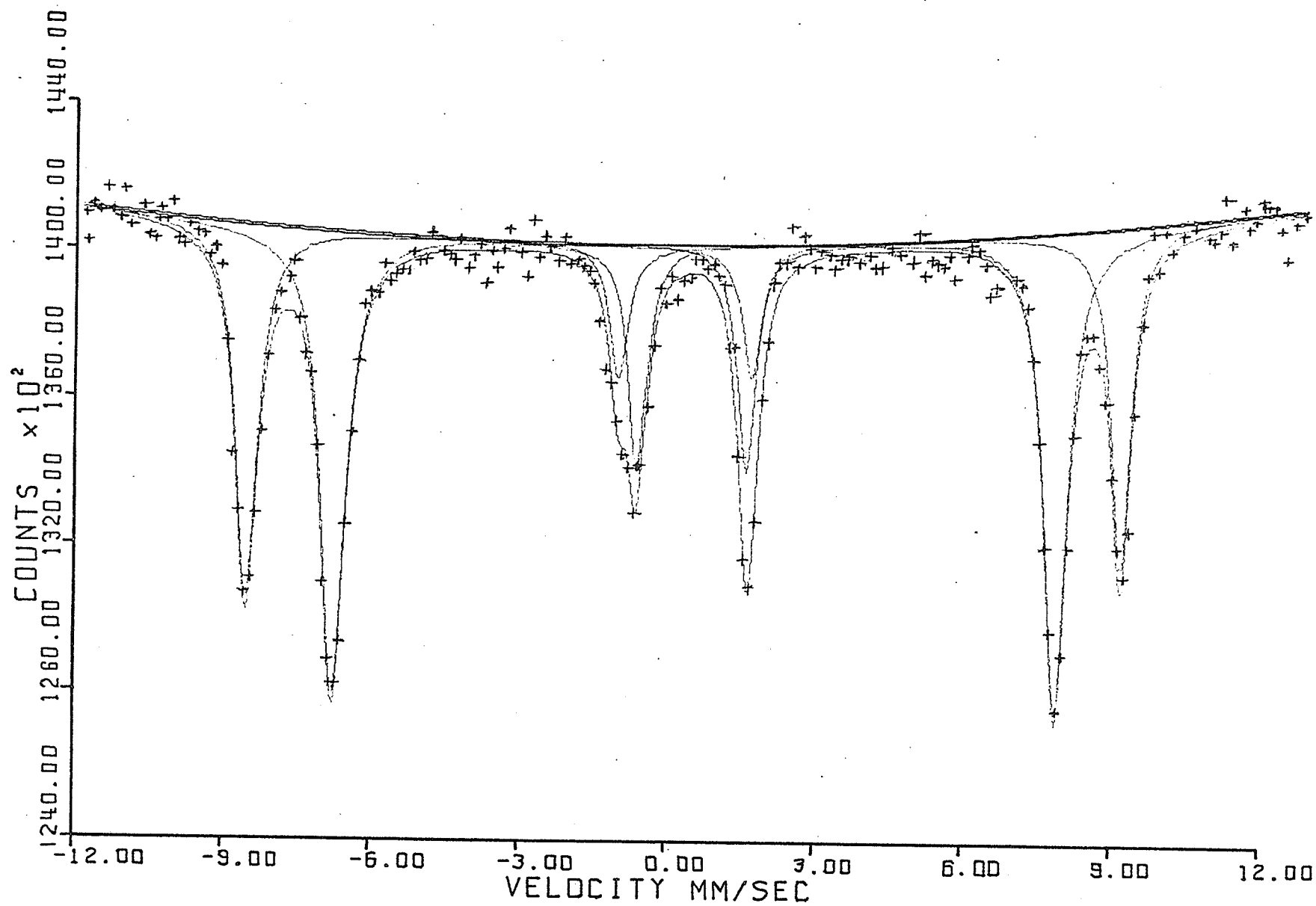
TABLE XVI

HYPERFINE FIELDS AND ISOMER SHIFTS

Sample Number	Mole % Cobalt	Isomer Shift mm/sec (relative to Chromium) ± 0.03 mm/sec		Hyperfine Field kOe ± 4kOe	
		A Site	B Site	A Site	B Site
1	0	0.33	0.55	502	503
8	4.5	0.34	0.56	498	505
10	9.9	0.32	0.54	503	512

The hyperfine fields found by using an applied field were like those of pure γFe_2O_3 and compare favourably with other results.[44] The increase in the hyperfine field for sample 10 (9.9 mole % cobalt) was approximately within the experimental error. Again there was no Fe^{2+} present within experimental error; these ions would cause a decreased hyperfine field which was not observed.

One noticeable feature of the spectra was the increased B site line width for the cobalt doped samples. Widening can be caused by Fe^{2+} ions, or by cobalt ions in the A sites producing a decrease in the predominant A-B superexchange interaction.[45] However both these effects would cause an asymmetric line and a decreased hyperfine field neither of which were present. A further effect leading to symmetric broadening is the dipolar field of the Co^{2+} ions in the B sites. The classical expression for the dipolar field is

$$\vec{H}_{dip} = - \frac{\vec{\mu}}{r^3} \frac{(3\vec{\mu} \cdot \vec{r}) \vec{r}}{r^3}$$

where $\vec{r}$ is the position vector from the Co^{2+} ion and $\vec{\mu}$ is the dipole moment. The field at one B site can be calculated from averaging the fields from Co^{2+} ions in the six

nearest neighbour B sites. The broadening is symmetrical because of the symmetry of a B site. The results are shown in Table XVII. Thus the broadening of sample 8 ($4\frac{1}{2}$ mole % cobalt) may be accounted for by Co^{2+} ions on the iron B sites or vacancies but not on the A sites. There is still some broadening in sample 10 (9.9 mole % cobalt) that is not accounted for by the dipolar field. However if interstitial ions were present the distance r would be less than that between nearest neighbours resulting in an increased dipolar field.

Area Ratios

If the recoilless fractions are the same, the area ratio of the A to B site lines gives the ratio of the number of iron ions in each site. The area ratio of the B to A site lines in $Fe(Fe_{5/3} \square_{1/3})O_4$ should be 1.67 and in $Fe(Fe_{3/2} H_{1/2})O_4$ it should be 1.5. If cobalt ions replaced iron on the B sites of either structure a decrease in the area ratio of 0.12 for sample 8 ($4\frac{1}{2}$ mole % cobalt) and 0.26 for sample 10 (9.9 mole % cobalt) would be expected.

TABLE XVII

BROADENING OF B SITE LINES

Cobalt Ion Replaces	Sample Number	Mole % Cobalt	Broadening Due to Dipolar Field (kOe)	Experimentally Observed Broadening (kOe)
vacancies	8	4.5	1.1	1.7 ± 1
	10	9.9	2.4	4.3 ± 1
B site iron	8	4.5	0.8	1.7 ± 1
	10	9.9	1.8	4.3 ± 1

The area ratio at room temperature calculated from the computer fits both with and without constraints and from measurements with a planimeter are shown in Table XVIII, which shows no difference in the area ratios of the doped and undoped samples.

Mossbauer Spectra at 4.2^O K

The spectra obtained at 4.2^O K using liquid helium are shown in Figures 35 and 36 and the data obtained from them is shown in Table XIX.

It is of interest to note that when a field was applied at 4.2^O K the second and fifth lines did not disappear, demonstrating that the material was not saturated at 50 kOe at this temperature. The intensities of these lines were however reduced to about 1/10 of the intensity of the other lines. This may indicate that the coercive forces at low temperatures should be higher than those measured. There were no Fe^{2+} or Fe^{4+} lines observable in either spectrum.

The spectrum taken with no applied field was the characteristic six line spectrum but with partial resolution of the A and B sites in the sixth line.

TABLE XVIII

AREA RATIOS OF B TO A SITE LINES AT ROOM TEMPERATURE

Sample Number	Mole % Cobalt	Average Area Ratio ±0.08	Area Ratio Measured With a Planimeter ±0.08	Area Ratio Calculated From Computed Lorentzians	
				With Constraints	Without Constraints
1	0	1.45	1.43	1.49	1.445
8	4.5	1.47	1.555	1.44	1.505
10	9.9	1.50	1.47	1.49	1.445

FIGURE 35

Mossbauer spectrum of Sample 7 at 4.2° K with no applied field.
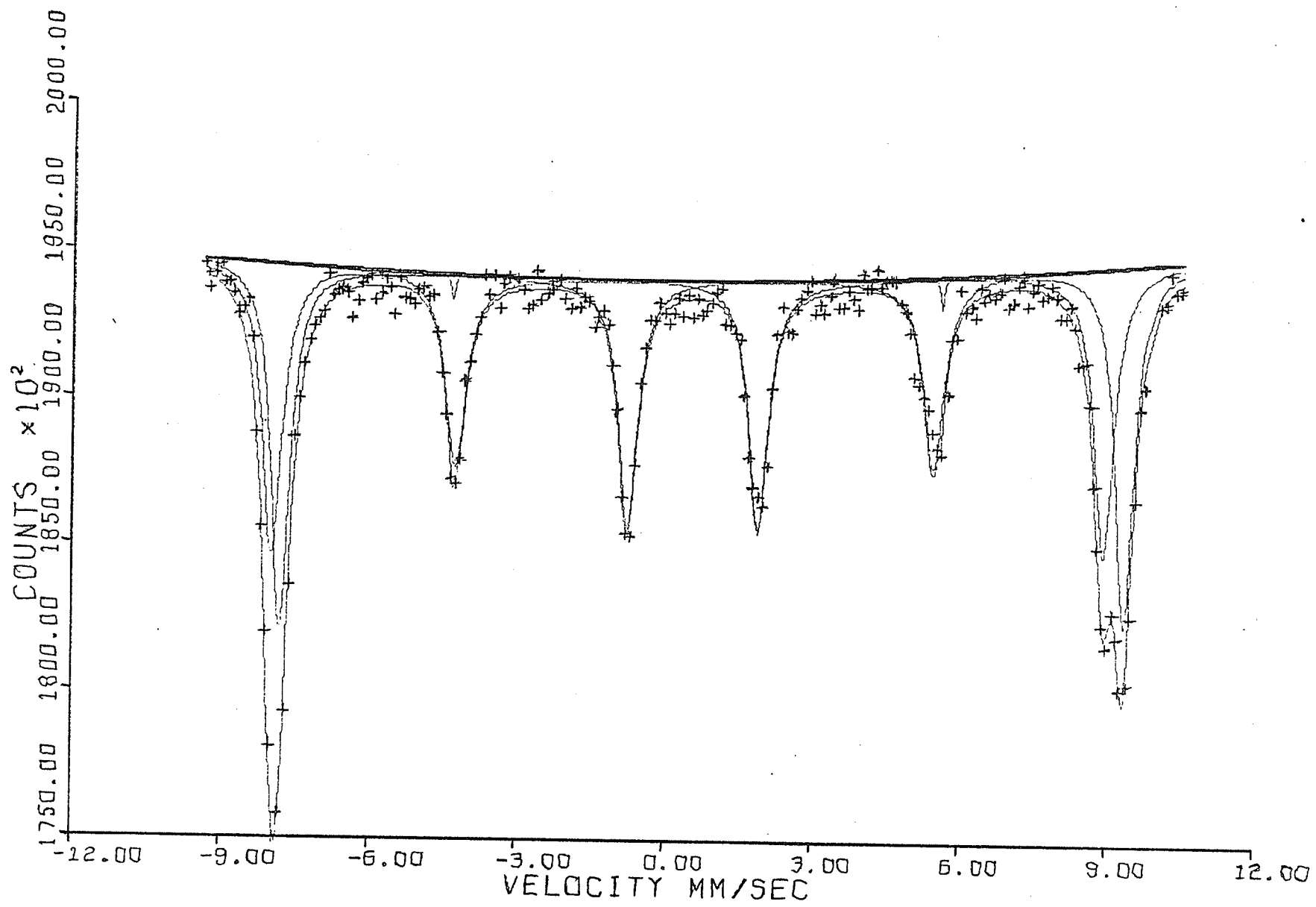
FIGURE 36

Mossbauer spectrum of sample 7 at 4.2° K with an applied field of 50 kOe.
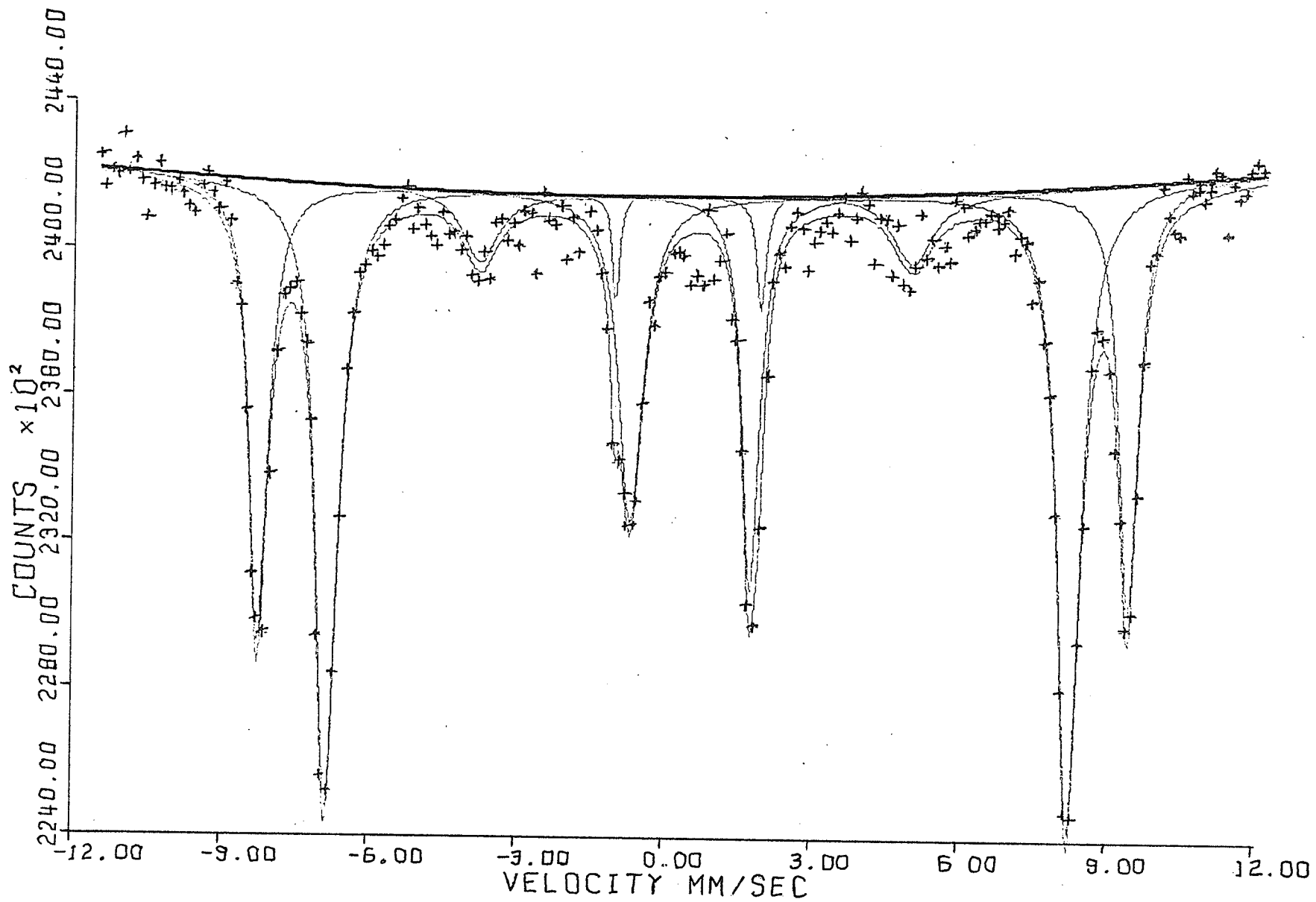
TABLE XIX

MÖSSBAUER RESULTS AT 4.2° K

HYPERFINE FIELDS ISOMER SHIFTS AND QUADRUPOLE INTERACTION

	Spectra Taken With an Applied Field		Spectra Taken Without an Applied Field	
	A Site	B Site	A Site	B Site
Hyperfine field kOe	521 ± 3	537 ± 3	528 ± 5	536 ± 5
Isomer Shift mm/sec	0.60 ± 0.03	0.71 ± 0.03	0.53 ± 0.1	0.70 ± 0.1
Quadrupole Interaction	−	−	0.06 ± 0.1	0.07 ± 0.1

AREA RATIOS

	Spectra Fitted To					
	10 Peaks	10 Constraints	10 Peaks	0 Constraints	12 Peaks	12 Constraints
Area Ratio $\frac{B}{A}$	1.64		1.582	1.697		1.639

Average Area Ratio $\frac{B}{A} = 1.64 \pm 0.06$

The difference in hyperfine fields at the A and B sites increased to about 15 kOe and the difference in isomer shifts remained about the same.

Area Ratios at 4.2° K

The area ratios of the B to A site was about 10% higher at 4.2° K than at room temperature, and the average value of 1.64 ± 0.06 is much more consistent with an area ratio of 1.67 expected for $Fe^{3+}(Fe^{3+}_{5/3} \square_{1/3})O_4$. This suggests that there is little water in the lattice but an area ratio of 1.64 may have 20 mole % of $Fe^{3+}(Fe^{3+}_{3/2} H_{1/2})O_4$ and an area ratio of 1.60 may have 40 mole % of this phase. Thus the possibility of water in the lattice is not eliminated but if present it comprises less than half of the sample.

Quadrupole Interaction

A quadrupole splitting of the Mössbauer absorption peaks is obtained when the nuclear quadrupole moment interacts with the electric field gradient due to other charges in the crystal. The nuclear quadrupole moment reflects the deviation of the nucleus from spherical symmetry. Large magnetostrictive effects are often associated with Co^{2+} ions, thus a quadrupole interaction may possibly be expected

in cobalt doped gamma ferric oxide due to tetragonal distortion. However no quadrupole interaction was observed at 4.2° K, but as quadrupole interactions for Fe^{3+} ions in B sites are usually about 0.1 mm/sec, there may still be a quadrupole interaction within experimental error.

Conclusions from Mössbauer Experiments

Within experimental error the samples did not contain any iron other than Fe^{3+}, and most ions did not go into B sites as no area ratio change was found. There was effectively no difference in the spectra of pure and cobalt doped samples apart from an increased B site line width that could be accounted for by the dipolar field of the nearest neighbour cobalt ions. It is difficult to conceive a mechanism whereby the cobalt goes into the lattice with no iron valence change and with no large number of cobalt ions in the iron B sites, however many configurations can be found with small amounts of Fe^{2+} and Fe^{4+} present and relatively small amounts of Co^{2+} on B iron sites. By using data for the isomer shift and hyperfine fields in $Fe^{2+/3+}$ on B sites and Fe^{3+} on B sites in magnetite and the experimental errors involved here, it is found possible to have 3% of the total iron as Fe^{2+}.

CHAPTER VI

CONCLUSION

A. EFFECT OF COBALT ON THE BULK PROPERTIES OF GAMMA FERRIC OXIDE

The cobalt ion has a very significant effect on
the bulk magnetic properties of γFe_2O_3, the predominant
effect being a large increase in coercive force especially
at low temperatures. These properties have been analyzed
and discussed previously and are best accounted for by the
one ion model which requires most cobalt in B sites espec-
ially in vacancies.

Magnetic Moment

The magnetic moment is dependent on the microscopic
distribution of the ions and should yield significant re-
sults on such a distribution. The magnetic moments of
samples that have a linear relationship between cobalt
content and coercive force (except sample 2) are the same
as that of pure γFe_2O_3 to within 2%. Two of the samples
which had no superstructure lines and whose coercive forces
did not follow the same linearity as the others, had much
lower magnetic moments. If such a decrease was produced

by cobalt ions only a large increase in area ratios of B to A site lines would be observed. Another possibility is if these samples were the hydrogen phase doped with cobalt and the pure moment would then be within about 2% of the doped moments. This also leads to the possibility of the original pure γFe_2O_3 sample being partially $Fe(Fe_{3/2} \, H_{1/2})O_4$; for a moment of 69 emu/gm a ratio of 4:10 of the hydrogen phase would be required which is within the experimental error of the Mossbauer area ratios.

Remanence to Saturation Ratios

The Mossbauer results confirm the idea that the material is not saturated at low temperatures. As fields of less than 20 kOe were used to measure the ratio of the remanence to saturation, and no saturation was found even at 50 kOe the increase in the ratio at low temperatures may be accounted for. Thus it is probable that the particles are single domain reversing coherently.

B. EFFECT OF COBALT ION ON CRYSTALLOGRAPHIC STRUCTURE AND POSITION OF THE ION

There is an increase in lattice parameter when γFe_2O_3 is doped with cobalt; however this yields little information about the distribution of ions except the

possible exclusion of Fe^{4+} ions which would probably decrease the lattice parameter.

If a cobalt ion goes into the lattice the charge must be balanced. To account for the experimental results it would be desirable to have very few cobalt ions on iron B sites, many cobalt ions in vacancies, some hydrogen present, very little Fe^{2+} or Fe^{4+} present and a spin arrangement that would result in little change in magnetic moment. For the magnetic moment to be constant, there must be many Co^{2+} on iron B sites and few in vacancies, whereas for the area ratios to be constant very few Co^{2+} ions must go into the B sites and many in the vacancies. Several distributions of ions were calculated (Table XX and Table XXI) by constraining the charge to be balanced and allowing the cobalt ions to be predominantly in B sites (as they have a B site preference energy in other ferrites) and varying the other parameters. Only the most simple arrangements are shown, that satisfy charge balance and at least one other condition.

There are three structures that approximately fit all data within experimental error. One third of the cobalt ions in vacancies and two thirds in iron B sites is

TABLE XX

SITES FOR Co^{2+} IONS IN $Fe(Fe_{5/3} \square_{1/3})O_4$

	xCo^{2+} Ion Replace	Other Changes Necessary For Charge Balance	Fractional Moment Change	Fractional Area Change	Fraction of Co^{2+} in A Sites to Total Iron Content	Fraction of Fe^{2+} or Fe^{4+} to Total Iron Content
a)	$\frac{1}{3}$ x Fe(A) $\frac{1}{3}$ x Fe(B) $\frac{1}{3}$ x vacancies	none	0.27 m	0	0.3 m	0
b)	x vacancies	$2xFe^{3+}$ becomes Fe^{2+}	0.8 m	0	0	2 m
c)	x vacancies	oxygen polarisation	2.4 m	0	0	0
d)	$\frac{1}{3}$ x vacancies $\frac{2}{3}$ x Fe(B)	none	-0.27 m	-1.1 m	0	0
e)	x Fe(B)	xFe^{3+} becomes Fe^{4+}	-1.6 m	-1.6 m	0	1 m
f)	$\frac{1}{2}$ x vacancies $\frac{1}{2}$ x Fe(B)	$\frac{1}{2}$ x Fe^{3+} becomes Fe^{2+}	0	-0.8 m	0	0.5 m
g)	x vacancies	oxygen polarisation	2.4 m	0	0	0

TABLE XXI

SITES FOR Co^{2+} IONS IN $Fe(Fe_{3/2} H_{1/2})O_4$

	xCo^{2+} Ion Replace	Other Changes Necessary For Charge Balance	Fractional Moment Change	Fractional Area Change	Fraction of Co^{2+} in A Sites to Total Iron Content	Fraction of Fe^{2+} or Fe^{4+} to Total Iron Content
a)	x H(B)	polarisation of oxygen ions	3.0 m	0	0	0
b)	x H(B)	2 x hydrogen removed from lattice	3.0 m	0	0	0
c)	x H(B)	x Fe^{3+} becomes Fe^{2+}	2.0 m	0	0	1.0 m
d)	x/4 Fe(A) x/4 Fe(B) x/2 H(B)	none	1.5 m	0	m/4	0
e)	x/2 H(B) x/2 Fe(B)	none	0.5 m	-0.8 m	0	0
f)	2x/3 H(B) x/3 Fe(B)	x/3 Fe^{3+} become Fe^{2+}	2.5	-0.55 m	0	0.3 m
g)	x Fe(B)	polarisation of oxygen	-5.0 m	-1.7 m	0	0

(Also as Table XX e)

one possibility, equal numbers of cobalt ions in the iron

B sites and in the vacancies and half this number of Fe^{3+}

becoming Fe^{2+} also satisfies the conditions. For the

structure with hydrogen in the B sites, agreement is ob-

tained with equal numbers of cobalt ions in the hydrogen

and iron B sites. The magnetic moment change in sample 10

is not within the experimental error but, as indicated by

previous results, if there are interstitial ions the ef-

fective per cent of cobalt would be less and the results

would fit.

The actual distribution may be a mixture of these

and others but this shows that there are ionic arrangements

with approximately equal numbers of cobalt ions in the

vacancies or hydrogen sites and the B sites, which fit

experimental data.

Evidence that Cobalt Ions are in the Lattice

The most significant evidence in support of cobalt

ions being in the lattice randomly and not in clusters is

the linearity of the coercive forces and anisotropy con-

stants with cobalt content, and the fit to the one ion mo-

del. Also the increase in lattice parameter with cobalt

doping tends to indicate cobalt ions in the lattice. The

broadening of the B site Mossbauer absorption peaks can
be explained reasonably by assuming cobalt ions are in the
nearest neighbour B sites. By using the fact that the ma-
terial is unsaturated at low temperatures the remanence
to saturation ratio also suggests this model.

There is no evidence in conflict with the cobalt
ions being in the lattice and the lack of extra lines due
to another phase, in the diffraction patterns does not
refute the idea of clusters being present.

Thus although many results can be accounted for by
cobalt ions in clusters or in the lattice, it appears that
most results point to cobalt ions being in the lattice.
The experiments also indicate that the cobalt ions are in
the iron B sites and vacancies and that the micropowder
consists of single domain particles whose magnetization
vectors reverse coherently.

C. SUGGESTIONS FOR FURTHER EXPERIMENTS

Further experiments should be of a chemical nature,
to determine the amount of Fe^{2+} and water present accurately.
To do so requires a large amount of material. Another area

to be investigated is the method of preparation of the
samples, the ionic distribution is dependent on the heat
treatment used in the preparation of some materials[45]
If it were at all possible to grow single crystals of cobalt
doped gamma ferric oxide the anisotropy constants and
magnetostriction measurements would yield valuable infor-
mation.

REFERENCES

1. A. H. Morrish, The Physical Principles of Magnetism, John Wiley, 1965.

2. Luborsky, F.E., J. Appl. Phys., 32 1715 1961.

3. Bate, G., J. Appl. Phys. 1961 32 2395

4. Wohlfarth, E. P., J. Appl. Phys. 30, 41, 1175 1959

5. Neel, L., Compt. Rend (Paris) 224 1488 1947

6. Van Oosterhout, G., W., Rooijmans CJM Nature 181, 44, 1958

7. Braun, P.B., Nature 1952, 1123.

8. David I., Welch A.J.E., Trans. Faraday Soc., 15 1642 1956.

9. Aharoni, A. Frei E.H., Schieber, M., J. Phys. Chem. Solids 23, 545, 1962.

10. Van Oosterhout, G.W., Acta Cryst 13, 932, 1960

11. Eagle, D.F., Mallinson, J.C., J. Appl. Phys. 28, 3, 995 1967.

12. Berkowitz, A.E., Schrieber, W.J., Flanders, P.J. , J. Appl. Phys. 39 2 1261 1968.

13. Osmond W.P., Proc. Phys. Soc. B 65 121 1952, B 66 265, 1953.

14. Henry, W.E., Boehm, M.J., Phys. Rev. 101,4, 1253 1956.

15. Brown, W.F., Johnson, C.W., J. Appl. Phys. 33, 91 2753 1962.

16. Speliotis, D.E., Morrison, J.R., Bate, G., Proc. Int. Conf. on Magnetism, Nottingham, 1964 p. 623.

17. Watt, L.A.K., Morrish, A.H., J. Appl. Phys., 31, 715, 1960.

18. Morrish, A.H., Watt, L.A.K., J. Appl. Phys., 29, 7, 1029, 1958.

19. Morrish, A.H., Yu S.P., Phys. Rev. 102, 3, 670, 1956.

20. Morrish, A.H., Valstyn, H., J. Phys. Soc. Japan 17, Suppl. B1, 392, 1962.

21. Wohlfarth, E.P., J. App. Phys. 30, 1465, 1959.

22. Morrish, A.H., Sawatzky, G.A., (in press)

23. Kachi, S., Momiyama, K., Shimuzu, S., J. Phys. Soc. Japan 18, 106, 1963.

24. Deboer, J., Selwood, H., J. Amer. Chem. Soc. 76, 3365 1954.

25. Bando, Y., Kiyama, M., Takada, T., Kachi, S., Jap. J. Appl. Phys. 4, 240 1965.

26. Senno, H., Tawara, Y., Jap. J. Appl. Phys. 6, 509, 1967.

27. Senno, H., Tawara, Y., Jap. J. Appl. Phys. 6, 1347, 1967.

28. Krones, F., Technik der Magnetspeicher, Springer Verlag Berlin, 1963, p. 479.

29. Bickford, L.R., Brownlow, J.M., Penoyer, R.F., I.E.E. Proc. 1048, Suppl. No. 5, 288, 1957.

30. Miyamoto, S., Tanaha, N. Iida, S., J. Phys. Soc. Japan, 20, 753, 1965.

31. Pearson, R.F., Phys. Soc. (London) 74, 505, 1959.

32. Tachiki, M., Progr. Theor. Phys. 23, 6, 1055, 1960.

33. Slonczewski, J.C., J. Appl. Phys. 32, 3, 2535, 1961.

34. Slonczewski, J.C., J. Appl. Phys. 29, 3, 448, 1958.

35. Slonczewski, J.C., J. Phys. Chem. Solids 18, 4, 269, 1961.

36. Becher, J.J., J. Appl. Phys. 39, 12, 1270 1969.

37. Westendorp, F.F., Solid State Comm. 8, 139, 1970.

38. Buschow, K.H.J., Naastepad, P.A., Westendorp, F.F., J. App. Phys. 40, 10, 4029, 1969.

39. Greenough R.D., Lee, E.W., Phys. Soc. D. (Lond.) 13, 11 1595, 1970.

40. Gorter, E., J. Phys. Radium 12, 184, 1951.

41. Iida, S., J. Phys. Soc. Japan, 12, 222, 1957.

42. Shur, Y.S., Ivanov, B.A., Shtol'ts E.V. Sov. Phys. Sol. State 9, 1, 30, 1967.

43. Ivanov C. A., Shur, Y.S., Shtol'ts, E.V., Sov. Phys. Sol. State 9, 4, 857, 1967.

44. Coey, J. M. D., Morrish, A. H.,Sawatzky, G.A., J. Physique (in press).

45. Sawatzky, G.A., Van der Woude, F., Morrish, A.H., J. Appl. Phys. 39, 2, 1968.

46. Sawatzky, G.A., Ph. D. Thesis University of Manitoba 1969.

47. Wohlfarth, E.P., J. Phys., Radium 20, 295, 1959.